



ANTIOXI - Development of oxide model for activity buildup in LWRs – Validation of model

Author William Eek (ALARA Engineering)

Confidentiality Public

Report's title ANTIOXI - Development of oxide model for activity buildup in LWRs – Validation of model	
Customer, contact person, address EC / Marc Deffrennes, Commission européenne, Rue du Champ de Mars 21, B-1050 Brussels, Belgium	Order reference
Project name ANTIOXI	Project number/Short name 6402 ANTIOXI
Author William Eek, ALARA Engineering AB, Vasterås, Sweden	Pages 57 p.
Keywords activity buildup, water chemistry, LWR	Report identification code VTT-R-04208-09
Summary The objective of this project is to develop a deterministic model for the activity build-up in the oxide on the out-of core primary system surfaces in both BWR plants using different water chemistries and PWR plants. The oxide is divided into two layers since the oxide appears different close to the alloy compared to the oxide close to the coolant. The activities in the two oxide layers are calculated using transport equations. Since the oxide appears different close to the alloy compared to close to the coolant, also different transport equations were used for the two oxide layers. Concentration profiles are obtained for both activated and non-activated nuclides. It is also studied how the different water chemistries in BWR affects the thickness of the oxide.	
Confidentiality	Public
Signatures  Pentti Kauppinen Technology Manager	
 Petri Kinnunen Senior Research Scientist, Coordinator	
VTT's contact address VTT Technical Research Centre of Finland, P.O. Box 1000 (Kemistintie 3, Espoo), FI-02044 VTT, FINLAND. Tel. +358 20 722 111, Fax +358 20 722 7002	
Distribution (customer and VTT) European Commission 1 original ALARA Engineering 1 original VTT 1 original	
<i>The use of the name of the Technical Research Centre of Finland (VTT) in advertising or publication in part of this report is only permissible with written authorisation from the Technical Research Centre of Finland.</i>	

Preface

The work discussed in the present report has been carried out as a part of the Work Package 4 of the project FP6-036367 A deterministic model for corrosion and activity incorporation in nuclear power plants (ANTIOXI) in 2006 - 2008. The ANTIOXI project is a part of the EURATOM FP6 Programme “Advanced tools for nuclear safety assessment and component design”.

The ANTIOXI project in EURATOM FP6 concentrates on development of modelling tools for activity incorporation and corrosion phenomena into oxide films on construction materials in light water reactor environments.

The main funding source of the work has been the Sixth Framework Programme of the European Commission. The cooperation of the Members of the Advisory Board of the ANTIOXI project is gratefully acknowledged.

Espoo, Finland, 4 June 2009.

Author

Contents

1	Introduction	5
2	Model description	6
3	Determination of model parameters	9
4	Validation of the model	10
4.1	BWR	11
4.1.1	NWC	11
4.1.2	HWC	21
4.1.3	DZO+HWC	35
4.2	PWR	45
5	Conclusion	55
6	References	57

List of Acronyms

LWR	Light Water Reactor (BWR, PWR and WWER)
BWR	Boiling Water Reactor
PWR	Pressure Water Reactor
WWER	Water-Water Energy Reactor
NWC	Normal Water Chemistry
HWC	Hydrogen water Chemistry
DZO	Depleted Zinc Oxide
ECP	ElectroChemical Potential
O2	Oskarshamn 2
B2	Barsebäck 2
R1	Ringhals 1
R2	Ringhals 2
R3	Ringhals 3
RHR	Residual Heat Removal
OLA	On-Line Activity

1 Introduction

The objective of the ANTIOXI project is to develop a deterministic model for the build-up of activated ions in the oxide layers at the LWR out-of core primary system surfaces. The main focus in the development is to be able to model and predict the radioactivity build-up occurring on these surfaces.

This report covers both BWR and PWR power plants. The BWR and PWR data is obtained from:

1. BWRs:

- a. Oskarshamn 2 (O2): 1975 - , 1700 → 1800 MWt
- b. Barsebäck 2 (B2): 1975 – 1999, 1700 → 1800 MWt
- c. Ringhals 1 (R1): 1976 – , 2270 → 2500 MWt

2. PWRs:

- a. Ringhals 2 (R2): 1975 – , 2660 MWt
- b. Ringhals 3 (R3): 1981 – , 2775 MWt

Note that the B2 plant has been phased-out in 2005.

The O2 plant started operation in 1974. The characteristics of O2 from the water chemistry point of view can be summarised in the following way:

- The concentration of Zn and Cu in the reactor water were high during the first four cycles due to brass condenser tubes. An exchange to titanium tubes has thereafter meant low levels of Cu. The concentration of Zn maintained low until 2003. Thereafter depleted zinc oxide (DZO) injection was started in order to control radiation fields. A major decontamination campaign of primary piping system was performed during the 2003 outage, i.e. DZO injection started with decontaminated pipes.
- HWC operation has been applied since 1993. ECP monitoring has been done both in the recirculation lines and in the residual heat removal system (RHR) lines. The hydrogen injection has been determined to control the corrosion potential in the recirculation lines. Operation without hydrogen injection is normally designated Normal Water Chemistry (NWC).

The B2 plant started operation in 1977 and was finally phased-out during 2005. The plant has a similar design as O2. The characteristics of B2 from the water chemistry point of view can be summarised in the following way:

- The concentration of Zn and Cu in the reactor water were high during the first two cycles due to brass condenser tubes. An exchange to titanium tubes has thereafter meant low levels of Cu, and also Zn up to the 1998 outage. DZO was, however, started in the beginning of 1999 and maintained to the phase-out in 2005. The Zn reactor water concentration during the DZO injection has, however, been kept somewhat lower than in O2.

- HWC operation has been applied since 1992. As in O2, ECP monitoring has been performed both in the recirculation lines and in the RHR lines.

The R1 plant started operation in 1975. The characteristics of R1 from the water chemistry point of view can be summarised in the following way:

- The concentration of Zn and Cu in the reactor water were high during the first five cycles due to brass condenser tubes. An exchange to titanium tubes has thereafter meant low levels of Zn and Cu. No Zn injection has been applied.
- HWC operation has been applied since 1984, with a short interruption 1992-93 (noticed by significantly increased Cr concentration in reactor water). The degree of reducing conditions has, however, been varying, i.e. some cycles with HWC has in reality only resulted in a slight reduction of the corrosion potential in the primary piping. In 2003 new internals were installed in R1 which improved the effect of HWC injection.

In R1 the residual heat removal system has been equipped with an on-line gamma monitoring (On-Line Activity - OLA) which makes it possible to detect some short-lived activated corrosion products. In R1, OLA has been in operation since 1996.

R2 is the oldest Scandinavian PWR, which started operation in 1975. R3 started operation in 1981. The characteristics of R2 and R3 from the water chemistry point of view can be summarised in the following way:

The pH was changed in the fuel cycle 1999-2000 from $\text{pH}_{300} = 7.2$ to $\text{pH}_{300} = 7.4$ (pH_{300} is pH at 300°C) during most of the cycles. This was accomplished by increasing the maximum Li from 2.2 ppm to 3.5 ppm in the reactor water.

Despite of the fact that the change in pH from 7.2 to 7.4 clearly affected the reactor water no consideration of the pH change is taken into account in the calculations. The reason for this is that the fluctuation of pH during a fuel cycle is significant. In the data from R2 and R3 the activities in the out-of-core primary systems are measured in both hot leg (320°C) and cold leg (280°C). However, since the activities in the oxide are very similar in both hot leg and cold leg, the model parameters are only optimized against cold leg data.

2 Model description

The focus of the project has been to predict the build-up of activated ions in the oxide at the out-of core primary system surfaces. A model for evaluation of the measured data has been developed by Lundgren /1-2/. His model compares the activity in the oxide layer with the activity in the reactor water to obtain the enrichment factor for each specific radionuclide, see equation 1 -

$$\text{Eq. 1} \quad C_0 = KC_w$$

where –

C_0 = Concentration in the outer part of the oxide layer [Bq/kg]

C_w = Concentration in the reactor water [Bq/kg]

K = Enrichment factor [-]

The enrichment factor is calculated according to –

$$\text{Eq. 2} \quad K(t) = \frac{A(t)\sqrt{\lambda}}{\rho C_w(t)\sqrt{D}}$$

where

$A(t)$ = Activity in oxide film [Bq/m^2] at time “ t ” of a specific nuclide

λ = Decay constant [s^{-1}] of the nuclide

ρ = Assumed density for oxide layer [3500 kg m^{-3}]

D = Assumed average diffusion rate in oxide layer [$10^{-18} \text{ m}^2 \text{ s}^{-1}$]

However, a more sophisticated model is necessary since we would like to follow the transport of ions as the oxide is building up. Also, according to the work of Bojinov et al /3/ the oxide appears to be different in the region close to the alloy compared with the oxide close to the coolant. Therefore we divide the oxide into two layers using different transport equations. Both oxide layers are assumed to be present from the beginning. The transport equations are obtained from the report of Bojinov et al /3/ -

For the inner layer (between $x = 0$ and $x = L_i$) –

$$\text{Eq. 3} \quad \frac{\partial C_{XX}}{\partial t} = D_{XX} \frac{\partial^2 C_{XX}}{\partial x^2} + \frac{V_{XX} F \bar{E} D_{XX}}{RT} \frac{\partial C_{XX}}{\partial x}$$

Where –

C_{XX} = Concentration of specie XX (mol / m^3)

D_{XX} = Diffusion constant of specie XX (m^2 / s)

V_{XX} = Valence of specie XX (-)

F = Faradays constant (C / mol)

E = Field strength (V / m)

R = Universal gas constant ($\text{J K}^{-1} \text{mol}^{-1}$)

T = Temperature (K)

using the boundary conditions –

$$\text{Eq. 4} \quad C_{XX}(0, t) = C_{XX,a}$$

$$\text{Eq. 5} \quad C_{XX}(L_i, t) = \frac{k_{1,XX} C_{XX,a}}{V_{m,MO} k_{3,XX}} + K_{enr,XX,i} C_{XX}(sol)$$

Where –

$C_{XX,a}$ = Concentration of specie XX at the alloy (mol / m³)

$k_{1,XX}$ = Rate constant of oxidation of the specie XX at the alloy (cm⁴ mol¹ s⁻¹)

$k_{3,XX}$ = Rate constant of oxidation of the specie XX at the inner layer/solute (cm / s)

$V_{m,MO}$ = Molar volume of the phase in the inner layer (m³ / mol)

$K_{enr,XX}$ = Enrichment factor for specie XX (-)

$C_{sol}(sol)$ = Concentration of specie XX in the solute (mol / m³)

The first part of equation 3 is the diffusion term and the second, the migration term. However, notice that the migration term is dependent on the diffusion constant.

For the outer layer between ($x = L_i$ and $x = L_o$) –

$$\text{Eq. 6} \quad \frac{\partial C_{XX}}{\partial t} = D_{XX} \frac{\partial^2 C_{XX}}{\partial x^2}$$

using the boundary conditions –

$$\text{Eq. 7} \quad C_{XX}(L_i, t) = \frac{k_{1,XX} C_{XX,a}}{V_{m,MO} k_{3,XX}} + K_{enr,XX,i} C_{XX}(sol)$$

$$\text{Eq. 8} \quad B_{XX}(L_o, t) = C_{XX}(L_o, t) / C_{XX}(L_i, t)$$

$$\text{Eq. 9} \quad C_{XX}(L_o, t) = \frac{k_{1,XX} C_{XX,a}}{V_{m,MO} k_{3,XX}} B_{XX}(L_o, L_i, t) + (1 + B_{XX}(L_o, L_i, t)) K_{enr,XX,i} C_{XX}(sol)$$

The boundary conditions are the same as in the work of Bojinov except for the inner layer. The field strength and rate constants are assumed unaffected by the surrounding environment, i.e., they are constant throughout the calculation. The same is assumed for the diffusion coefficients except that these depend on the zinc concentration.

As can be seen in equations 8 and 9 the boundary condition between the outer layer and the coolant is dependent of the ratio between the boundary condition at the outer layer and the inner layer. This ratio is obtained from the work of Bojinov. These ratios are assumed constant and independent of the environment. In case of activated ions these ratios are set equal to unity due to lack of reference values. If the selected ions in the solution come from the oxide then this is a good approximation. However, if the ions come exclusively from the solute then this is a poor approximation. This can be seen in equations 8 and 9 in case of activated species comes exclusively from the solute. Then $C_{XX,a}$ is zero and the fraction between the concentration in the outer and inner layers is unity. However, according to equations 7 too 9 the concentration in the outer layer becomes twice the concentration in the inner layer despite that the fraction was set to unity. But since we do not have any reference values for this fraction for activated species we nevertheless use equation 9 with the fraction set to unity to obtain the boundary condition at the outer layer.

The calculations are performed using a Crank-Nicholson method in order to obtain the concentration profile in the oxide. The initial concentration profile is obtained by assuming steady-state. Both oxide layers are assumed to be present from the beginning and are set to 10 nm each. Since the two oxide layers are only connected through the boundary condition at the inner layer, in which the concentration is

constant through time, the two oxide layers can be regarded as independent of each other.

The oxide layers are growing using moving boundaries in accord with the work of Macdonald /4/. The rate, at which the oxide is growing, is dependent on the particle flux at the outer boundary for each oxide, see equation 11 below.

It can be seen in the report of Bojinov that the addition of zinc affects the rate constants, the diffusion coefficients, enrichment factors and also the field strength to some extent. In our simplified model the addition of zinc only affects the diffusion coefficients and enrichment factors. According to reference /3/ it is assumed that zinc occupies the empty cation interstices and/or cation vacancies. The number of available cation interstices and vacancies therefore decreases. In order to maintain the steady-state concentrations for the cations in the oxide more cations have to be dissolved. As the zinc concentration increases in the oxide it occupies the defects, which makes it difficult for the cations from the alloy to move towards the solution and the diffusion coefficients for these cations therefore decrease.

3 Determination of model parameters

Most of the parameters in the model are obtained from the work of Bojinov. But in the work of Bojinov these parameters are not constant throughout the calculation as they are in this work. The considered stainless steel type during all calculations was AISI 304. The field strength can, as mentioned by Bojinov, be regarded as constant. The field strength was set to $3 \cdot 10^6$ V/m during all calculations. Also the values for k_1 , k_3 and diffusion coefficient were obtained from the work of Bojinov. In case of activated ions for which the diffusion coefficients are unknown, the diffusion coefficients were chosen in relation to ions with similar chemical properties for which the diffusion coefficients are known. As mentioned above the diffusion coefficients are dependent of the zinc concentration. The reason for this is that the rate of which the oxide layers grow should be reduced in the present of zinc. The influence of zinc was chosen to have the following form –

$$\text{Eq. 10 } D_{XX}(t) = D_{XX} * (0.01 + 0.99 * \exp(-\text{frac}(t)/0.08)),$$

where $\text{frac}(t)$ is the molar fraction in the oxide of species XX. The functional form was chosen so that both oxide layers grow with reasonable accuracy compared to the reference work done by Bojinov. As can be seen in the work of Bojinov the zinc concentration used was 30 ppb. In a BWR using zinc addition the concentration is about 5 ppb. Since the zinc concentration is only about one sixth of the concentration in the work of Bojinov, it will not reduce the oxide growth in the same extent in the calculations presented in this report.

According to the report of Bojinov, the field strength can be regarded as independent of both time and zinc concentration. The diffusion coefficients are, as mentioned above, reduced in the presence of the zinc concentration. But, as can be seen in the report of Bojinov the addition of zinc affects the diffusion coefficient in the two oxide layers differently. However, in order to reduce the number of variables, the diffusion coefficients are reduced in the same manner in both inner and outer oxide layers. This can, however, be regarded as a crude assumption in the sense that according to the report of Bojinov, the diffusion coefficient in the inner layer is reduced by a factor three to four and in the outer layer by a factor hundred. In our model the diffusion coefficients in both oxide layers are reduced to values between the diffusion coefficients in inner and outer oxide layers found in the report of Bojinov. The diffusion coefficients in the inner layer are therefore smaller than reference values and vice versa for the outer oxide layer. This will affect both the concentration profiles and the rate of which both

oxide layers are growing. But since the oxide layers are growing according to equation 11 using a user specified alpha value the growing rates can be calculated with reasonable accuracy according to references. In case of the concentration profiles both the migration and diffusion term becomes underestimated in the inner oxide layer. However, they still have the correct proportions to each other since the migration term is dependent of the diffusion coefficient. In the outer layer the concentration profiles are independent of the diffusion coefficient in the sense that steady-state is assumed as an initial condition and the size of the diffusion coefficient only affects the growing rates of the oxide.

$$\text{Eq. 11 } Oxiderate = \frac{Abs(Flux) * M * \exp(-Thickness * Alpha)}{Density}$$

Oxiderate = Growing rate of the oxide

Flux = Particle flux at the outer boundary for each oxide layer

M = Molar mass of the oxide

Thickness = Thickness of the oxide

Alpha = A user defined value which makes the oxide grow according to reference oxide, (5E5 in this work)

Density = Density of the oxide (3500 kg / m³ in this work)

The next part of the work is to find enrichment factors for all species. This was done by first optimizing the enrichment factor of zinc since it affects the rate of the oxide growth. This was done by doing a series of calculations for a specific year and comparing the ratio of the activity in the oxide with the activity in the water to reference values. The reference values were obtained from B2 and O2 for the BWR case /1/. In the case of PWR the reference values were obtained from R2 and R3 /2/. With the optimized enrichment factor for zinc the same procedure was done for the all other nuclides. In case of Co58 and Co60 the enrichment factors should be the same. But since they originate from different elements, Co58 from Ni and Co60 from Co, the different enrichment factors may be justified. Ni is dissolved from the internal parts of the reactor and Co originates from the fuel crud. The larger enrichment factor of Co60 may be justified since it can be assumed to be partially in particular form. It is known that particles in particular form has a higher tendency to deposit on surfaces.

4 Validation of the model

The activated nuclides treated in this work together with half lives and decay constants are presented in table 1.

Table 1: Half lives and decay constants for activated nuclides.

Nuclide	Fe59	Zn65	Cr51	Mn54	Co58	Co60	Sb124
Half lives	45.1 d	244.3 d	27.7 d	312.5 d	70.78 d	5.27 y	60.2 d
Decay constant (s ⁻¹)	1.78E-07	3.28E-08	2.90E-07	2.57E-08	1.13E-07	4.17E-09	1.33E-07

4.1 BWR

4.1.1 NWC

The optimized enrichment factors for NWC using the boundary conditions in equations 7-9 are shown in table 2.

Table 2: Optimized enrichment factors for NWC.

Nuclide	Fe	Zn	Ni	Cr	Mn	Co58	Co60	Sb
Enrichment Factor (-)	1.90E+08	7.50E+07	9.35E+07	1.72E+06	3.91E+07	4.04E+07	1.47E+08	1.40E+08

The calculated enrichment factors in table 2 are close to the enrichment factors calculated by Lundgren [1].

The figures 1 – 2 shows the calculated concentration profiles for the non-activated nuclides in the two oxide layers on the steel AISI 304 after 4000 respective 8000 h. Water concentrations of activated and non-activated nuclides are given in tables 3 – 4. The water concentration of Mn is set to 0.01% of the concentration of Mn54. The interface between the inner and outer oxide layer is indicated by the vertical line.

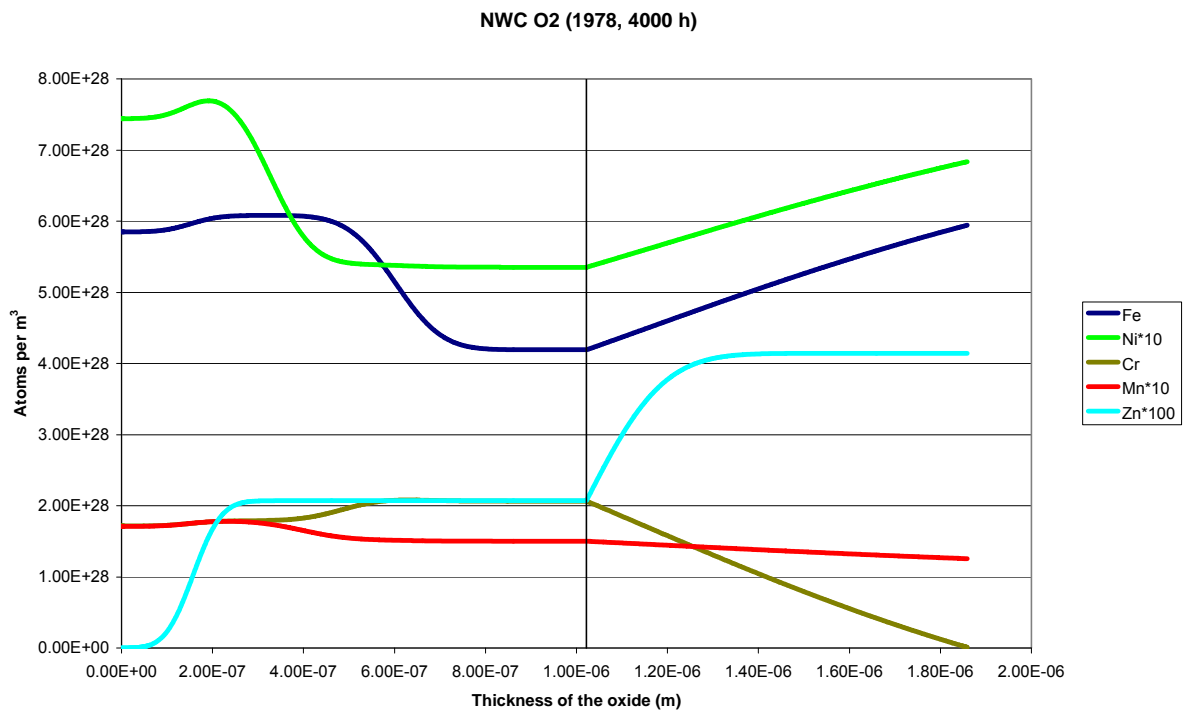


Figure 1: Concentration profile of the non-activated nuclides after 4000 h using NWC in O2.

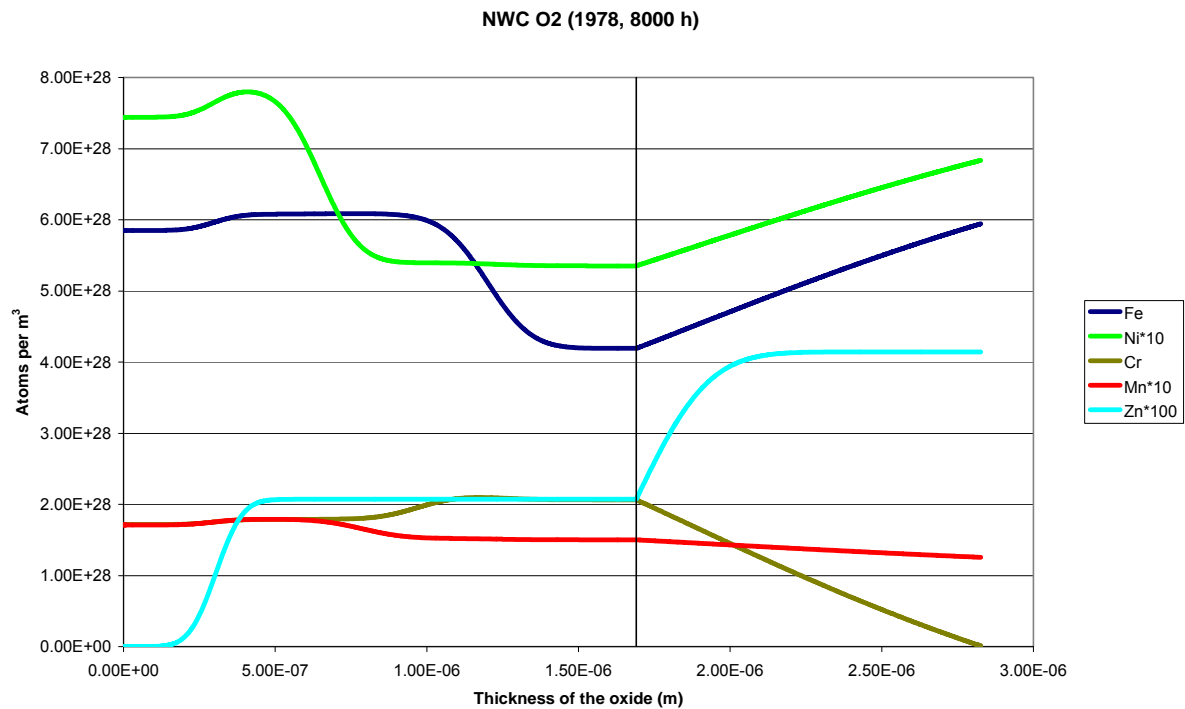


Figure 2: Concentration profile of the non-activated nuclides after 8000 h using NWC in O₂.

As can be seen in the figures above the concentration profiles do not change appreciably between 4000 and 8000 h. However, the oxide is nevertheless still growing. Despite the fact that no zinc were added during the year 1978 in O₂ there is still a high concentration of zinc in the coolant. This is due to that O₂ used brass condenser tubes for the first four cycles the reactor was in use. The tubes were thereafter changed to titanium tubes which lowered the zinc concentration in the coolant. The zinc concentration maintained low until 2003 when DZO injection started. The effect of the high concentration of zinc can be seen in the inner oxide layer in the figures above. As the zinc concentration increases the transport of other ions decreases. However, since there still is a constant flux of ions coming from the alloy the concentrations of ions increase above the concentrations in the alloy. The concentration profiles in the outer oxide layer seem to follow steady state solutions except for zinc. The reason for this is that the diffusion coefficients are not reduced as much as they should be according to reference work by Bojinov et al. However, the diffusion coefficient of zinc is nevertheless obtained from the reference work. There are therefore large differences between the diffusion coefficient of zinc and the diffusion coefficients of the other ions which results in that the oxide is growing faster than zinc is transported into the oxide. However, as can be seen in the figures above the concentration of zinc is overestimated compared to a steady state solution. This is due to the segments which are added as the outer oxide layer is growing. When the outermost segment towards the solution is increased to a certain length an extra segment is added. This segment then has the same concentration profile as the previous segment. Since the diffusion coefficient for zinc is much smaller than that for other ions only a small amount of zinc is transported to the nearest segment before a new segment is added. Therefore the zinc concentration profile in the outer oxide layer is overestimated. However, since the diffusion coefficients of the other ions are too large an overestimation of the zinc concentration actually reduces the diffusion coefficients closer to reference values.

The figures 3 – 4 shows the activity profiles for the activated nuclides in the two oxide layers on the steel AISI 304 after 4000 respective 8000 h.

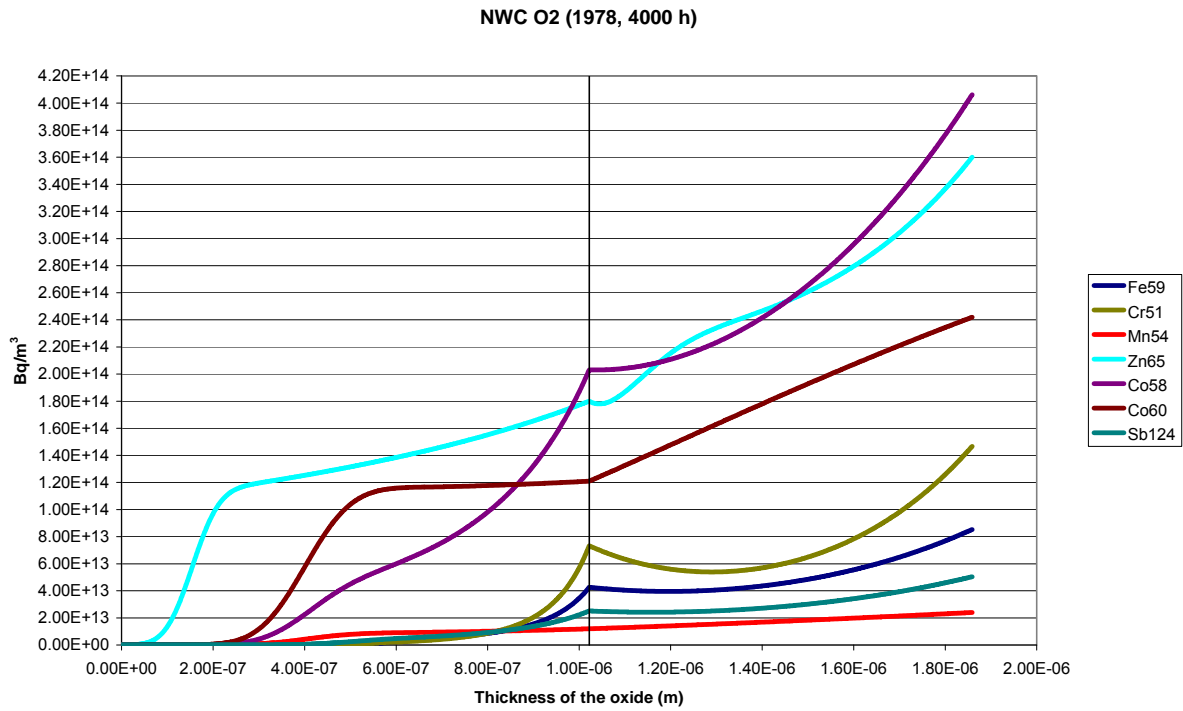


Figure 3: Activity profile of the activated nuclides after 4000 h using NWC in O₂.

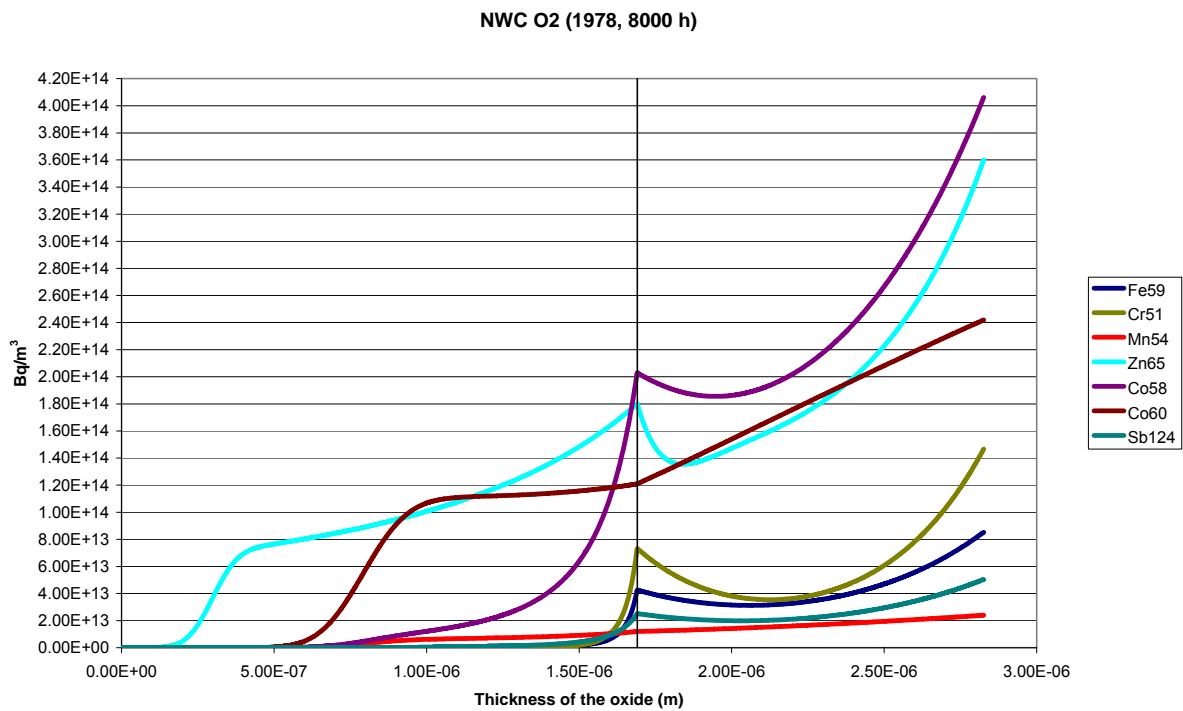


Figure 4: Activity profile of the activated nuclides after 8000 h using NWC in O₂.

As can be seen in the figures 3 – 4 the nuclides with longer half lives penetrates the inner oxide layer further than nuclides with shorter half lives. But also the

concentration in the coolant plays an important role. The differences in diffusion coefficients are small except for zinc which has a greater diffusion coefficient compared to the other nuclides since zinc lowers the diffusion coefficients for other nuclides. This is the reason to why zinc penetrates the inner oxide layer further than Co60 which has a longer half life.

In the outer oxide layer nuclides with long half life have an activity profile which appears like a steady-state solution similar to the concentration profile for non-activated nuclides shown in figures 1 – 2. Again zinc does not behave as expected since its relative long half life should give a more steady-state like behaviour for the activity profile. Again this is due to the overestimation of the other nuclide's diffusion coefficients. Nuclides with shorter half lives have activity profiles which appear like parabola. The reason for this is that nuclides with long half lives do not decompose in a significant extent during the calculation and therefore a steady-state like activity profile for them is obtained.

The figures 5 – 8 shows the same system, i.e. O₂, but for a different year. As can be seen in the figures 5 – 6 the increase in concentration close to the alloy of nuclides other than zinc is less pronounced compared to the year 1978. This is due to the fact that the zinc concentration were lower in the year 1988 compared to 1978. As also can be seen in the figures 1 – 2 and 5 – 6 is that the zinc concentration was not high enough in the year 1978 to reduce the oxide growth compare to year 1988 when the zinc concentration were more than halved.

The activity profiles look very much the same as in the year 1978, as can be seen in figures 3 – 4 and 7 – 8.

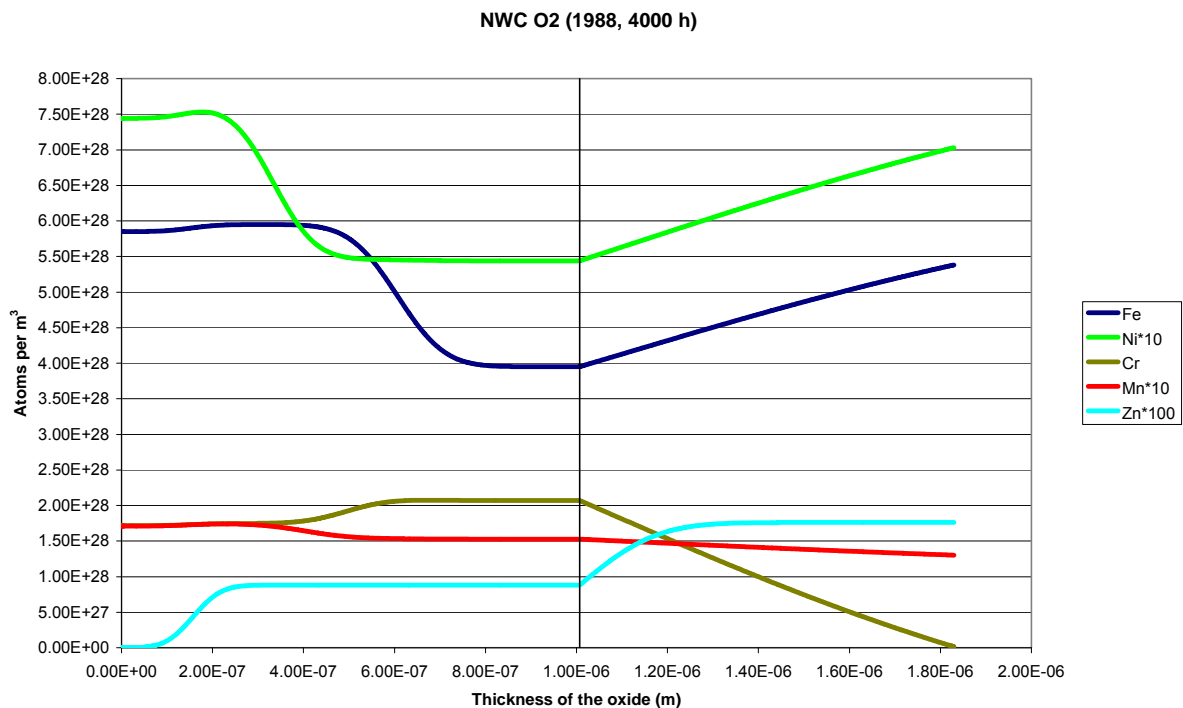


Figure 5: Concentration profile of the non-activated nuclides after 4000 h using NWC in O₂.

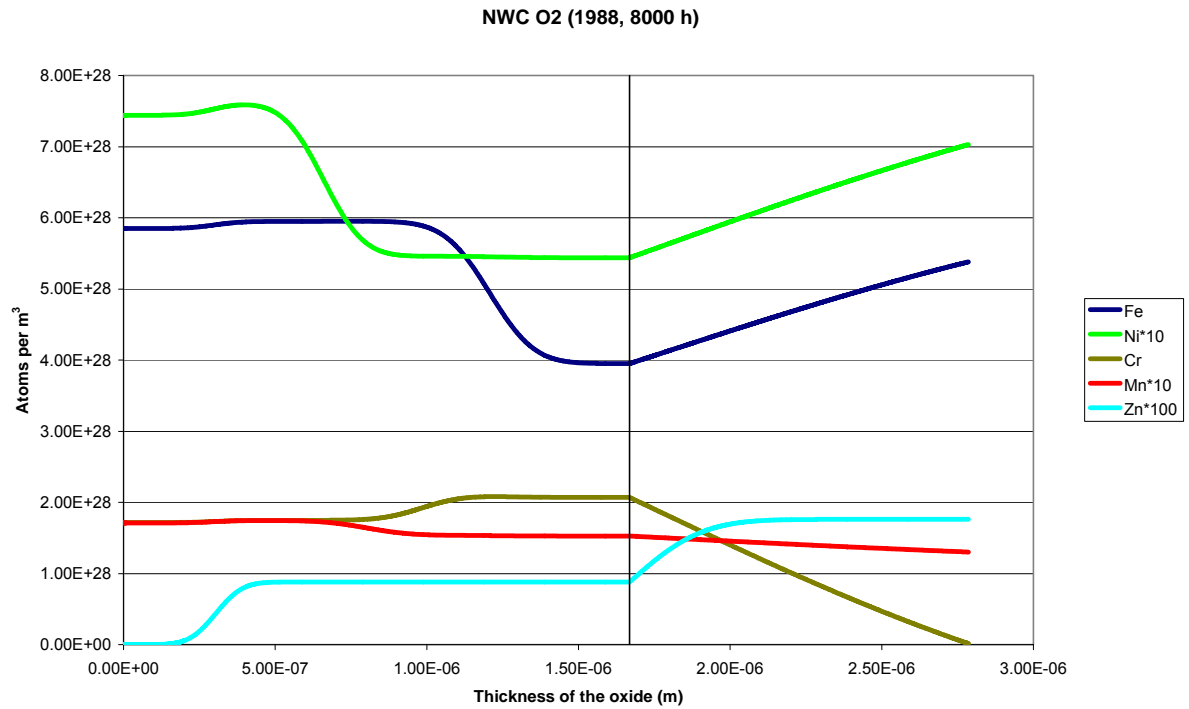


Figure 6: Concentration profile of the non-activated nuclides after 8000 h using NWC in O₂.

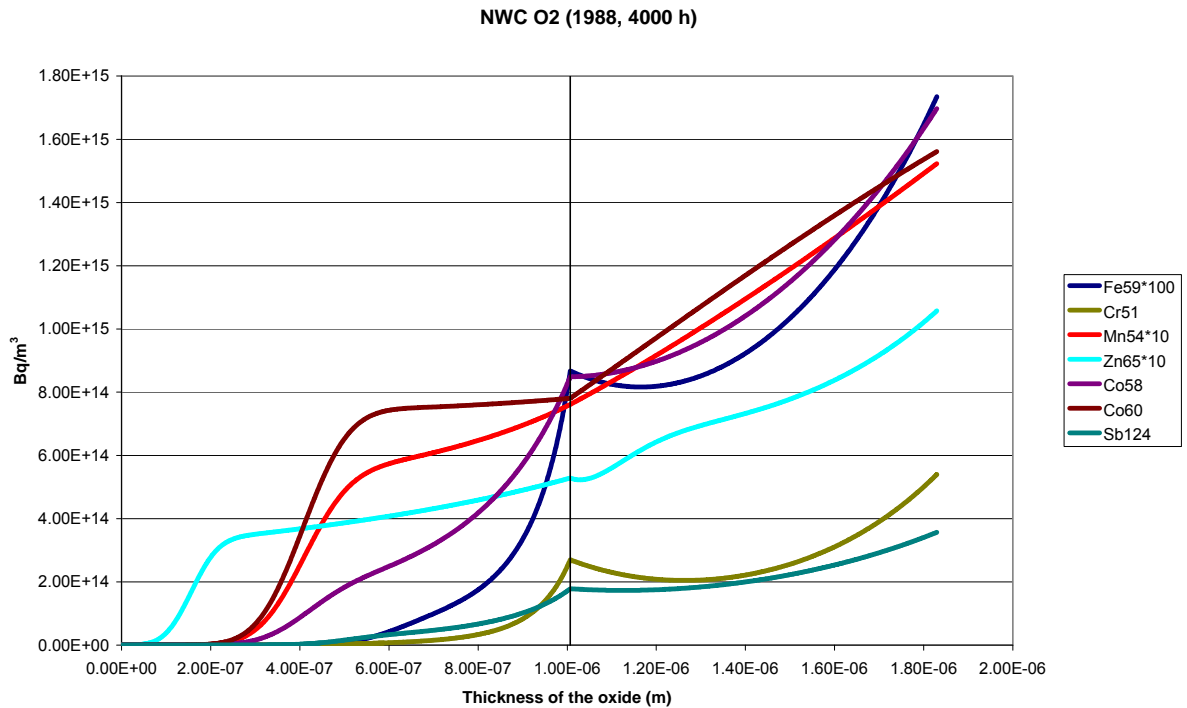


Figure 7: Activity profile of the activated nuclides after 4000 h using NWC in O₂.

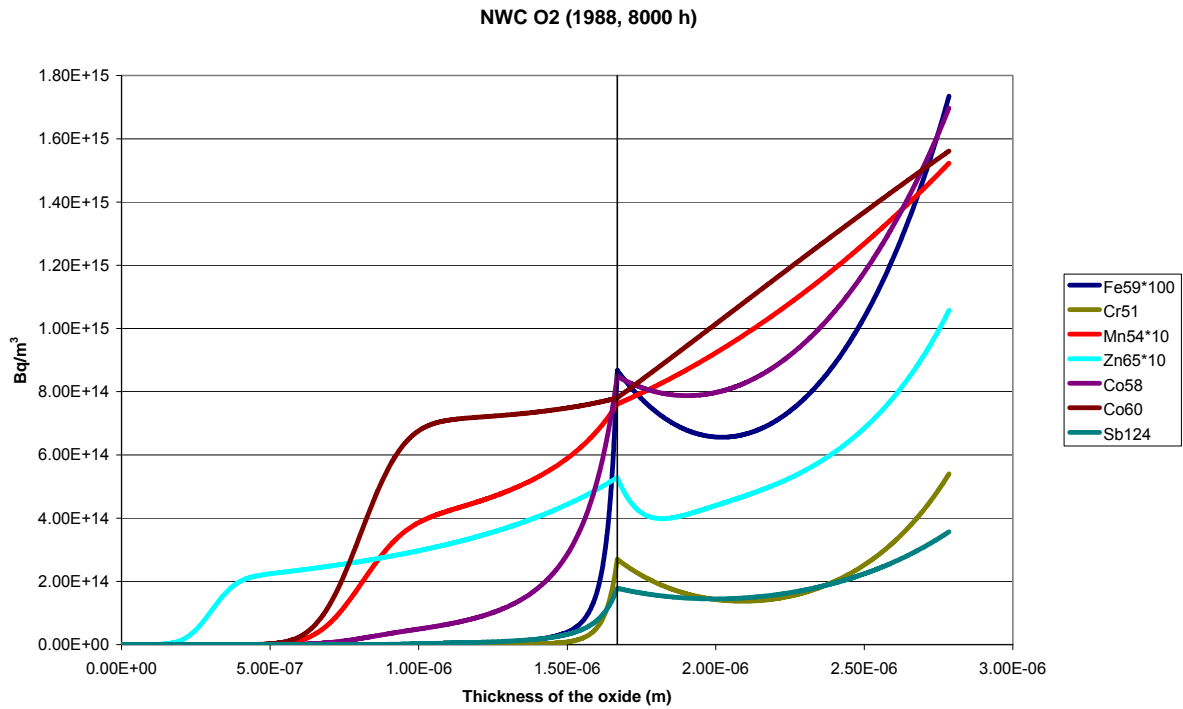


Figure 8: Activity profile of the activated nuclides after 8000 h using NWC in O2.

If the activity profiles are integrated over the oxide thickness these obtained activities can be compared with reference data /1/. The figures 9 – 15 compares the ratio between the activity in the oxide and the activity in the coolant with reference values. The reference values are obtained from O2 using values from the years 1978, 1988, 1990 and 1992.

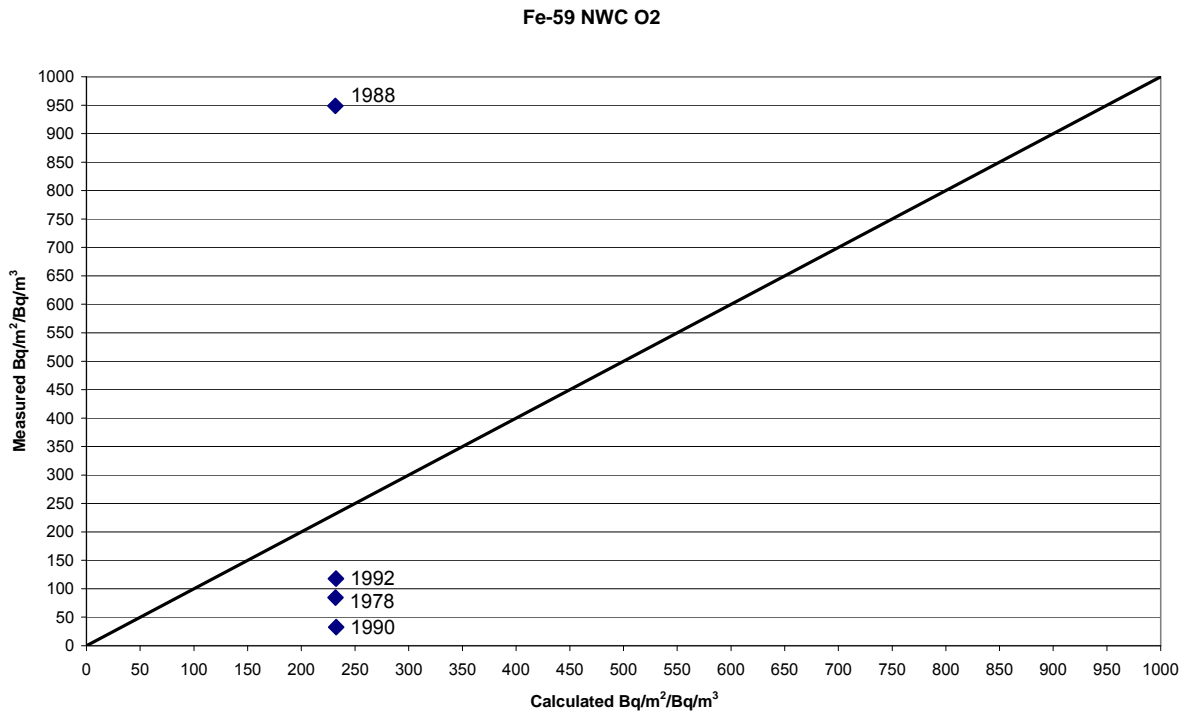


Figure 9: Measured verses calculated ratio between activity in the oxide and the activity in the coolant for Fe59.

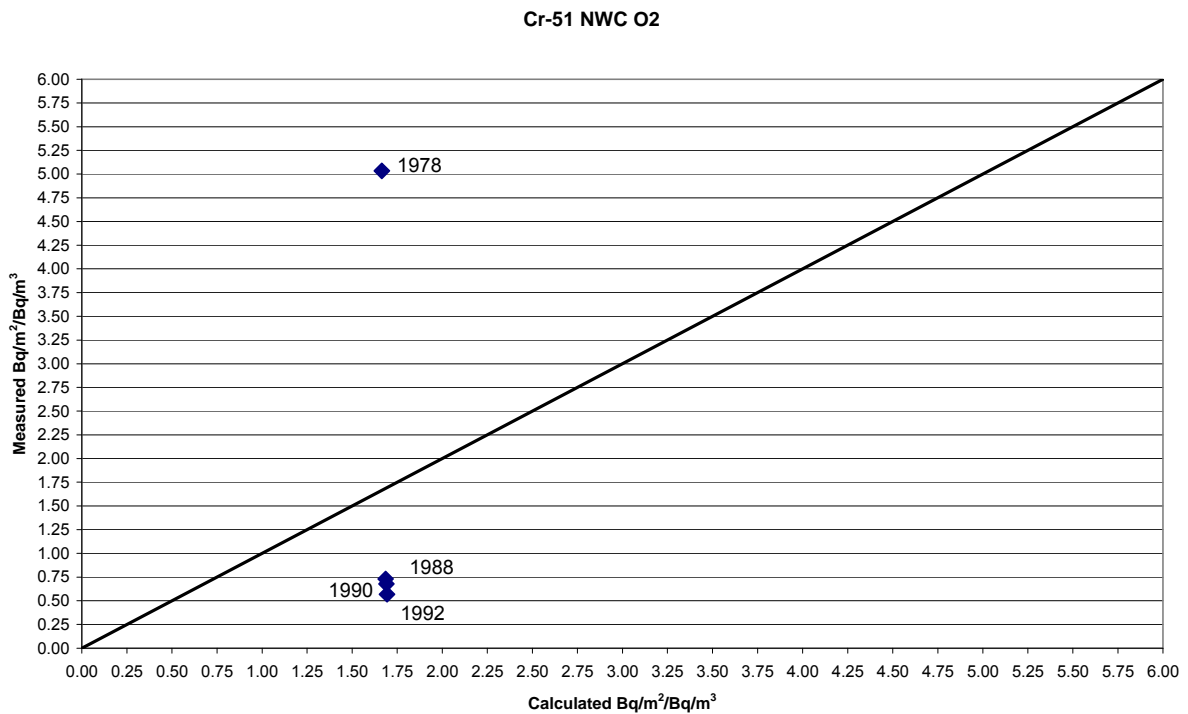


Figure 10: Measured verses calculated ratio between activity in the oxide and the activity in the coolant for Cr51.

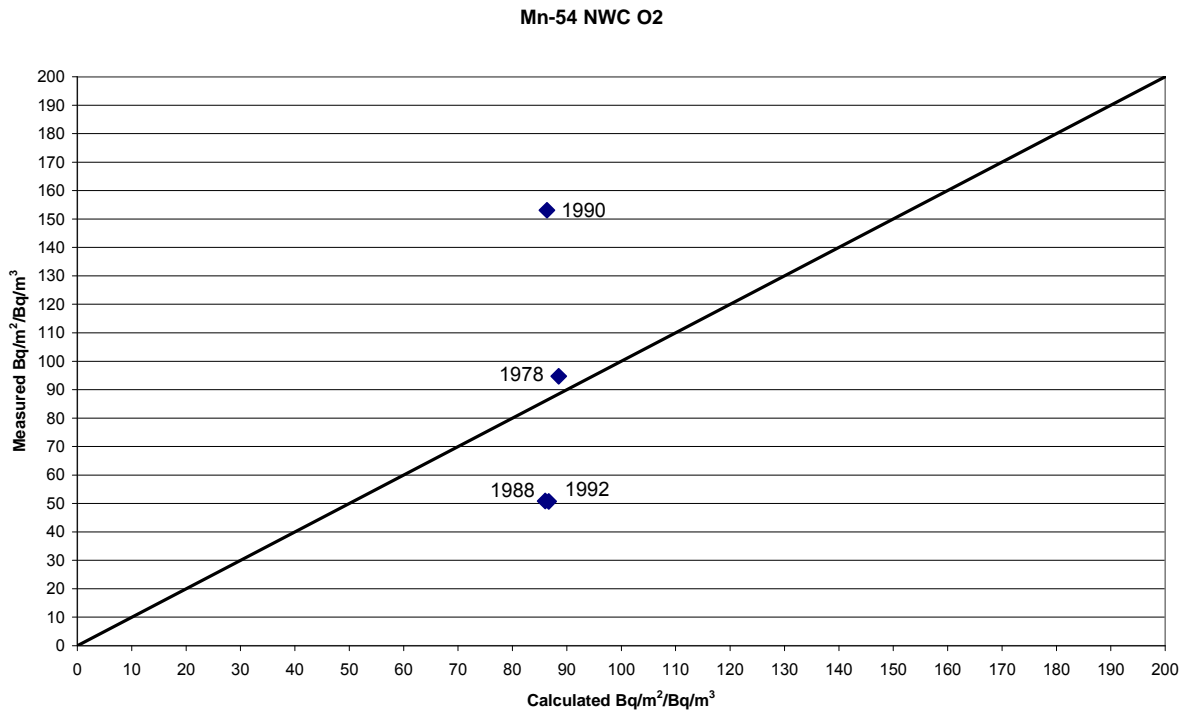


Figure 11: Measured verses calculated ratio between activity in the oxide and the activity in the coolant for Mn54.

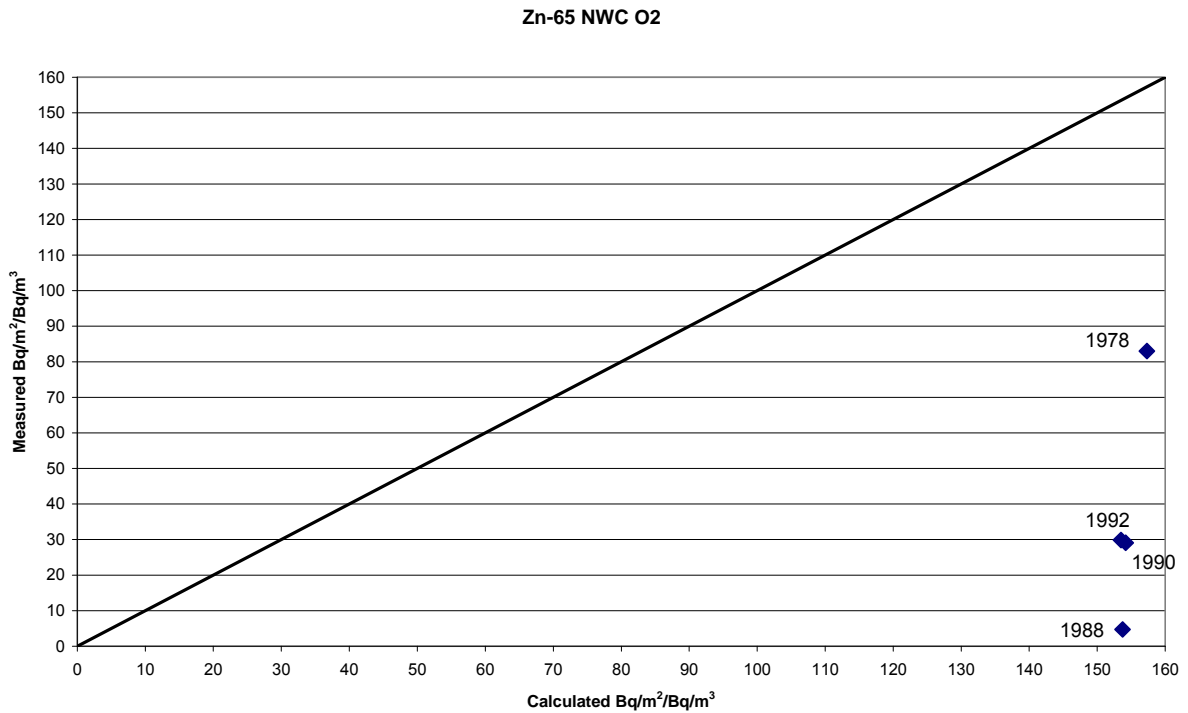


Figure 12: Measured verses calculated ratio between activity in the oxide and the activity in the coolant for Zn65.

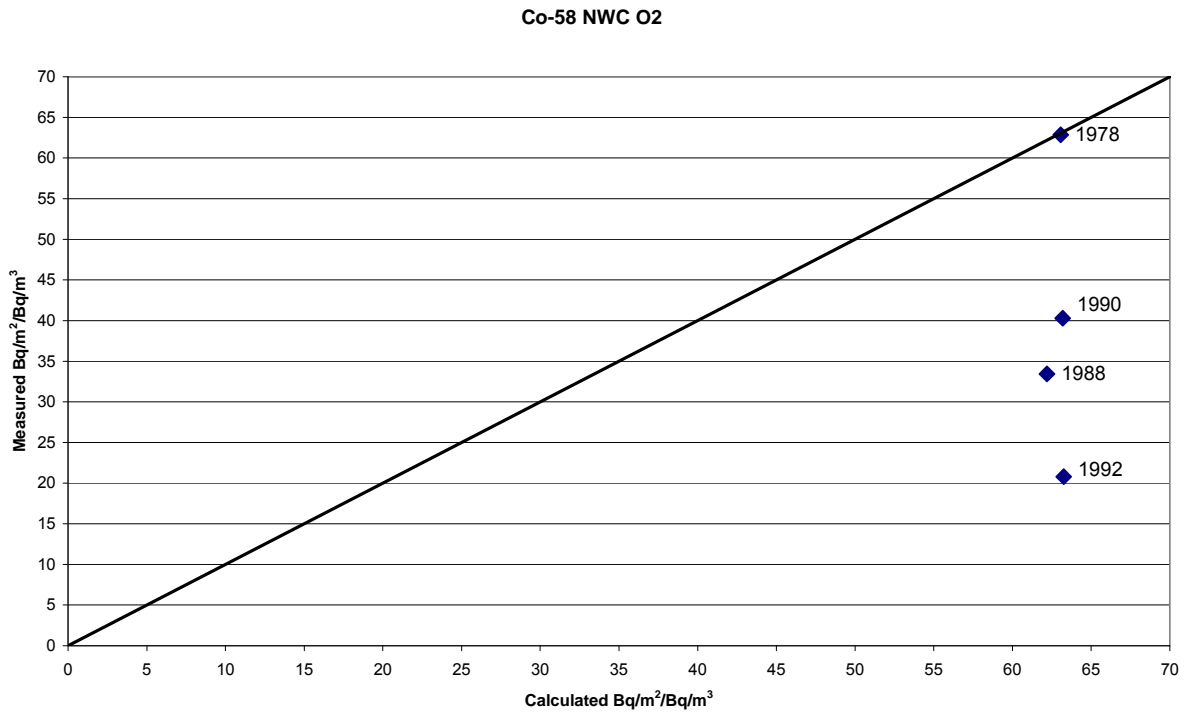


Figure 13: Measured verses calculated ratio between activity in the oxide and the activity in the coolant for Co58.

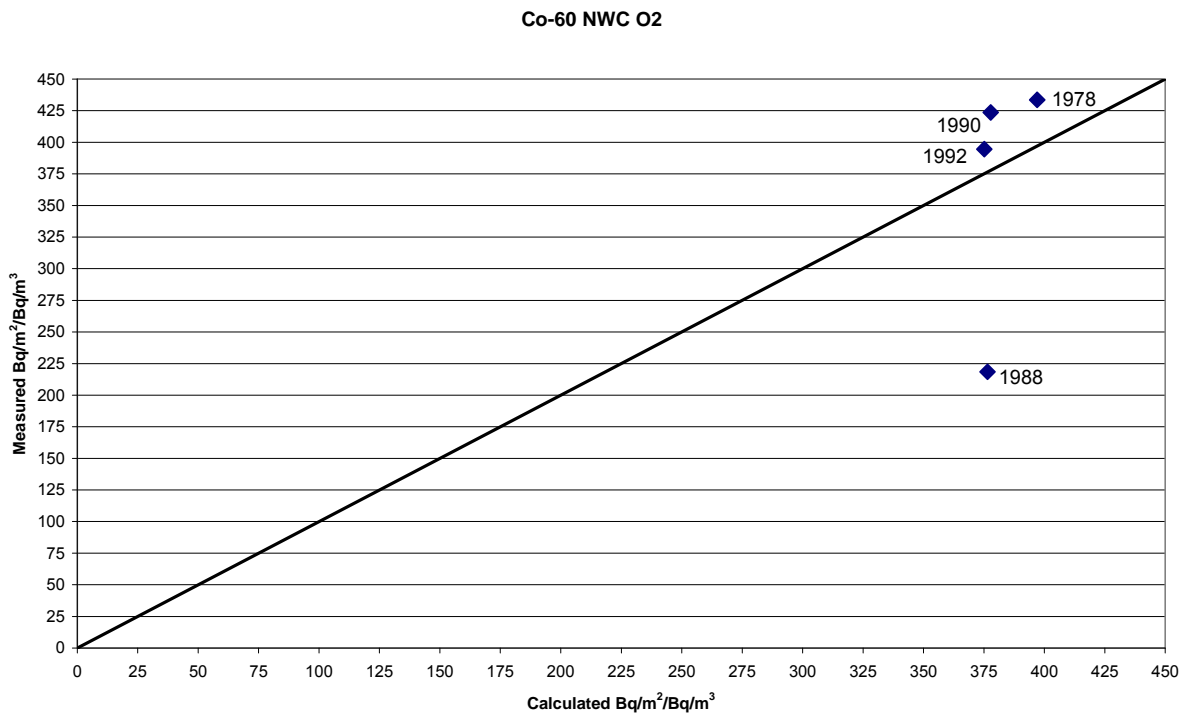


Figure 14: Measured verses calculated ratio between activity in the oxide and the activity in the coolant for Co60.

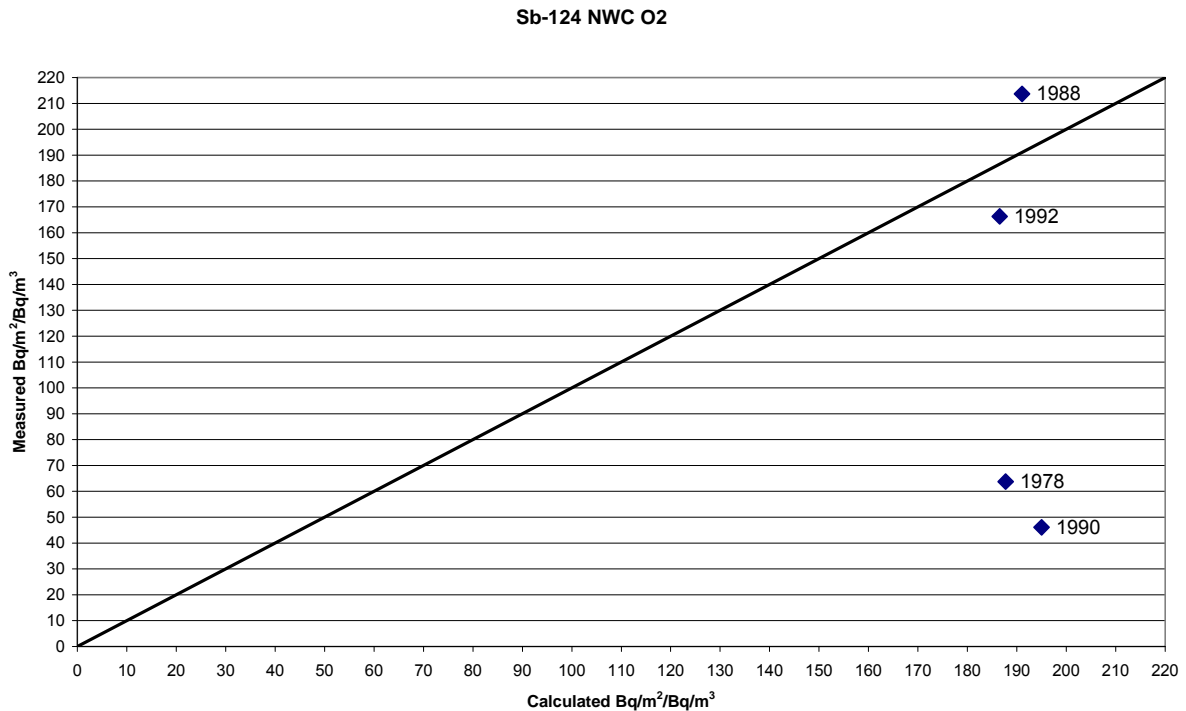


Figure 15: Measured versus calculated ratio between activity in the oxide and the activity in the coolant for Sb124.

As can be seen in the figures 9 – 15 the calculated activities are close to reference values. The calculated values of zinc, Co58 and Sb124 are, however, slightly too high compared to reference values. As also can be seen in the figures above the measured values tend to fluctuate much more than the calculated values.

Table 3: Oskarshamn 2 – Corrosion product reactor water chemistry data – Annual average data during reactor operation (NWC).

Year	C _w (t)			
	Fe [ppb]	Zn [ppb]	Ni [ppb]	Cr [ppb]
1978	2.30	0.40	0.20	0.60
1988	0.73	0.17	0.32	3.36
1990	0.74	0.15	0.50	2.66
1992	0.44	0.09	0.24	2.66

Table 4: Oskarshamn 2 – Corrosion product reactor water chemistry data – Annual average data during reactor operation (NWC)

Year	C _w (t)						
	Mn54 Bq/kg	Co58 Bq/kg	Co60 Bq/kg	Zn65 Bq/kg	Cr51 Bq/kg	Fe59 Bq/kg	Sb124 Bq/kg
1978	4.1E+02	6.7E+03	1.1E+03	3.2E+03	5.7E+04	3.0E+02	2.4E+02
1988	2.6E+03	2.8E+04	7.1E+03	9.4E+02	2.1E+05	6.1E+01	1.7E+03
1990	5.4E+02	3.9E+04	6.2E+03	1.3E+03	2.2E+05	3.5E+02	1.3E+03
1992	5.0E+02	3.1E+04	5.7E+03	1.0E+03	1.7E+05	1.3E+02	2.8E+02

4.1.2 HWC

The optimized enrichment factors for HWC are shown in table 5.

Table 5: Optimized enrichment factors for HWC.

Nuclide	Fe	Zn	Ni	Cr	Mn	Co58	Co60	Sb
Enrichment factor (-)	1.05E+08	7.50E+07	2.53E+08	2.27E+08	1.40E+07	1.31E+08	3.76E+08	5.53E+07

As can be seen in the table above the enrichment factor for Cr increase by a factor of 130 compared to its corresponding NWC value, when using HWC injection. The enrichment factors for the nuclides Fe, Mn and Sb decreases slightly compared to NWC. In case of Ni, Co58 and Co60 there is a small increase of the enrichment factors compared to NWC. The calculated enrichment factors in table 5 are somewhat high compared to the enrichment factors obtained by Lundgren [1]. However, there is nevertheless a strong correlation between the calculated enrichment factors in table 5 and the enrichment factors obtained by Lundgren.

The figures 16 – 17 shows the concentration profiles for the non-activated nuclides in the two oxide layers on the steel AISI 304 after 4000 respective 8000 h. Water concentrations of activated and non-activated nuclides are given in tables 6 – 7. The water concentration of Mn is set to 0.01% of the concentration of Mn54.

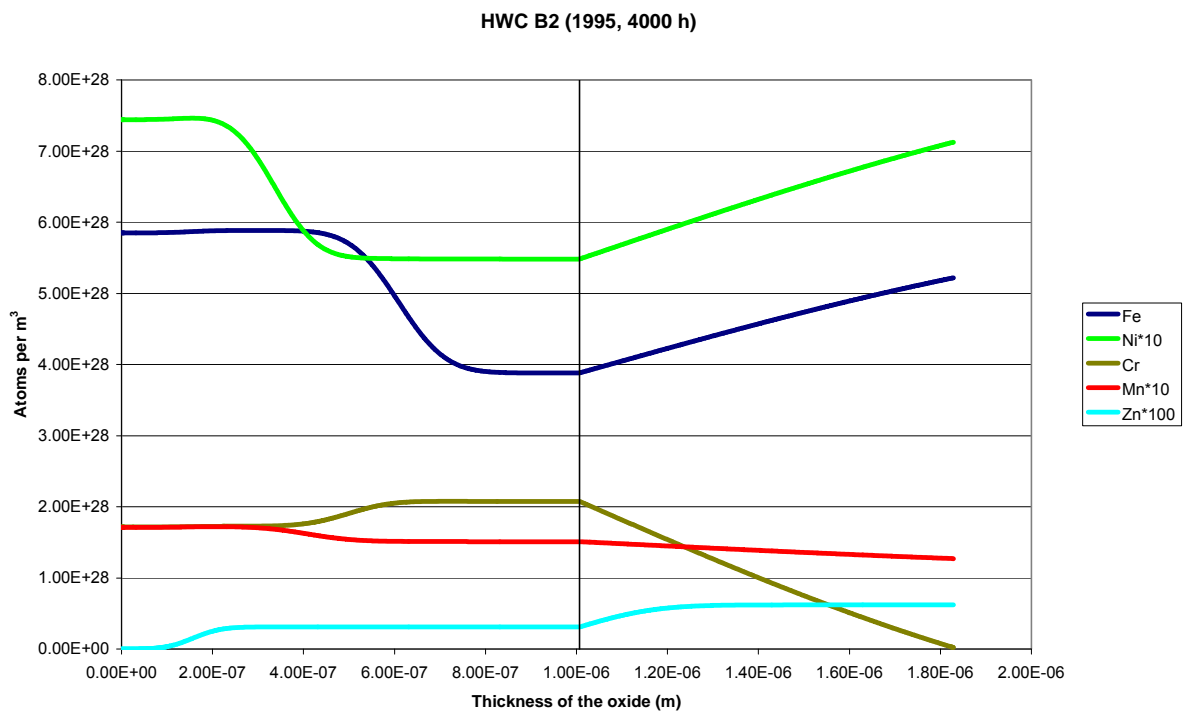


Figure 16: Concentration profile of the non-activated nuclides after 4000 h using HWC in B2.

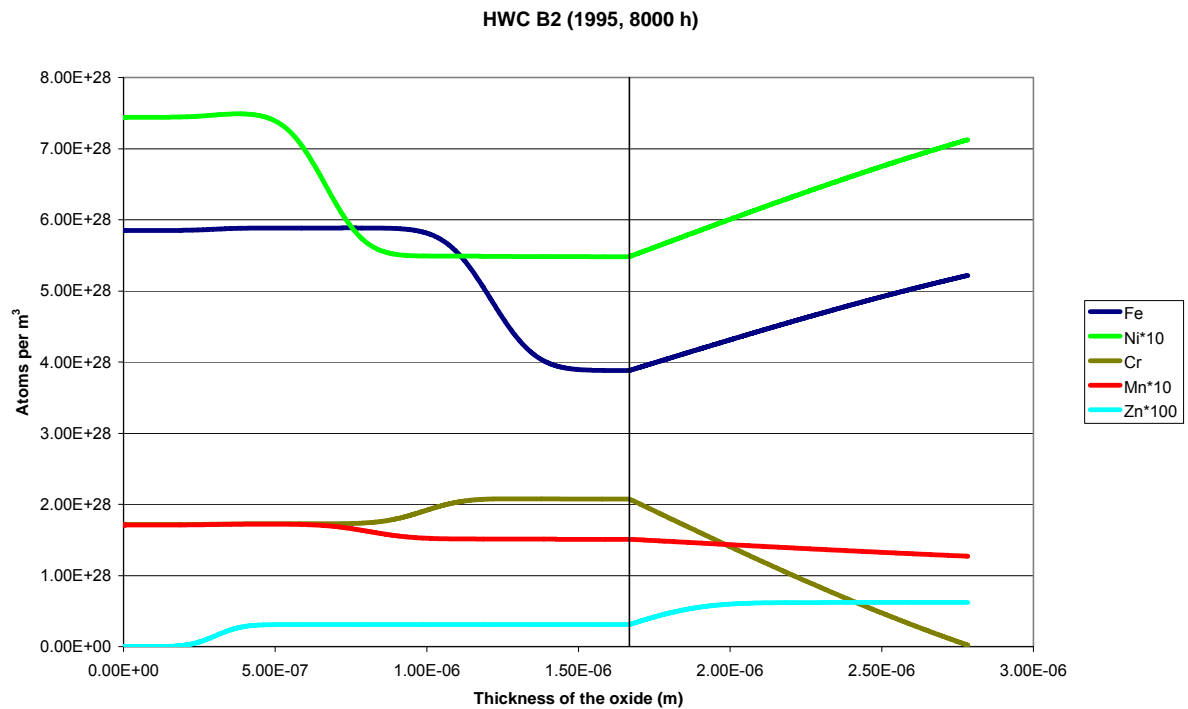


Figure 17: Concentration profile of the non-activated nuclides after 8000 h using HWC in B2.

As can be seen in figures 16 – 17 the concentration profiles look very much the same after 4000 h and 8000 h. However, the oxide is still growing. Since the zinc concentration is very low the concentration profiles are hardly affected. The concentration profiles are very similar to the NWC profiles explained above.

The figures 18 – 19 show the activity profiles for the activated nuclides in the two oxide layers on the steel AISI 304 after 4000 respective 8000 h.

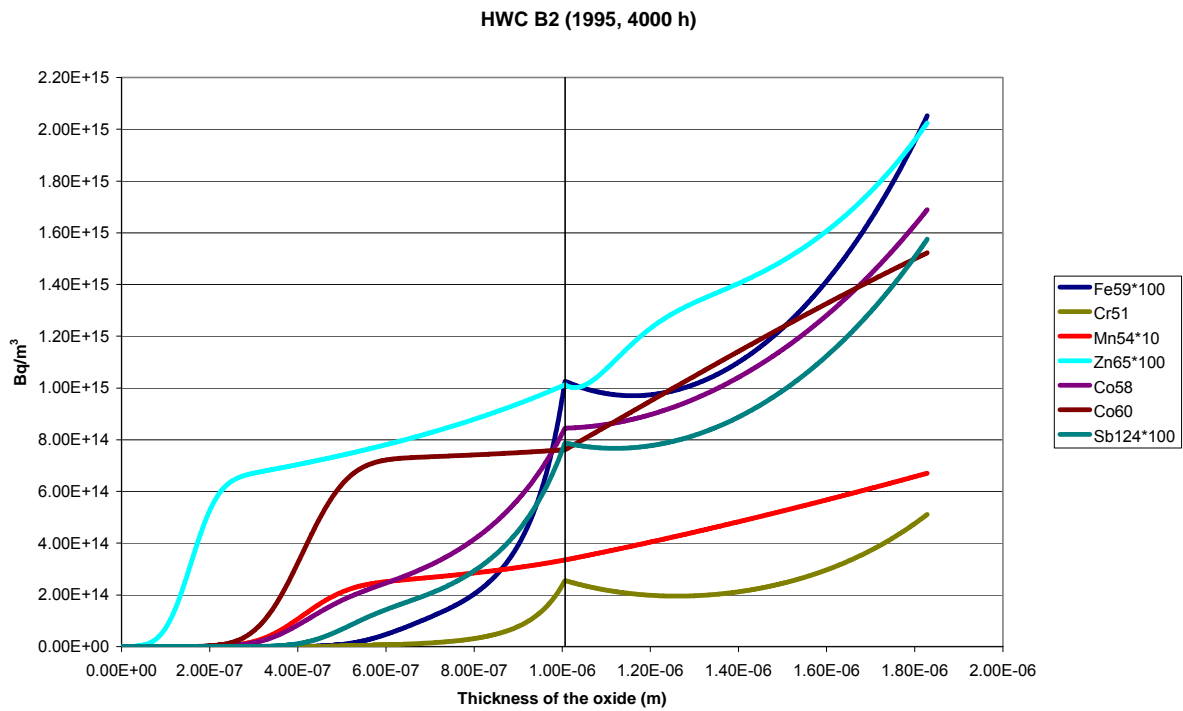


Figure 18: Activity profile of the activated nuclides after 4000 h using HWC in B2.

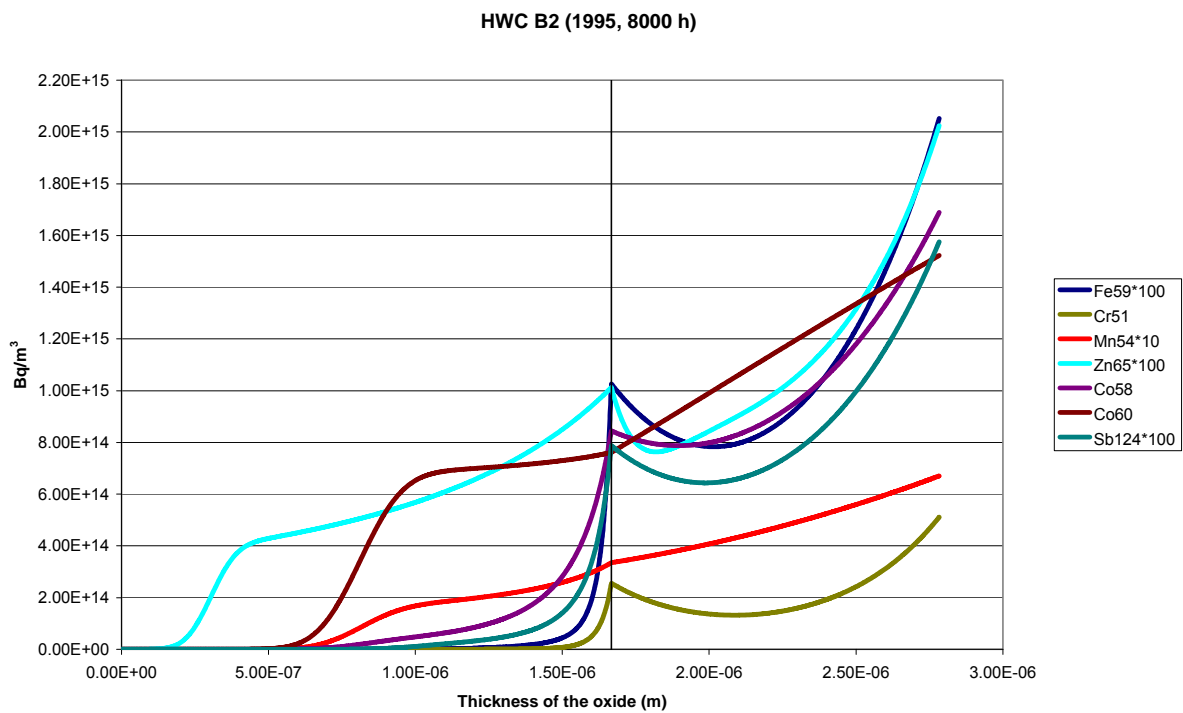


Figure 19: Activity profile of the activated nuclides after 8000 h using HWC in B2.

As can be seen in the figures 18 – 19 the largest part of the activity comes from Co60, as in the case of NWC. The second largest contribution of activity comes from Co58. As also can be seen in the figures above is that the activation profile for Cr51 looks

very much the same as in the case of NWC for O₂ in the year 1988, see figures 7 – 8, despite of the fact that the enrichment factor is increased by a factor of 130 when using hydrogen injection. The reason for the similarities between the activation profiles is that the concentration of Cr₅₁ in the coolant is about 130 times larger in the year 1988 compared to 1995. The figures 20 – 23 shows the concentration and activity profiles for the non-activated nuclides in the two oxide layers on the steel AISI 304 after 4000 respective 8000 h.

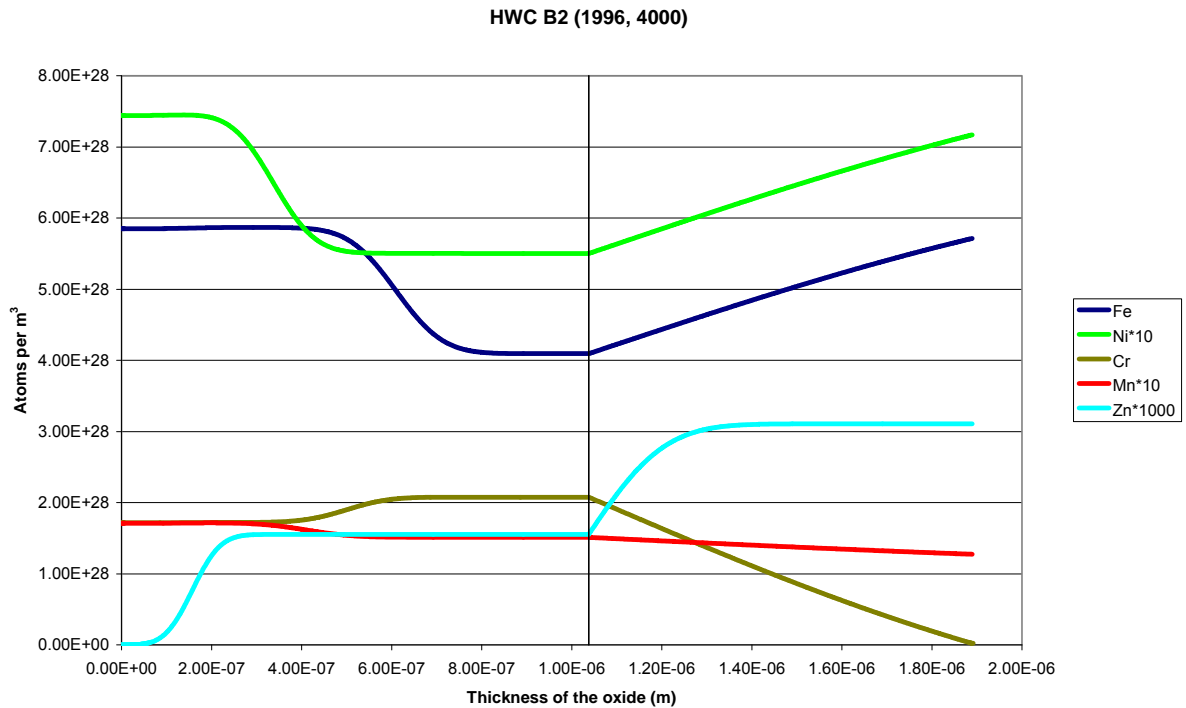


Figure 20: Concentration profile of the non-activated nuclides after 4000 h using HWC in B2.

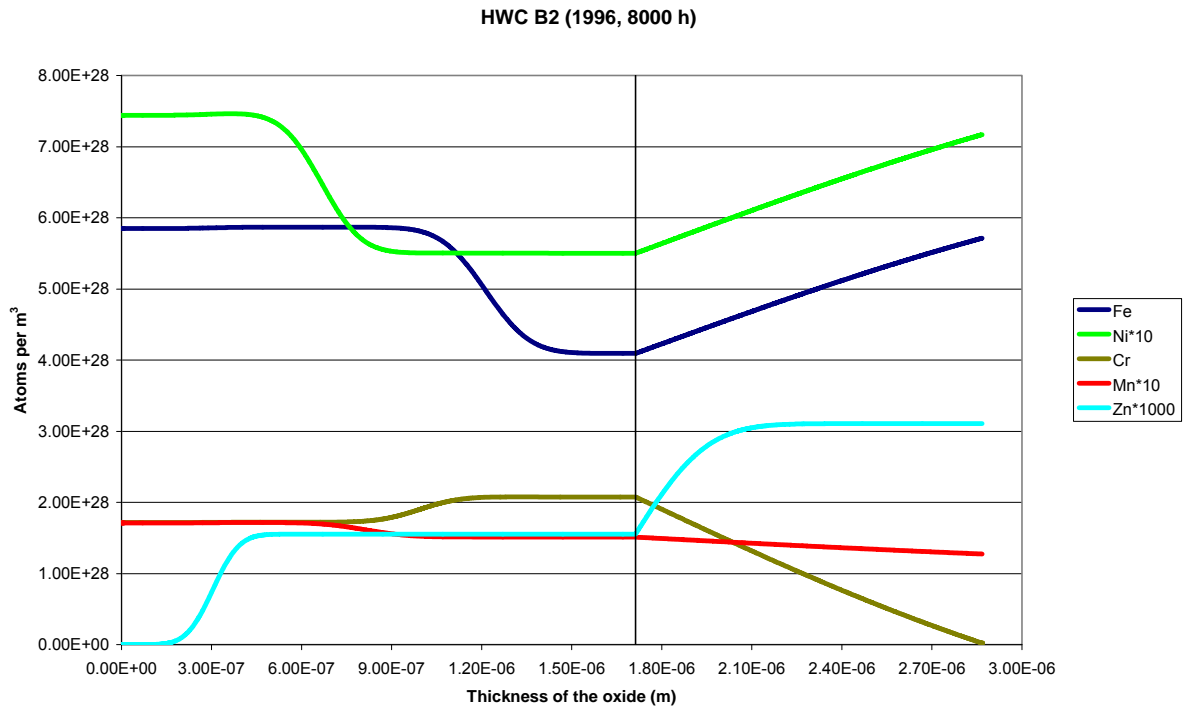


Figure 21: Concentration profile of the non-activated nuclides after 8000 h using HWC in B2.

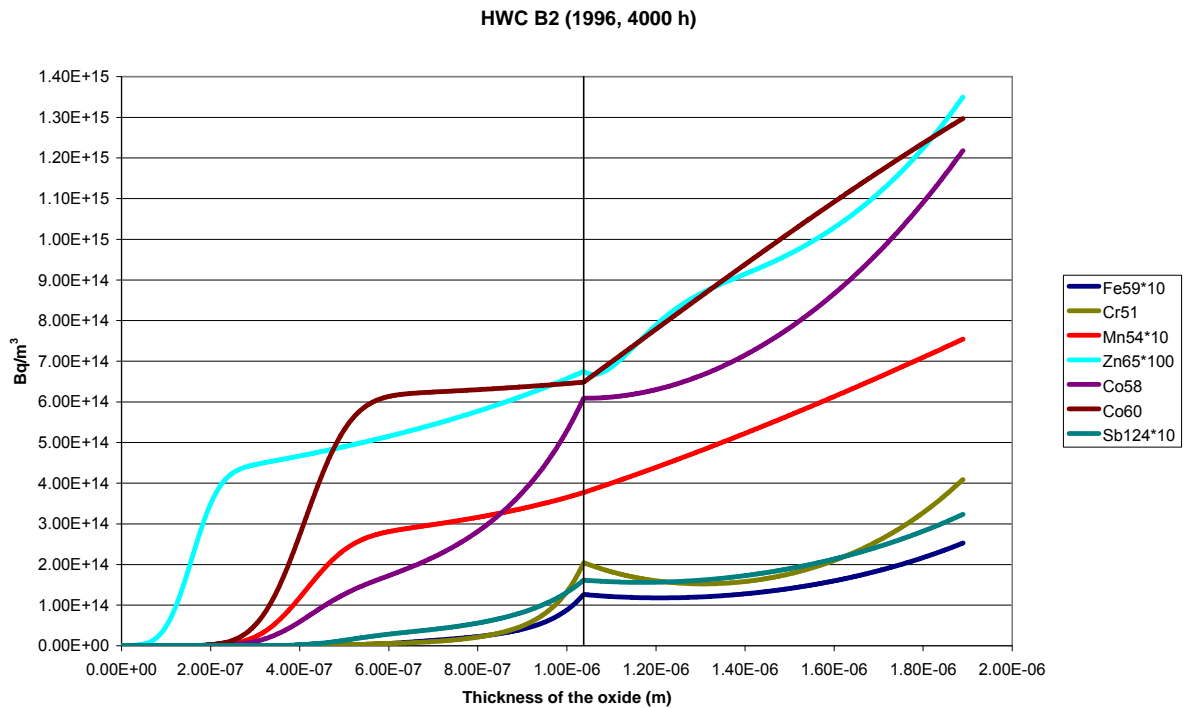


Figure 22: Activity profile of the activated nuclides after 4000 h using HWC in B2.

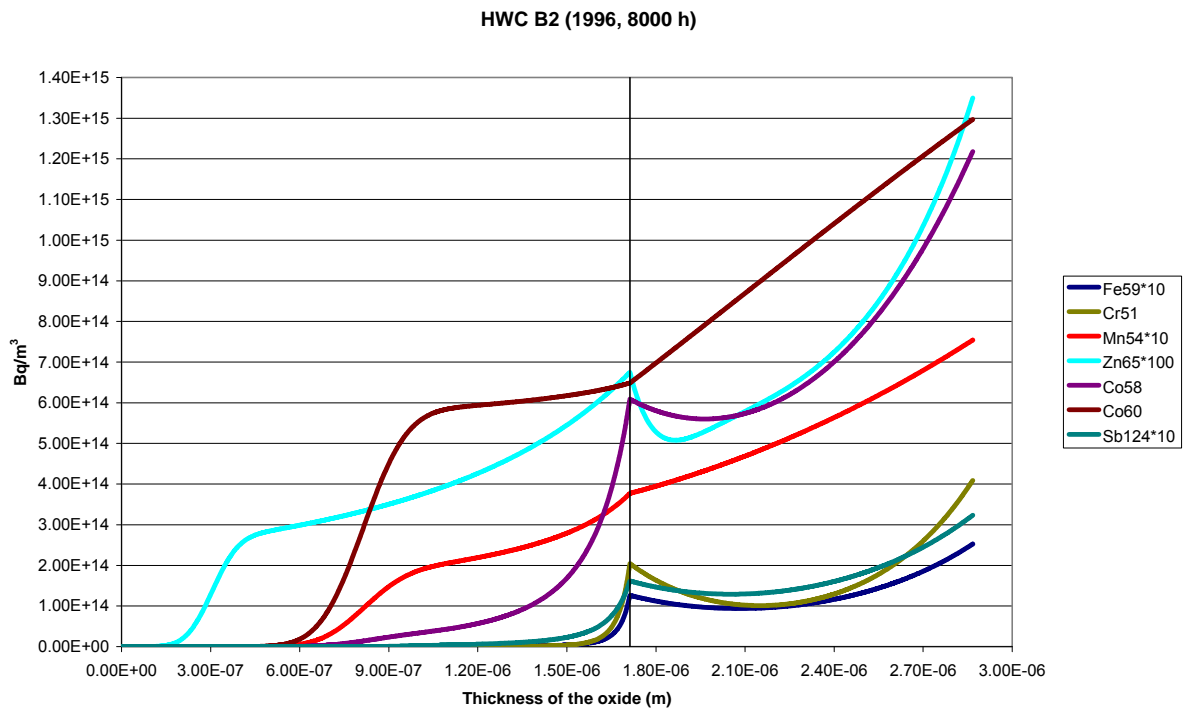


Figure 23: Activity profile of the activated nuclides after 8000 h using HWC in B2.

The concentration profiles in the figures 20 – 21 look very much the same for Ni, Cr and Mn ions as the corresponding profiles in the previous year, as can be seen in the figures 16 – 17. In case of zinc, the concentration is decreased by a factor of two and in case of Fe the concentration is increased by a factor of six. The oxide becomes therefore somewhat thicker compared to the previous year. In case of the activity profiles there are only small changes compared to previous year which again are due to small changes of the concentration in the coolant.

The figures 24 – 30 compares the ratio between the activity in the oxide and the activity in the coolant with reference values. The reference values are obtained from B2 using values from the years 1993, 1995, 1996 and 1997.

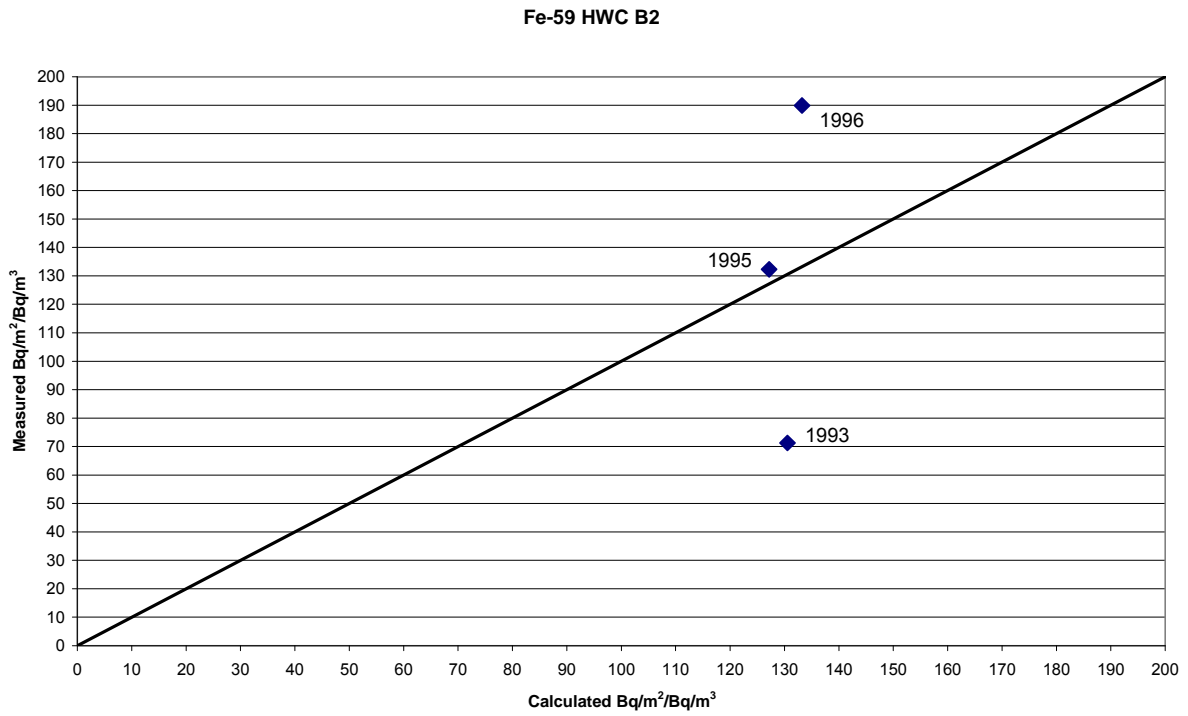


Figure 24: Measured versus calculated ratio between activity in the oxide and the activity in the coolant for Fe59.

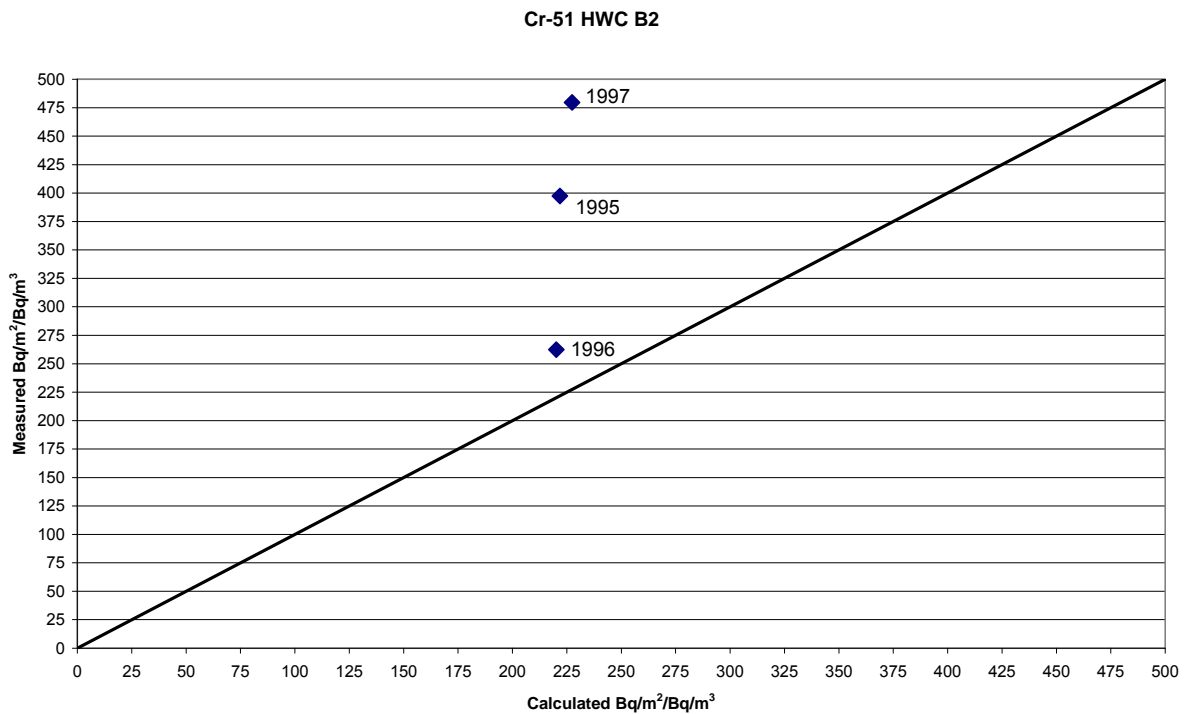


Figure 25: Measured versus calculated ratio between activity in the oxide and the activity in the coolant for Cr51.

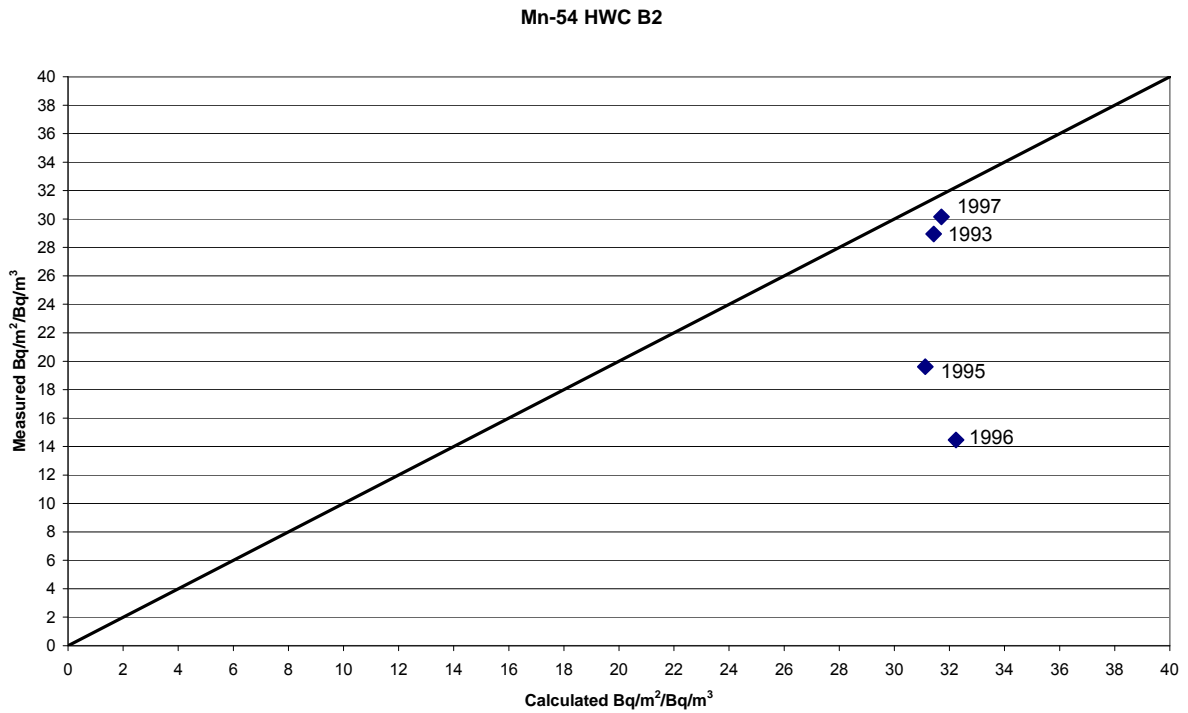


Figure 26: Measured versus calculated ratio between activity in the oxide and the activity in the coolant for Mn54.

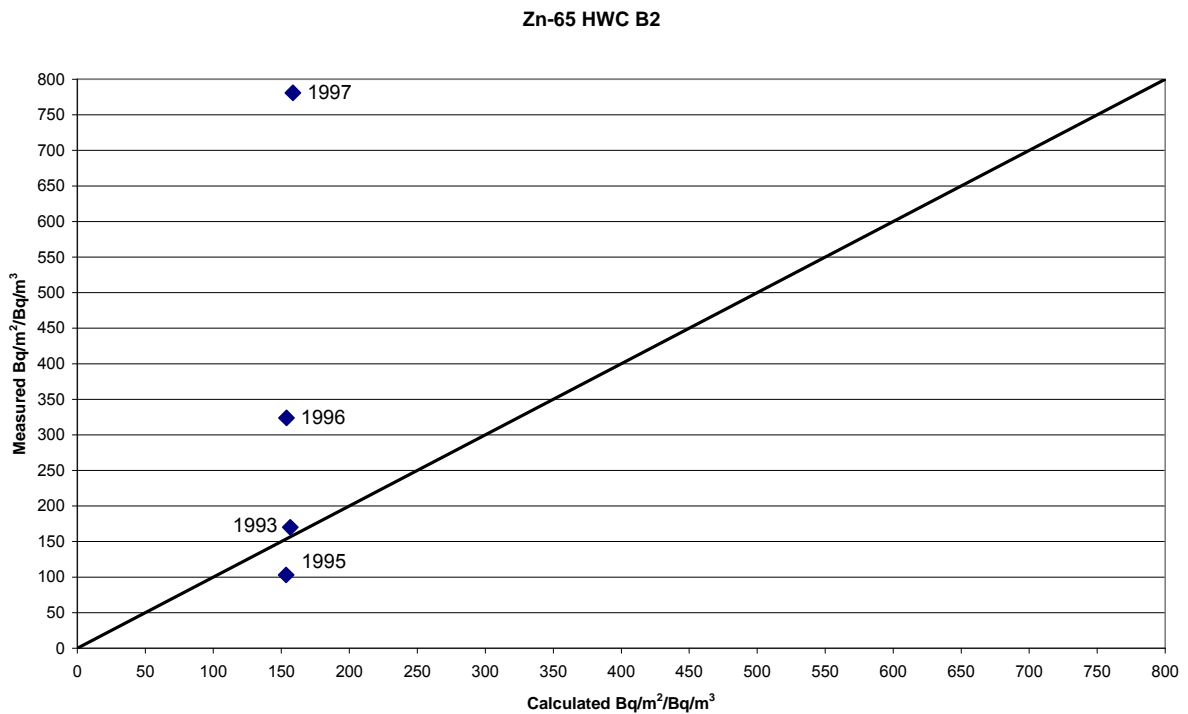


Figure 27: Measured versus calculated ratio between activity in the oxide and the activity in the coolant for Zn65.

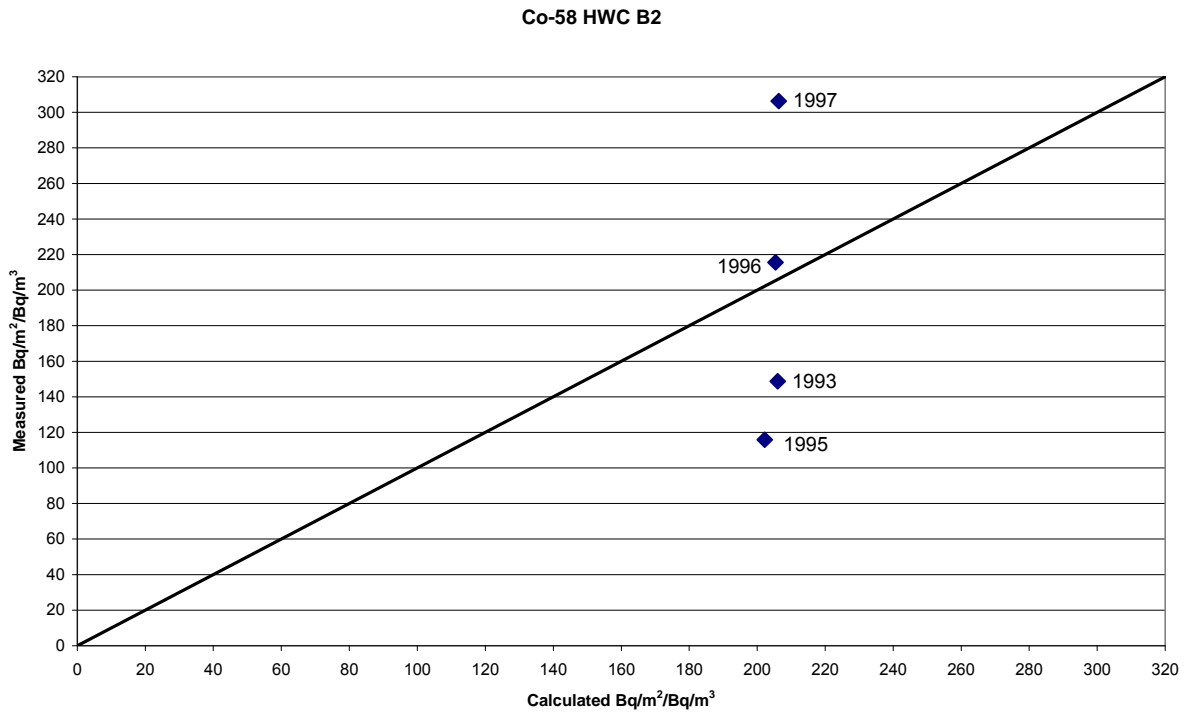


Figure 28: Measured versus calculated ratio between activity in the oxide and the activity in the coolant for Co58.

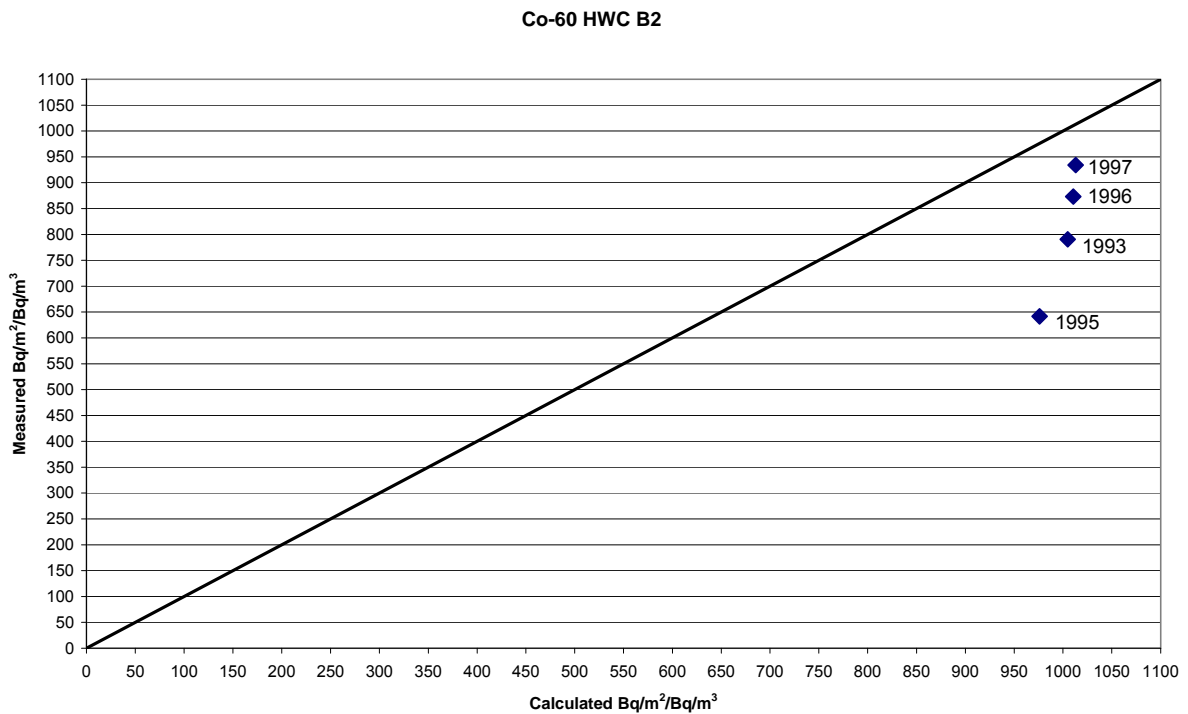


Figure 29: Measured versus calculated ratio between activity in the oxide and the activity in the coolant for Co60.

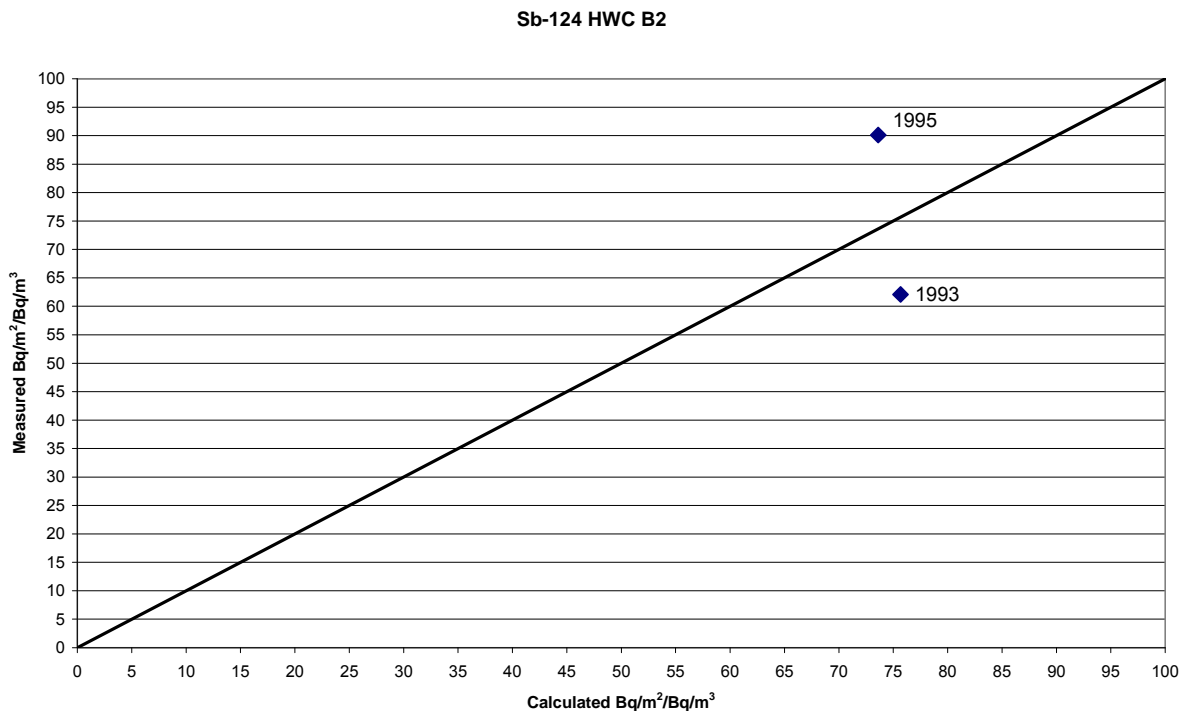


Figure 30: Measured versus calculated ratio between activity in the oxide and the activity in the coolant for Sb124.

As can be seen in the figures 24 – 30 the calculated activities are close to reference values. But as in the case of NWC the measured HWC values tend to fluctuate much more than the calculated values. The calculated values for Cr51 are somewhat underestimated and the calculated value for Co60 and Mn54 are somewhat overestimated. The reason for this is that the enrichment factors are optimized assuming that the ratio between the activity in the oxide and the activity in the coolant is a linear function of the enrichment factor. This is, however, a simplification since the ratio is also dependent of the coolant concentration of the non-activated ions especially the zinc concentration. This is because the coolant concentration of the non-activated ions affects the rate of which the oxide growth. In case of activated ions the concentration is too low to affect the oxide growth in any significant extent. In case of Cr51 the ratio between the activity in the oxide and the activity in the coolant is a factor of hundred greater in the case of hydrogen injection.

Table 6: Barsebäck 2 – Corrosion product reactor water chemistry data – Annual average data during reactor operation (HWC)

Year	$C_w(t)$			
	Fe [ppb]	Zn [ppb]	Ni [ppb]	Cr [ppb]
1993	2.20	0.07	0.16	0.20
1995	0.50	0.06	0.14	0.06
1996	2.99	0.03	0.15	0.06
1997	3.29	0.13	0.16	0.06

Table 7: Barsebäck 2 – Corrosion product reactor water chemistry data – Annual average data during reactor operation (HWC)

Year	C _w (t)						
	Mn54 Bq/kg	Co58 Bq/kg	Co60 Bq/kg	Zn65 Bq/kg	Cr51 Bq/kg	Fe59 Bq/kg	Sb124 Bq/kg
1993	3.1E+03	1.0E+04	2.9E+03	3.3E+02	4.1E+03	2.6E+02	3.1E+02
1995	3.2E+03	8.6E+03	2.7E+03	1.8E+02	1.5E+03	1.3E+02	1.9E+02
1996	3.6E+03	6.2E+03	2.3E+03	1.2E+02	1.2E+03	1.6E+02	3.9E+02
1997	3.4E+03	5.8E+03	2.0E+03	9.6E+01	1.6E+03	1.2E+02	2.1E+02

4.1.2.1 Nuclides with short half lives

In some plants (O1, B2, R1, O2) the residual heat removal system has been equipped with on-line gamma monitoring (On-Line Activity - OLA) which makes it possible to detect some short-lived activated corrosion products. In R1, OLA has been operational since 1996. The hydrogen injection started in 1984, with a short interruption 1992-1993.

Half lives and decay constants for nuclides with short half lives are presented in table 8 and their optimized enrichment factors are shown in table 9.

Table 8: Half lives and decay constants for activated nuclides.

Nuclide	Mn56	Sb122
Half lives	2.58 h	2.7 d
Decay constant (s ⁻¹)	7.46E-05	2.97E-06

Table 9: Optimized enrichment factors for nuclides with short half lives..

Nuclide	Mn56	Sb122
Enrichment Factor (-)	5.00E+07	1.49E+08

As can be seen in tables 5 and 9 the enrichment factors for nuclides with short half lives are larger than corresponding enrichment factors for nuclides with longer half lives. This correlation is also found in the work of Lundgren /1/. Figure 31 shows the concentration profiles for the non-activated nuclides in the two oxide layers on steel AISI 304 after 700 h. Water concentrations of activated and non-activated nuclides are given in tables 10 – 11. The water concentration of Mn is set to 0.01% of the concentration of Mn54.

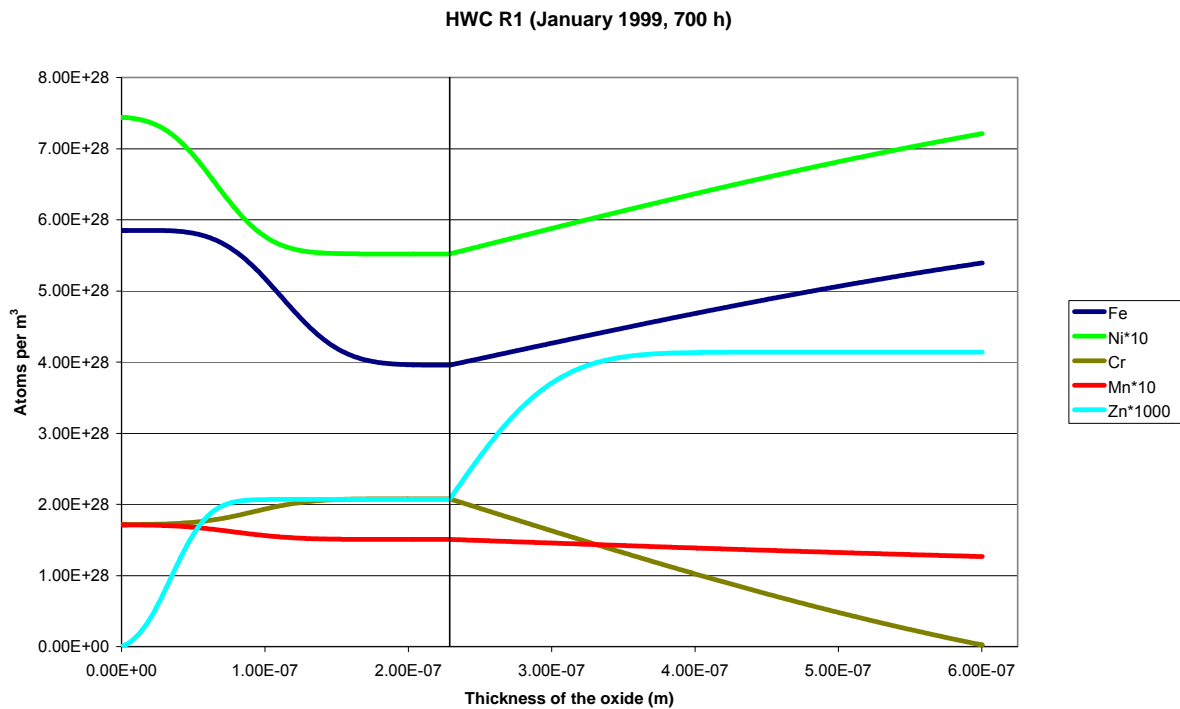


Figure 31: Concentration profile of the non-activated nuclides after 700 h using HWC in R1.

As can be seen in the figure above the concentration profiles look very much the same for 700 h as for 4000 h or 8000 h. As also can be seen in the figure above the inner oxide layer is thinner than the outer oxide layer after 700 h. However, for larger time scales the inner oxide layer becomes thicker than the outer oxide layer. This is due to the particle flux becomes greater in the outer boundary of the inner oxide layer compared to the outer boundary of the outer oxide layer for larger time scales.

Figure 32 shows the activity profiles for two activated nuclides with short half-lives in the two oxide layers on the steel AISI 304 after 700 h. The nuclides with long half-lives are excluded from the figure.

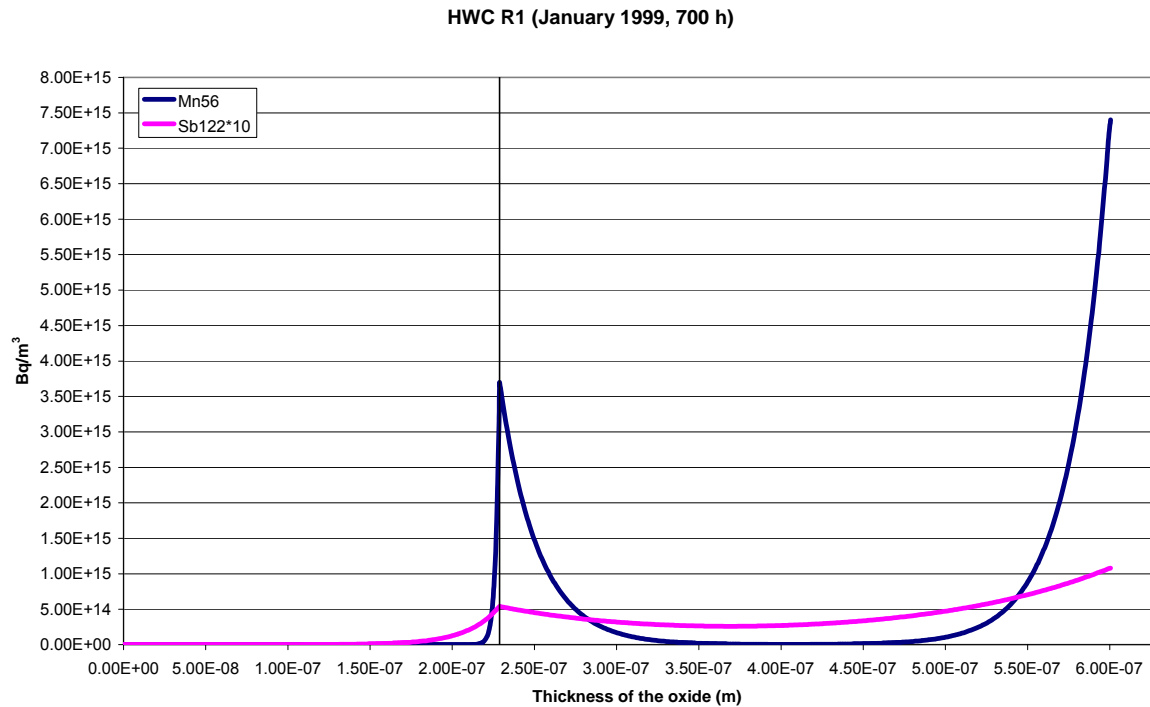


Figure 32: Activity profile of the activated nuclides after 700 h using HWC in R1.

As can be seen in figure 32 the largest part of the activity comes from Mn56. This is due to the larger enrichment factor of Mn56 compared to Sb122. Mn56 and Sb122 have approximately the same diffusion coefficients in the inner layer. Mn56 only penetrates the inner oxide layer on the surface. This is due to a short half life and small diffusion coefficient compared to the diffusion coefficient in the outer oxide layer. In the outer oxide layer the diffusion coefficients are much greater compared to the inner layer and the nuclides therefore penetrates the oxide further.

The figures 33 – 34 compares the ratio between the activity in the oxide and the activity in the coolant with reference values. The reference values are obtained from R1 using values from June 1998, January 1999, December 2001 and September 2002.

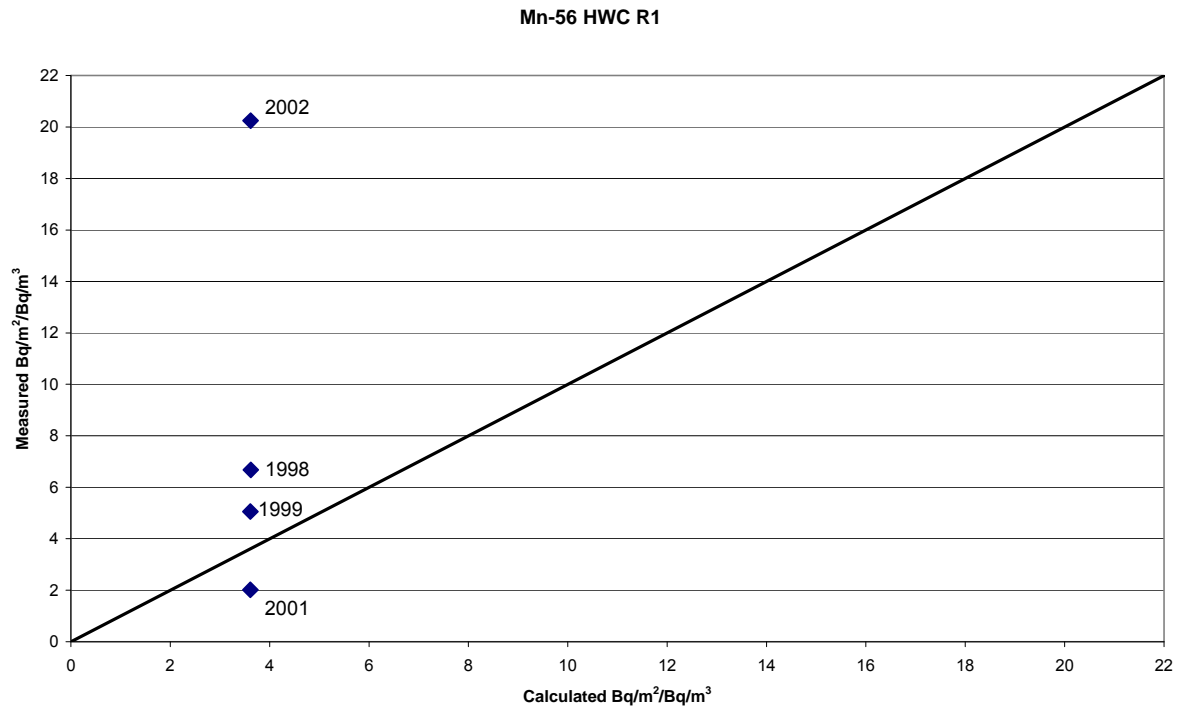


Figure 33: Measured versus calculated ratio between activity in the oxide and the activity in the coolant for Mn56.

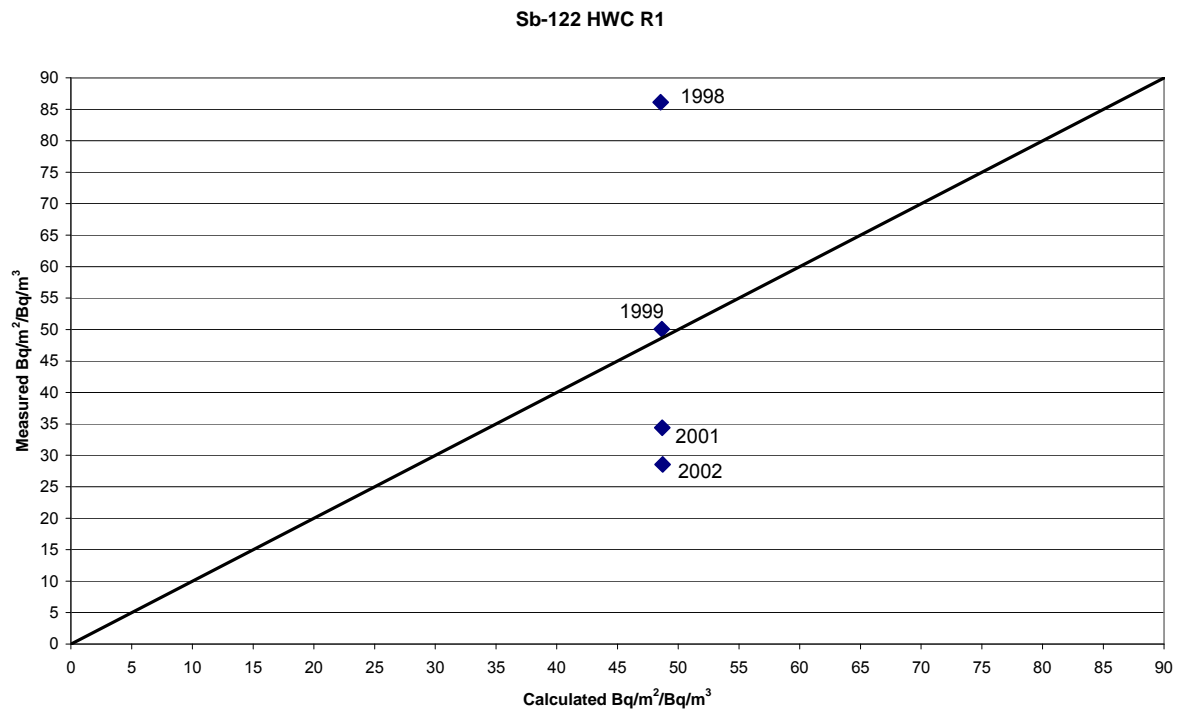


Figure 34: Measured versus calculated ratio between activity in the oxide and the activity in the coolant for Sb122.

As can be seen in the figures 33 – 34 the calculated activities are close to reference values. But as in the case of NWC the measured values tend to fluctuate much more than the calculated values.

Table 10: Ringhals 1 – Corrosion product reactor water chemistry data – Annual average data during reactor operation (HWC)

Year	$C_w(t)$			
	Fe [ppb]	Zn [ppb]	Ni [ppb]	Cr [ppb]
1998	1.56	0.01	0.19	0.09
1999	1.38	0.04	0.16	
2001	0.96	0.01	0.12	0.07
2002	1.83	0.01	0.10	0.07

Table 11: Ringhals 1 – Corrosion product reactor water chemistry data – Monthly average data during reactor operation (HWC). Nuclides with long half-lives are excluded from the table.

Year	$C_w(t)$	
	Mn56 Bq/kg	Sb 122 Bq/kg
June 1998	9.6E+04	4.5E+02
January 1999	9.9E+04	4.8E+02
December 2001	1.6E+05	6.3E+02
September 2002	2.4E+04	1.1E+03

4.1.3 DZO+HWC

The figures 35 – 36 shows the concentration profiles for the non-activated nuclides in the two oxide layers on the steel AISI 304 after 4000 respective 8000 h, at the condition prevailing in the B2 plant during 2000. The enrichment factors used for DZO+HWC are same as in HWC, see table 5. Water concentrations of activated and non-activated nuclides are given in tables 12 – 13. The water concentration of Mn is set to 0.01% of the concentration of Mn54.

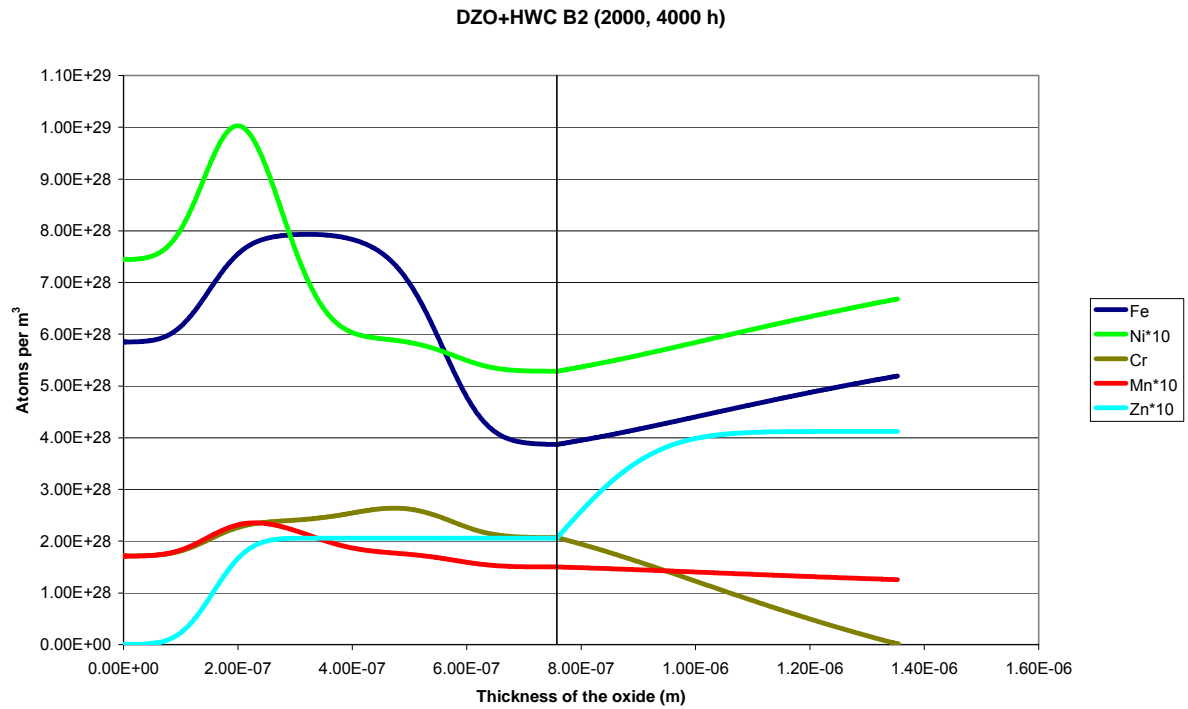


Figure 35: Concentration profile of the non-activated nuclides after 4000 h using DZO+HWC in B2.

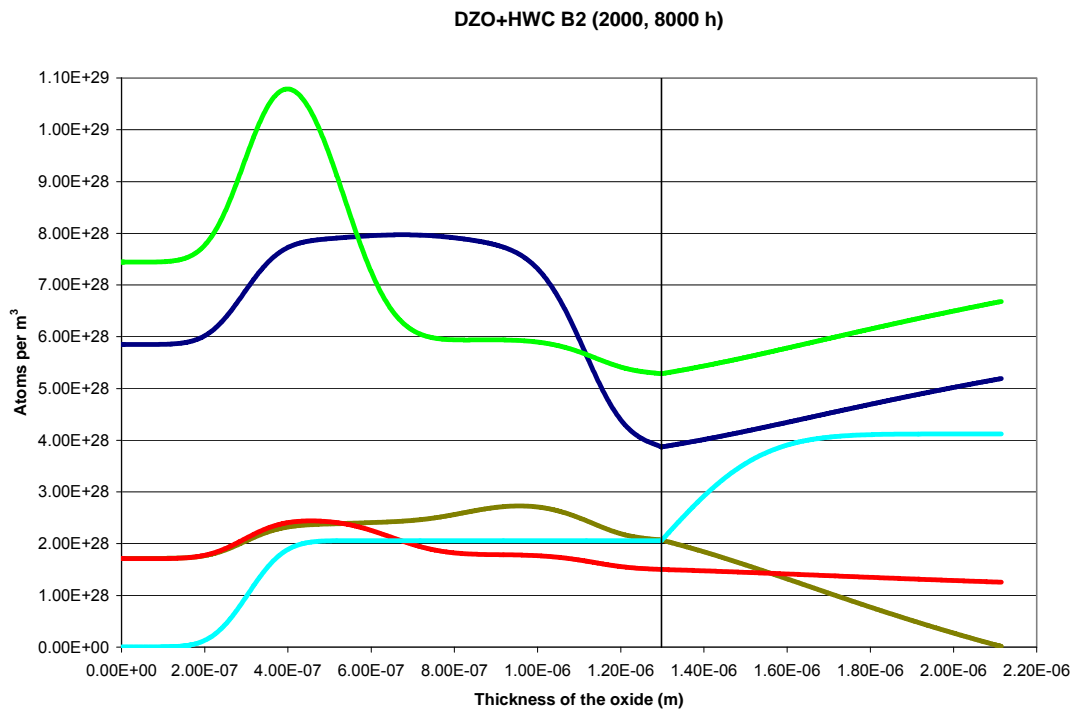


Figure 36: Concentration profile of the non-activated nuclides after 8000 h using DZO+HWC in B2.

As can be seen in the figures above the concentration profiles do not change appreciably between 4000 and 8000 h. However, the oxide is nevertheless still growing. The figures above shows similarities with the NWC concentration profiles using brass condenser tubes, see figures 1 – 2. The high concentration of zinc reduces the transport of the other ions and since there is a constant flux of ions coming from the alloy the concentration of ions increases above the concentration in the alloy. In the figures 35 – 36 the zinc concentration is a factor of ten larger than the concentration in figures 1 – 2. This reduces the oxide growth significantly, the oxide is therefore thinner in figures 35 – 36 compared to the oxide in the figures 1 – 2. The concentration profiles in the outer oxide layer seem to follow steady state solutions except for the zinc profile. The different appearance of the zinc concentration profile compared to the other nuclides is due to the large difference in the diffusion coefficients between zinc and the other ions and how the oxide grows within the model. This is described in the NWC subsection.

The figures 37 – 38 shows the activity profiles for the activated nuclides in the two oxide layers on the steel AISI 304 after 4000 respective 8000 h.

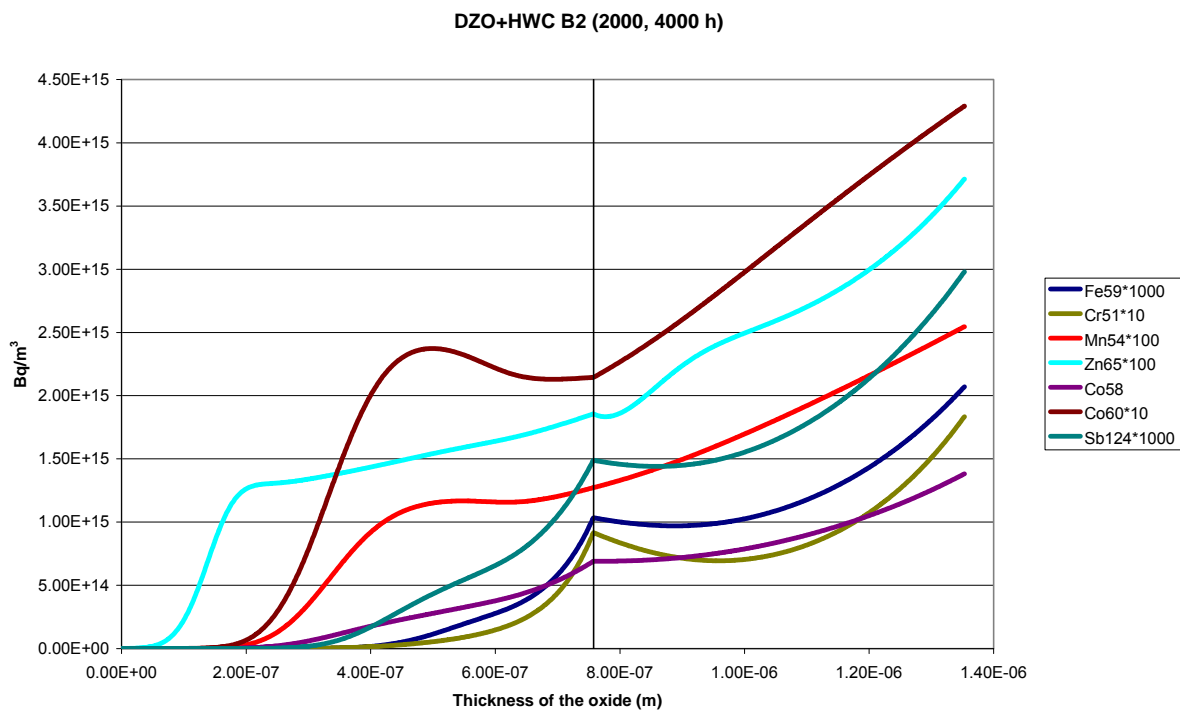


Figure 37: Activity profile of the activated nuclides after 4000 h using DZO+HWC in B2.

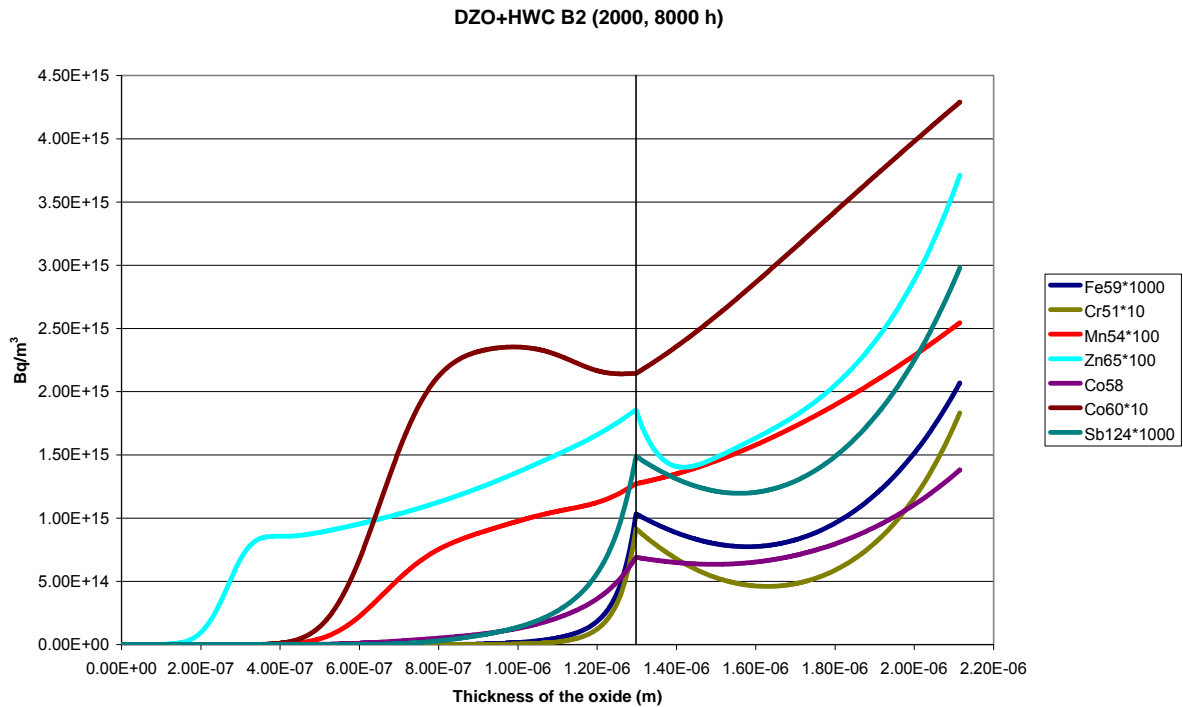


Figure 38: Activity profile of the activated nuclides after 8000 h using DZO+HWC in B2.

The high concentration of zinc also affects the activity profiles in the inner oxide layer, which can be seen in the figures 37 – 38. The high concentration of zinc reduces the diffusion coefficients which makes it harder for the nuclides to penetrate the oxide. If a lower concentration of zinc was used the activity close to the coolant would be lower but instead the nuclides would penetrate the oxide closer to the alloy and since the oxide growth is faster with the lower zinc concentration, the total activity in the oxide becomes larger.

The figures 39 – 42 shows the concentration and activity profiles for the non-activated nuclides in the two oxide layers on the steel AISI 304 after 4000 respective 8000 h corresponding to the 2003 B2 conditions.

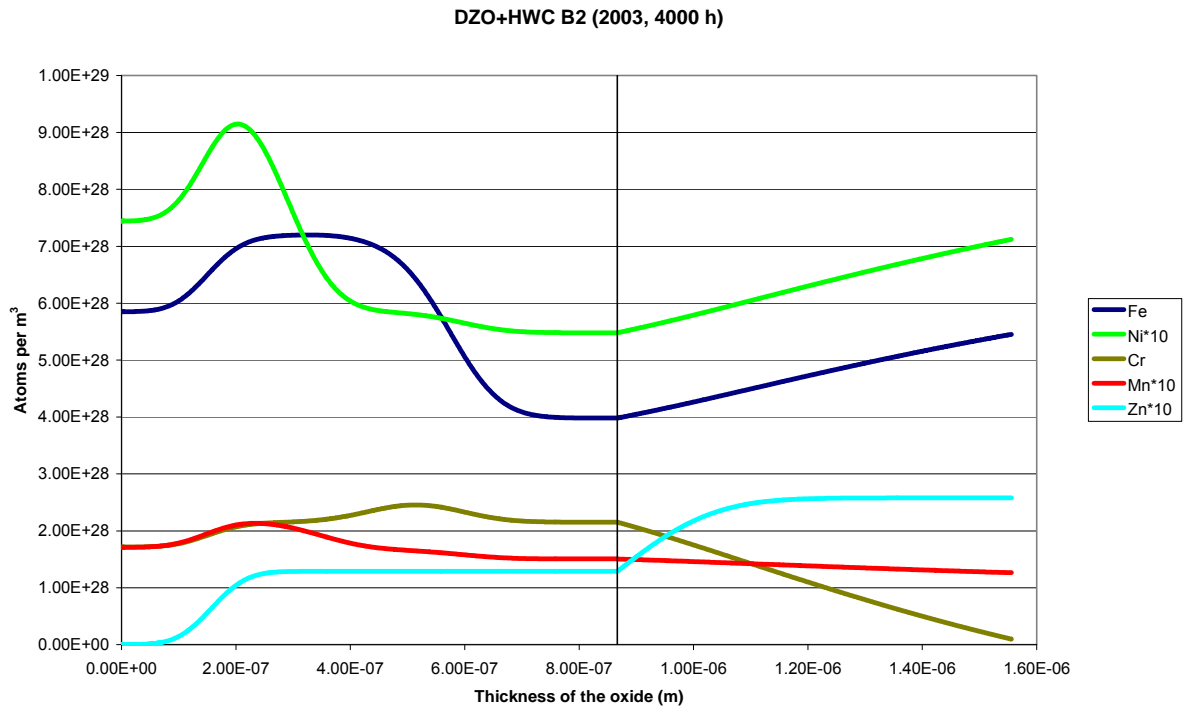


Figure 39: Concentration profile of the non-activated nuclides after 4000 h using DZO+HWC in B2.

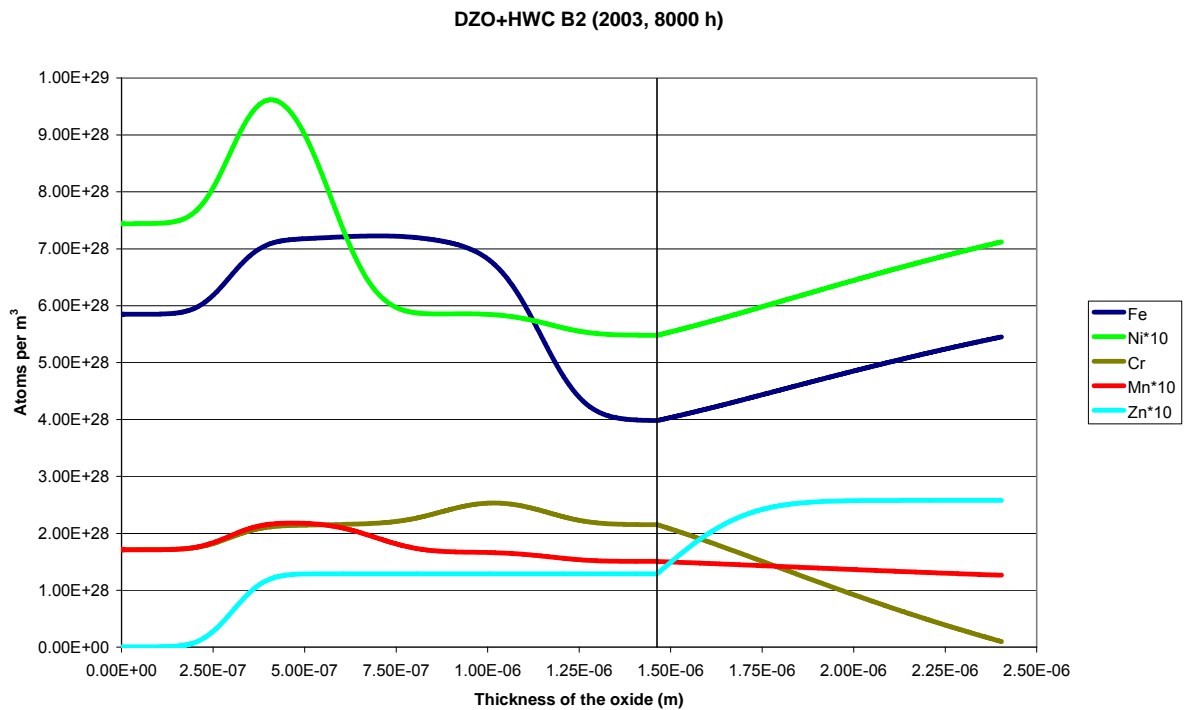


Figure 40: Concentration profile of the non-activated nuclides after 8000 h using DZO+HWC in B2.

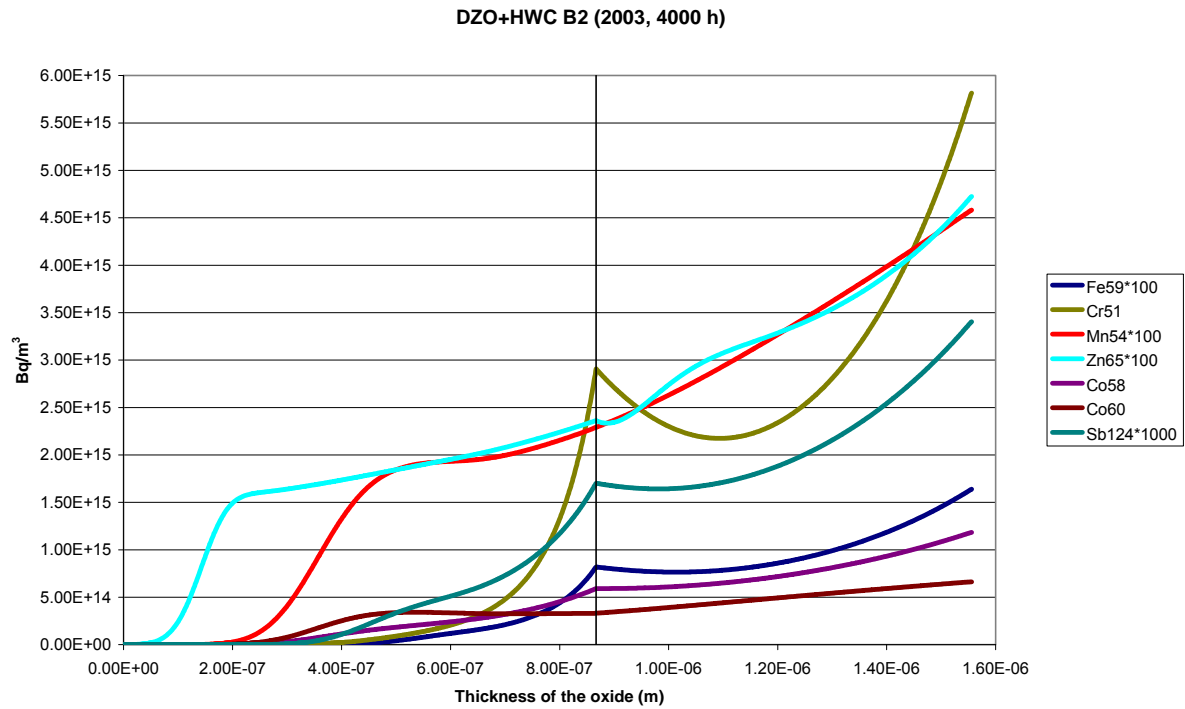


Figure 41: Activity profile of the activated nuclides after 4000 h using DZO+HWC in B2.

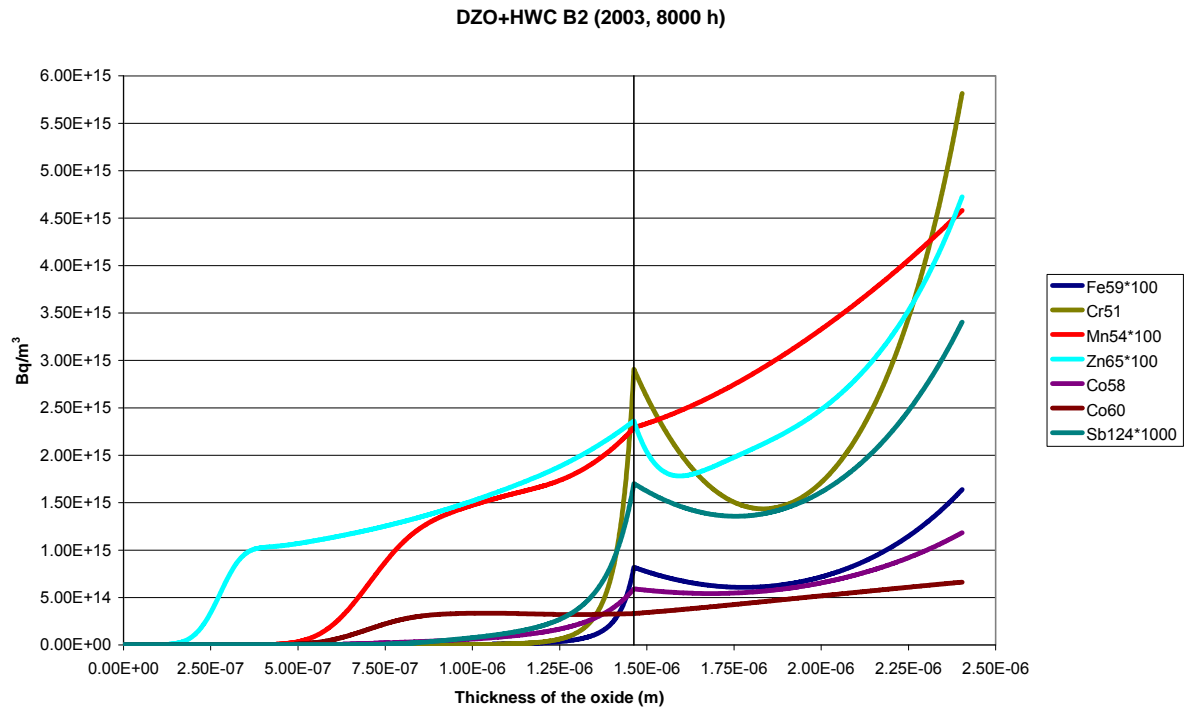


Figure 42: Activity profile of the activated nuclides after 8000 h using DZO+HWC in B2.

The figures 39 – 42 show the same system as above but for a different year. As can be seen in the figures 39 – 40 the increase of concentration of nuclides other than zinc is less pronounced as the zinc concentration increases compared to year 2000. This is due to that the zinc concentration was 40 % lower in the year 2003 compared to 2000. Since the zinc concentration was lower in the year 2003 the oxide became thicker than in the year 2000.

The figures 43 – 49 compares the ratio between the activity in the oxide and the activity in the coolant with reference values. The reference values are obtained from B2 using values from the years 2000, 2001, 2003 and 2004.

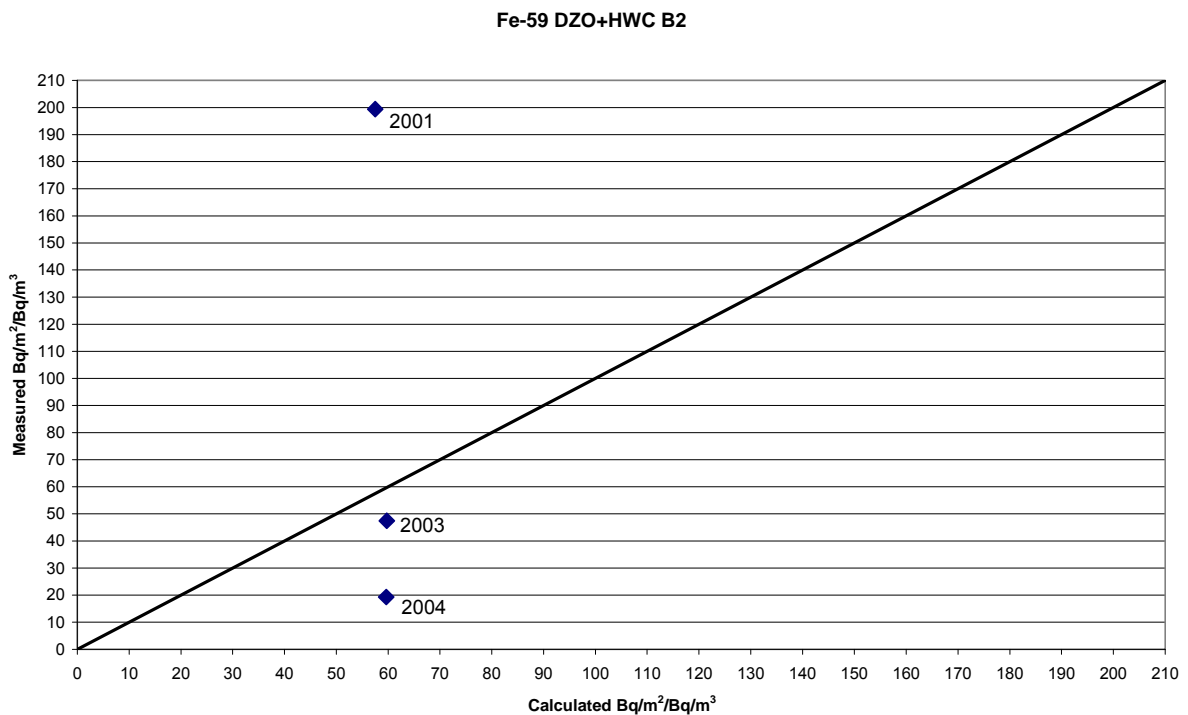


Figure 43: Measured versus calculated ratio between activity in the oxide and the activity in the coolant for Fe59.

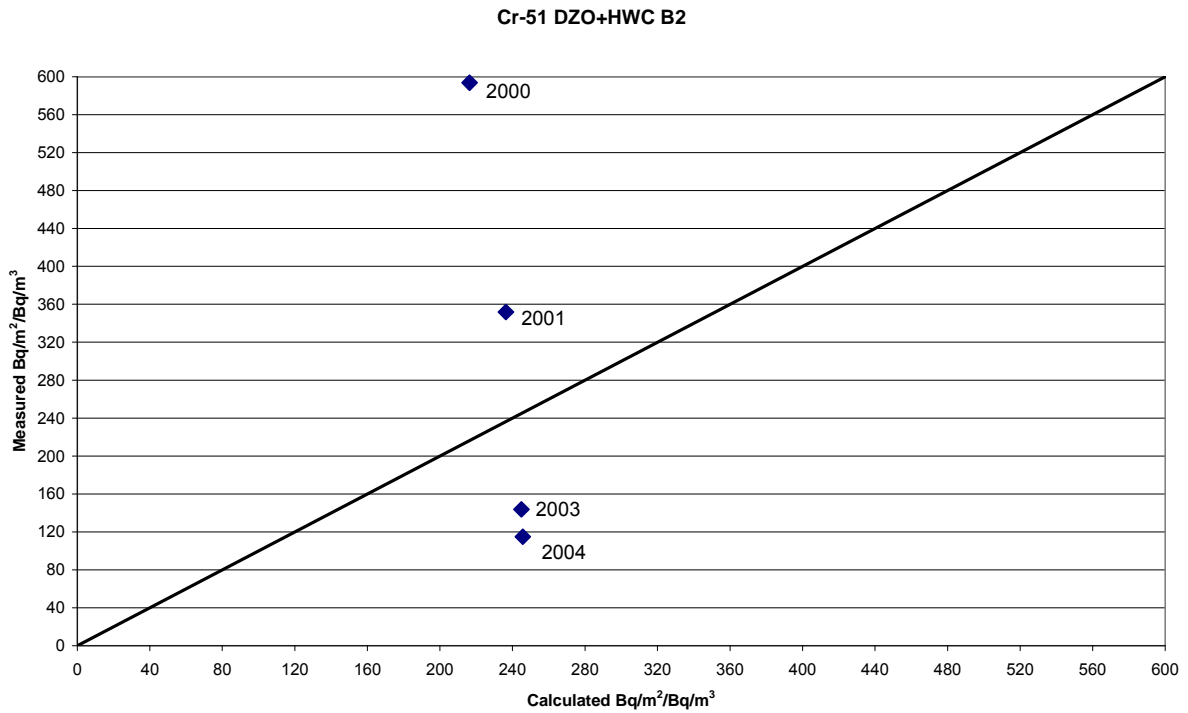


Figure 44: Measured versus calculated ratio between activity in the oxide and the activity in the coolant for Cr51.

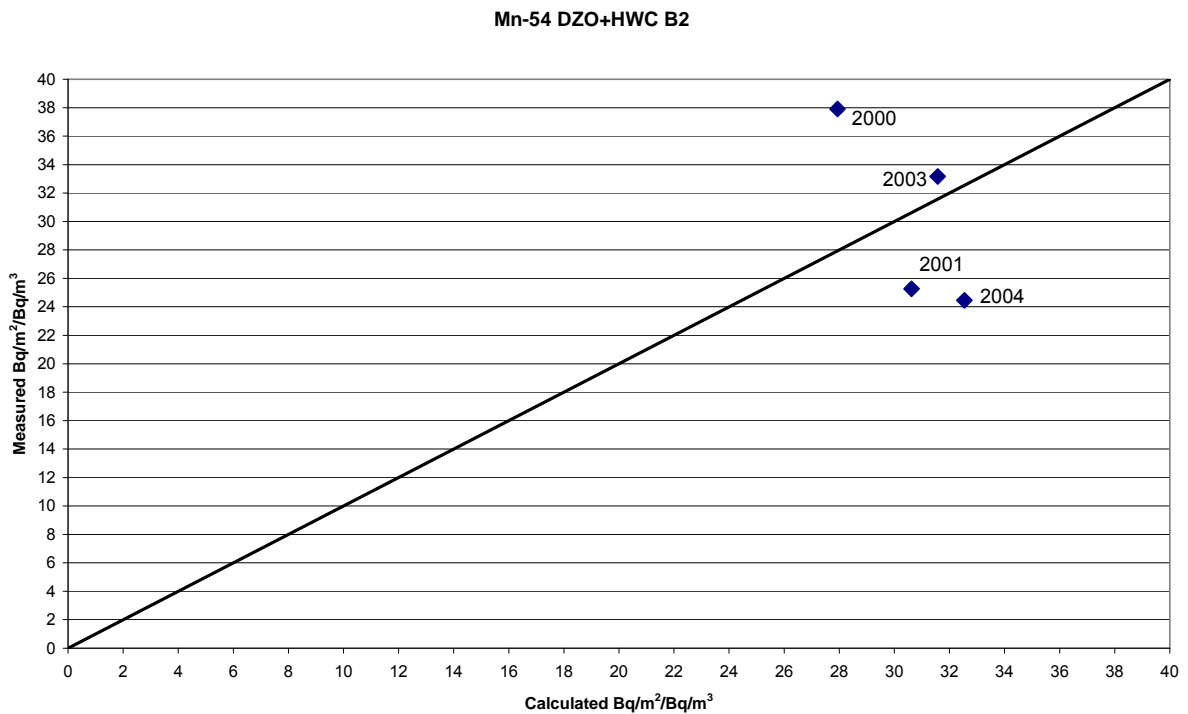


Figure 45: Measured versus calculated ratio between activity in the oxide and the activity in the coolant for Mn54.

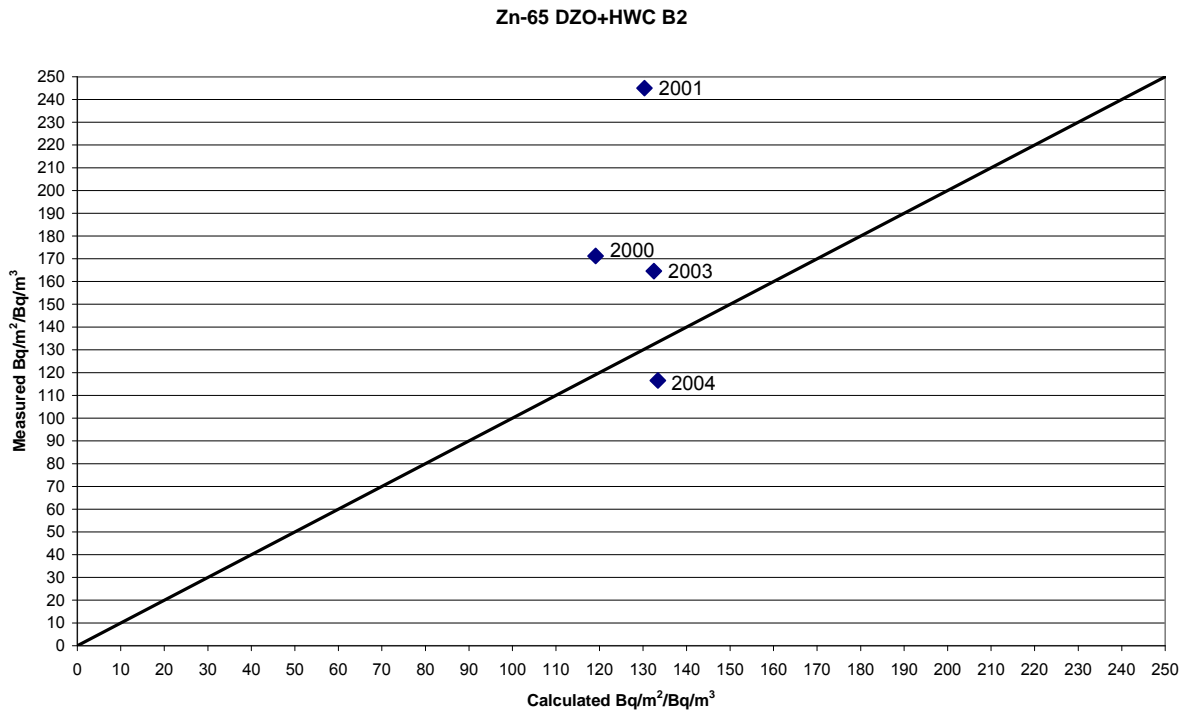


Figure 46: Measured versus calculated ratio between activity in the oxide and the activity in the coolant for Zn65.

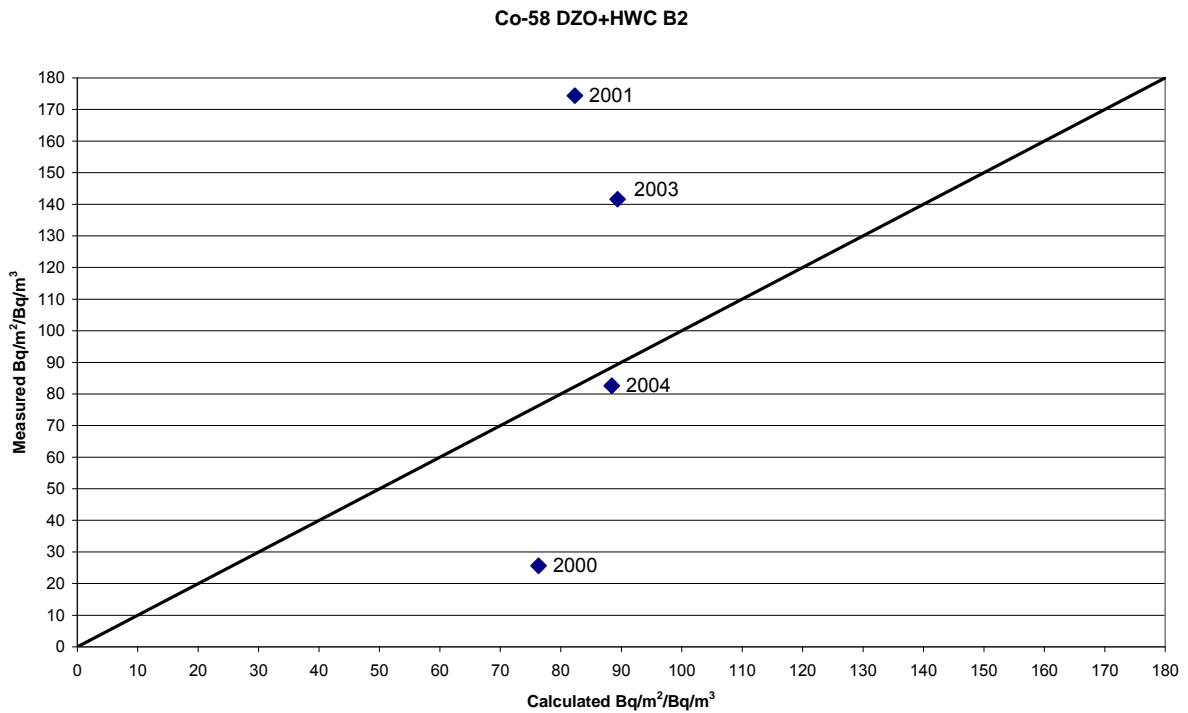


Figure 47: Measured versus calculated ratio between activity in the oxide and the activity in the coolant for Co58.

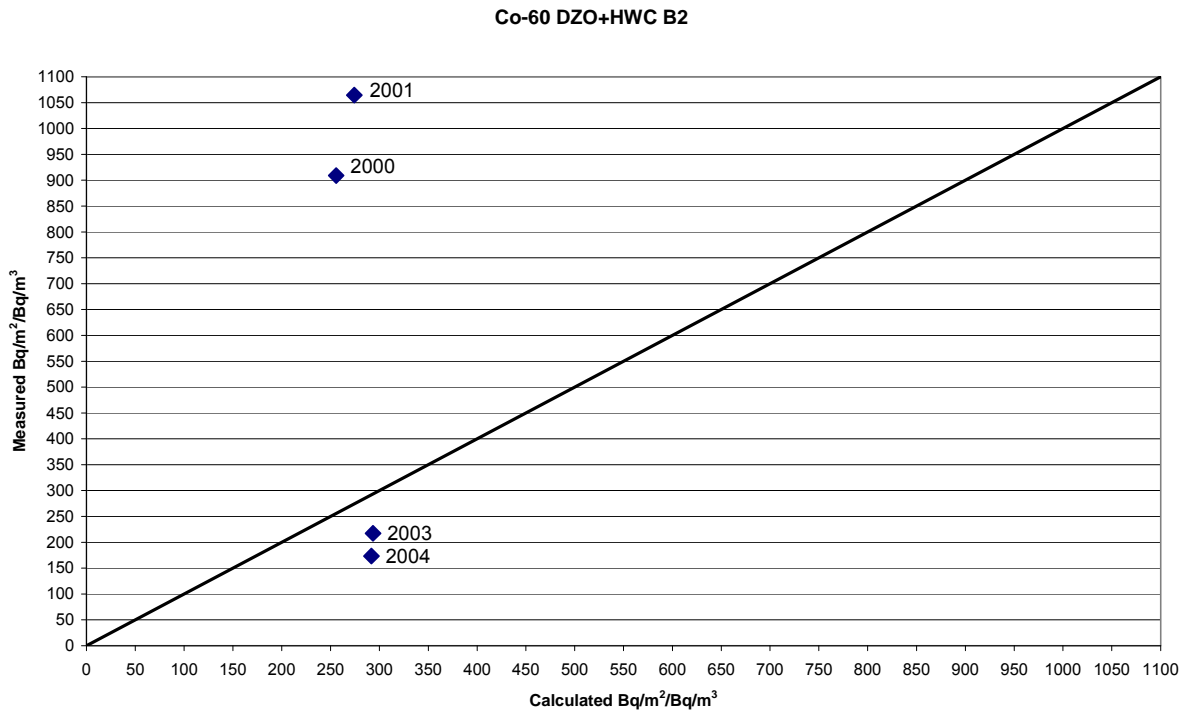


Figure 48: Measured versus calculated ratio between activity in the oxide and the activity in the coolant for Co60.

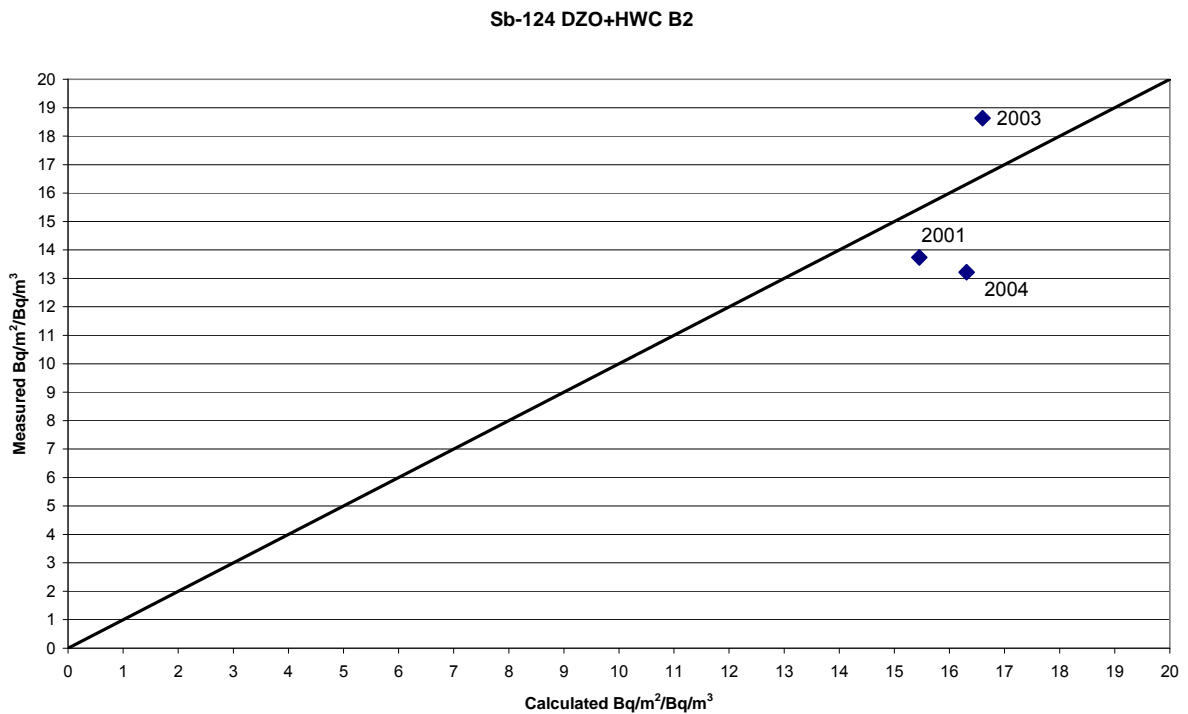


Figure 49: Measured versus calculated ratio between activity in the oxide and the activity in the coolant for Sb124.

As can be seen in the figures 43 – 49 the calculated activities are close to reference values. But as in the case of NWC and HWC the measured values tend to fluctuate much more than the calculated values.

Table 12: Barsebäck 2 – Corrosion product reactor water chemistry data – Annual average data during reactor operation (DZO+HWC)

Year	$C_w(t)$			
	Fe [ppb]	Zn [ppb]	Ni [ppb]	Cr [ppb]
2000	0.66	3.98	0.10	0.02
2001	0.70	2.65	0.11	0.05
2003	3.06	2.49	0.36	0.34
2004	1.94	2.34	0.28	0.46

Table 13: Barsebäck 2 – Corrosion product reactor water chemistry data – Annual average data during reactor operation (DZO+HWC)

Year	$C_w(t)$						
	Mn54 Bq/kg	Co58 Bq/kg	Co60 Bq/kg	Zn65 Bq/kg	Cr51 Bq/kg	Fe59 Bq/kg	Sb124 Bq/kg
2000	1.0E+03	1.4E+04	2.2E+03	3.3E+02	4.1E+02	2.4E+01	1.4E+02
2001	1.6E+03	1.3E+04	2.6E+03	3.6E+02	3.3E+03	6.5E+01	1.3E+02
2003	1.8E+03	1.2E+04	3.4E+03	4.2E+02	1.3E+04	1.9E+02	1.6E+02
2004	1.8E+03	1.4E+04	6.2E+03	5.5E+02	1.6E+04	2.7E+02	3.4E+02

4.2 PWR

The optimized enrichment factors for PWR are shown in table 14.

Table 14: Optimized enrichment factors for PWR.

Nuclide	Fe	Zn	Ni	Cr	Mn	Co58	Co60	Sb
Enrichment Factor (-)	1.57E+09	2.10E+08	1.84E+09	1.01E+09	2.91E+08	1.55E+09	2.13E+09	1.56E+08

The optimized enrichment factors in table 14 are an order of magnitude larger for the nuclides Fe, Ni, Mn Co58 and Co60 than the corresponding values for NWC, which can be seen in table 2. In case of Sb124 and Zn the enrichment factors are only slightly increased. The enrichment factor for Cr is almost increased by three orders of magnitude. The increase of the enrichment factors when comparing PWR with BWR is also found by Lundgren /2/. However, the calculated enrichment factors are in general larger than the enrichment factors obtained by Lundgren.

The figures 50 – 51 shows the concentration profiles for the non-activated nuclides in the two oxide layers on the steel AISI 304 after 4000 and 8000 h, respectively, for R2 in 1998.

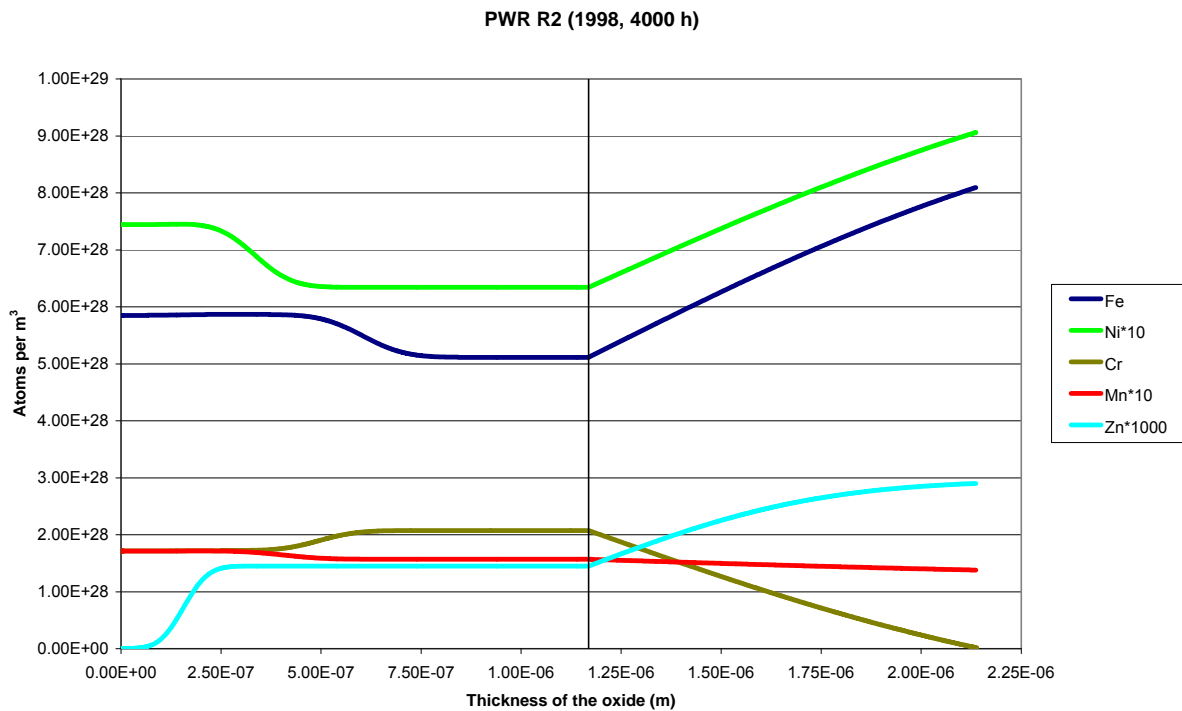


Figure 50: Concentration profile of the non-activated nuclides after 4000 h in R2.

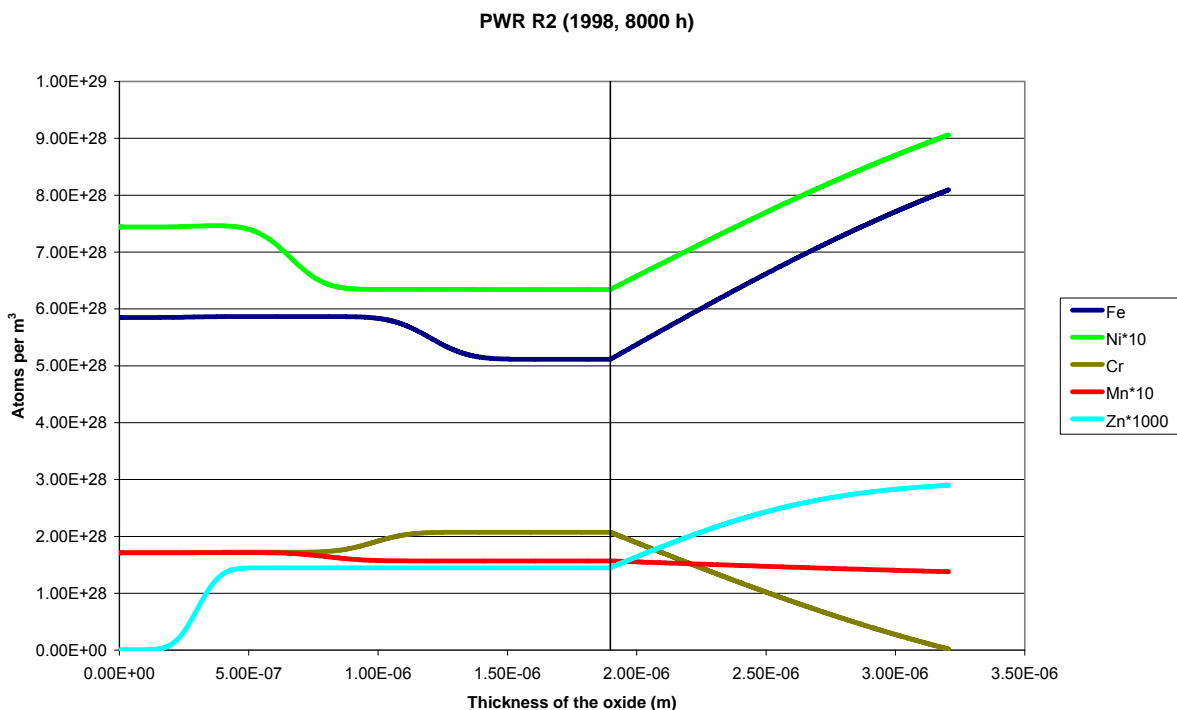


Figure 51: Concentration profile of the non-activated nuclides after 8000 h in R2.

As can be seen in figures 50 – 51 the concentration profiles look very much the same after 4000 h and 8000 h. However, the oxide is still growing. Since the zinc concentration is very low the concentration profiles are hardly affected. Therefore the concentration profiles are very similar to the HWC and NWC concentration profiles. As

also can be seen in the figures above the oxide becomes thicker in PWR than in BWR. This is due that the enrichment factors are larger in PWR than in BWR.

The figures 52 – 53 shows the activity profiles for the activated nuclides in the two oxide layers on the steel AISI 304 after 4000 respective 8000 h for R2 during 1998. Water concentrations of activated and non-activated nuclides are given in tables 15 – 16.

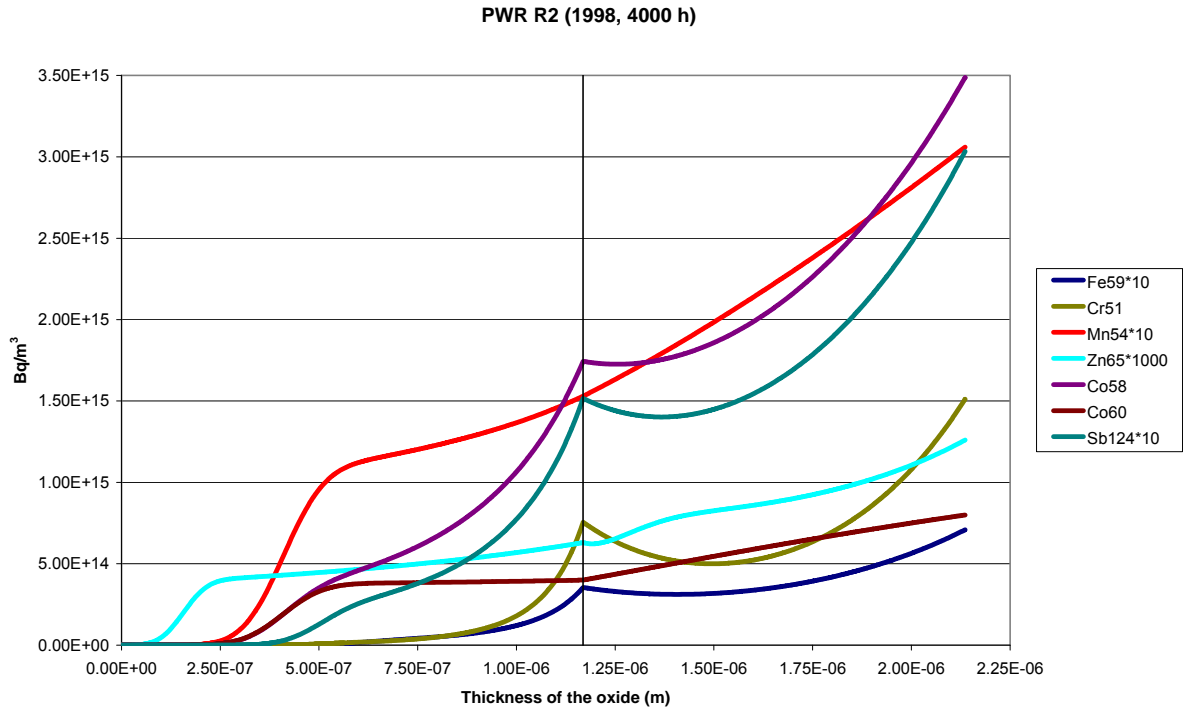


Figure 52: Activity profile of the activated nuclides after 4000 h in R2.

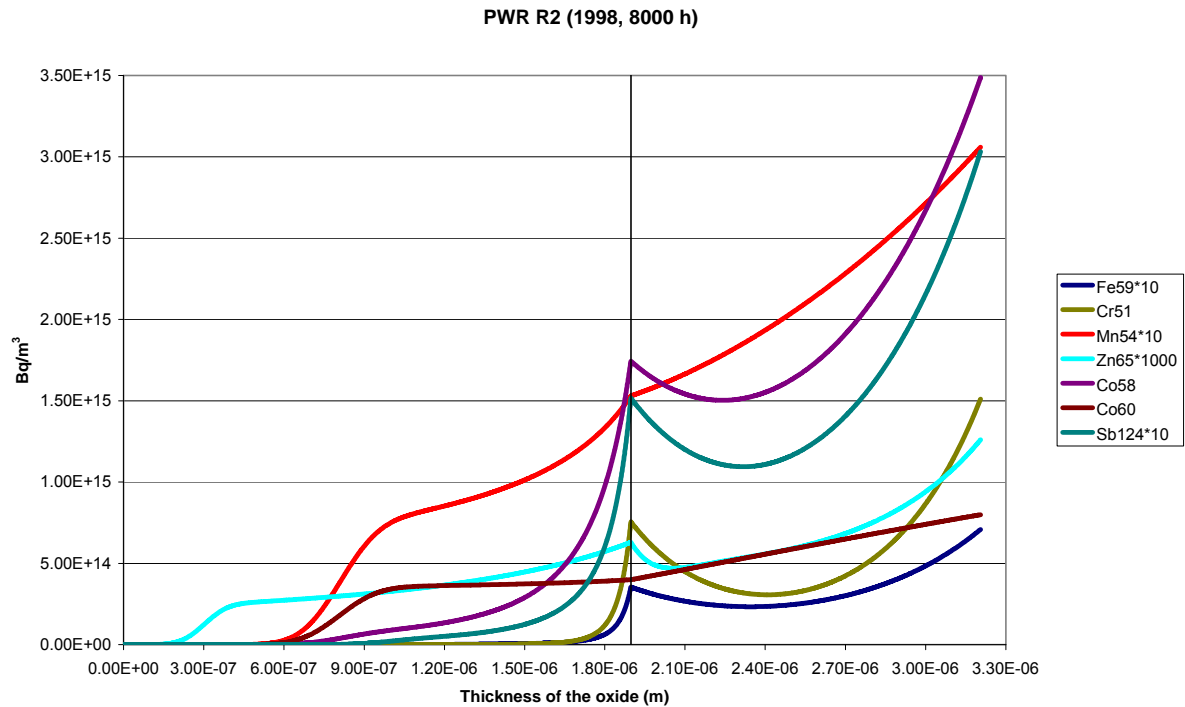
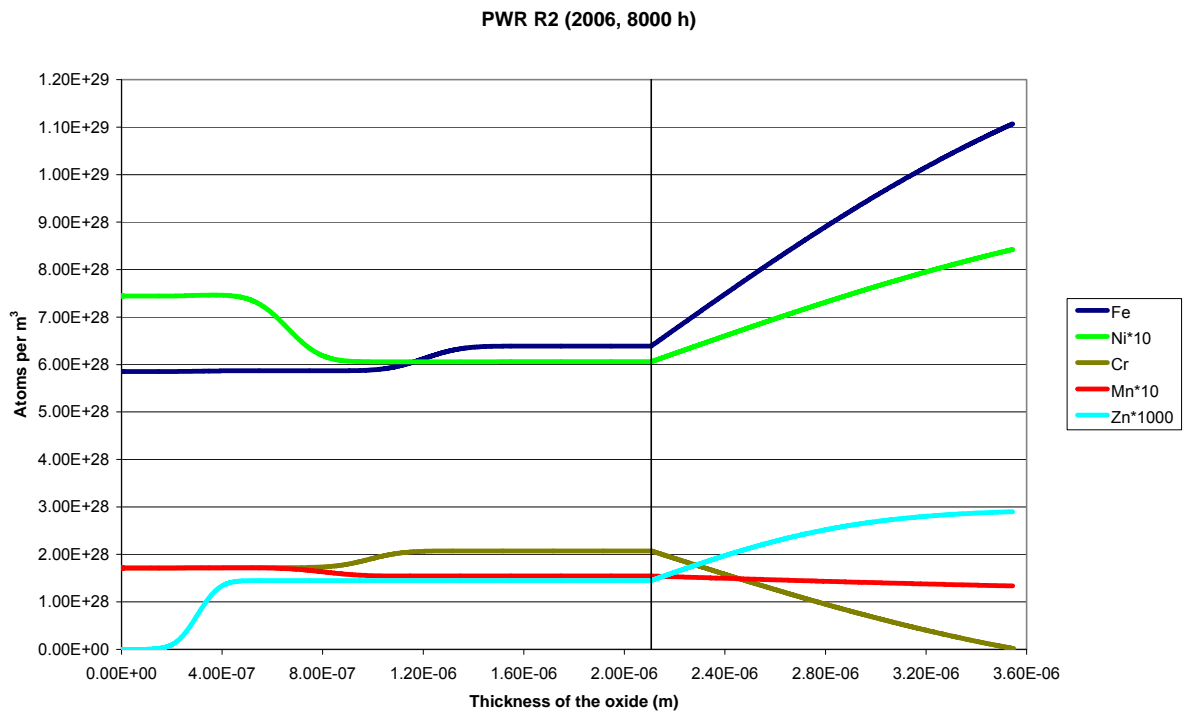
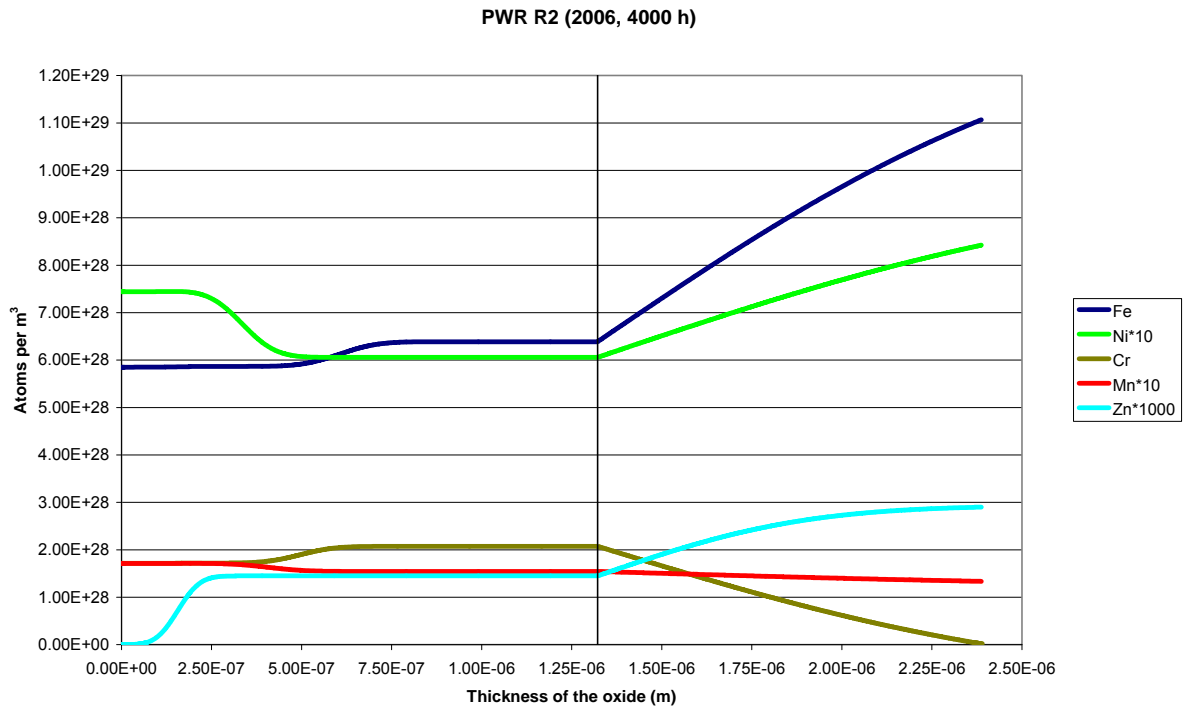


Figure 53: Activity profile of the activated nuclides after 8000 h in R2.

As can be seen in the figures 52 – 53 the largest part of activity comes from Co58 and second largest contribution comes from Co60 after 4000 h in the inner oxide layer. But after 8000 h the contributions are approximately the same. This is due to the larger half life of Co60. In the outer layer, however, the largest contribution comes from Co58 after both 4000 h and 8000 h. This is due the larger diffusion coefficients in the outer layer compared to the inner layer.

The figures 54 – 57 shows the concentration and activity profiles for the non-activated nuclides in the two oxide layers on the steel AISI 304 after 4000 respective 8000 h for R2 during 2006.



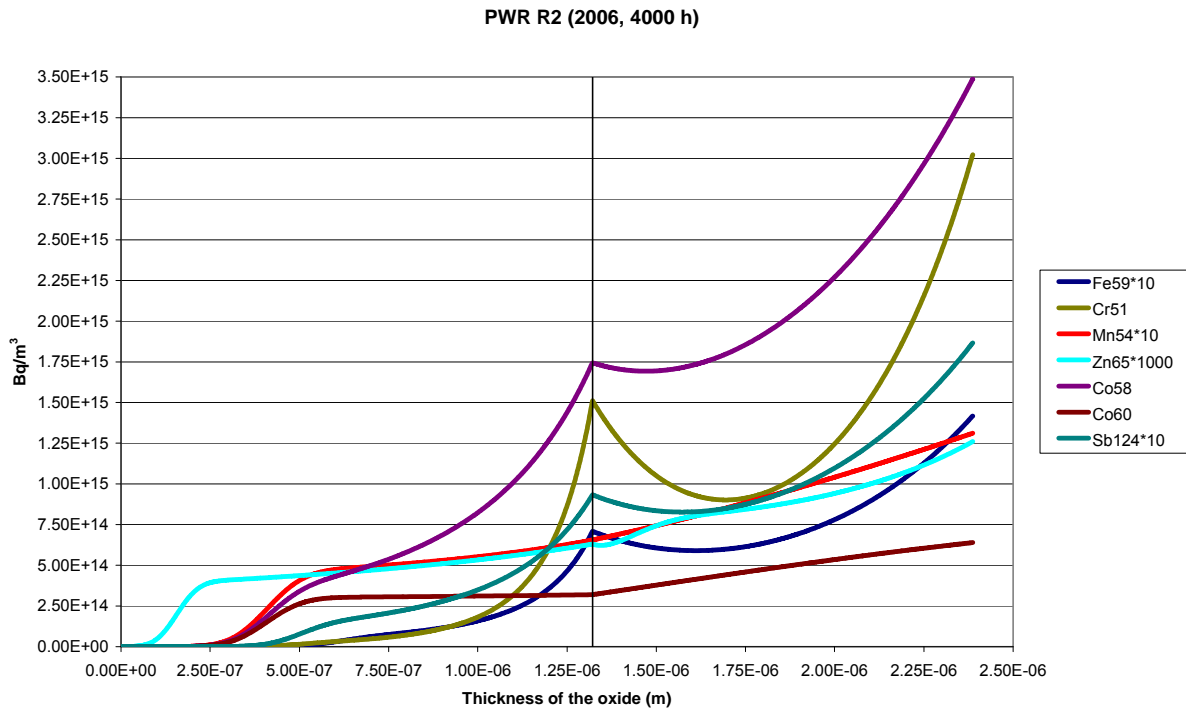


Figure 56: Activity profile of the activated nuclides after 4000 h in R2.

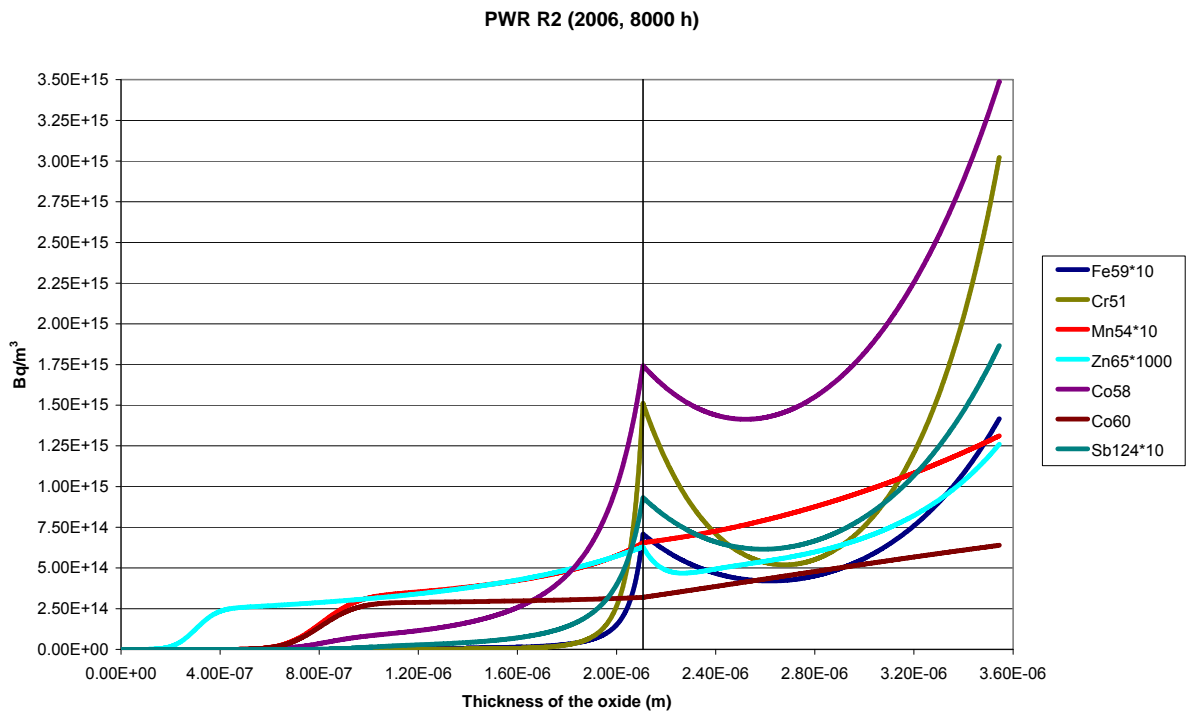


Figure 57: Activity profile of the activated nuclides after 8000 h in R2.

The figures 54 – 57 show the same system as above but for a different year. As can be seen in the figures 54 – 55 the concentration profiles look very much the same as in figures 50 – 51 except in the case of Fe. In the latter case the concentration of Fe in the coolant is doubled which makes the inner boundary concentration larger than in the alloy. Since the concentration of Fe in the coolant is doubled the oxide grows

faster. Therefore the oxide is about 10 % thicker in the latter case. The nuclides with shorter half lives benefit from faster oxide rate, which can be seen when comparing figures 52 – 53 with 56 – 57. In figures 56 – 57 can be seen that the largest part of activity comes from Co58 after both 4000 h and 8000 h.

The figures 58 – 63 compares the ratio between the activity in the oxide and the activity in the coolant with reference values. The reference values are obtained from R2 using values from the years 1998, 2002, 2004 and 2006. No figure on zinc is shown due to few reference values.

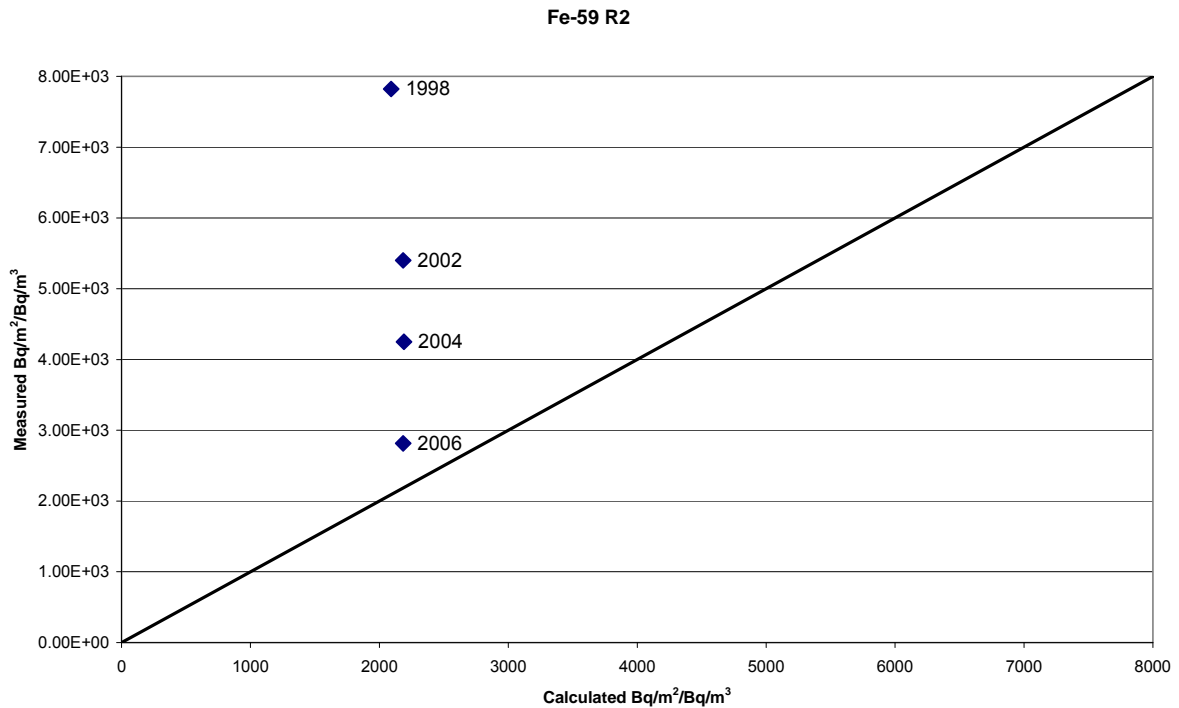


Figure 58: Measured verses calculated ratio between activity in the oxide and the activity in the coolant for Fe59.

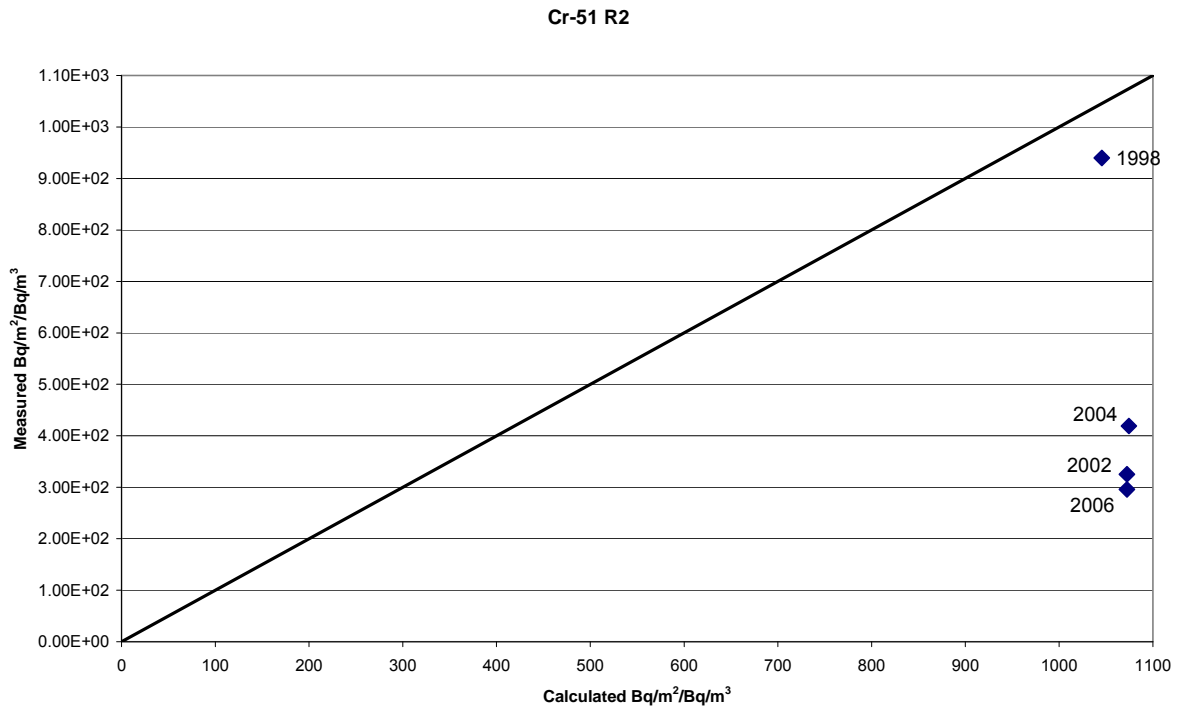


Figure 59: Measured versus calculated ratio between activity in the oxide and the activity in the coolant for Cr51.

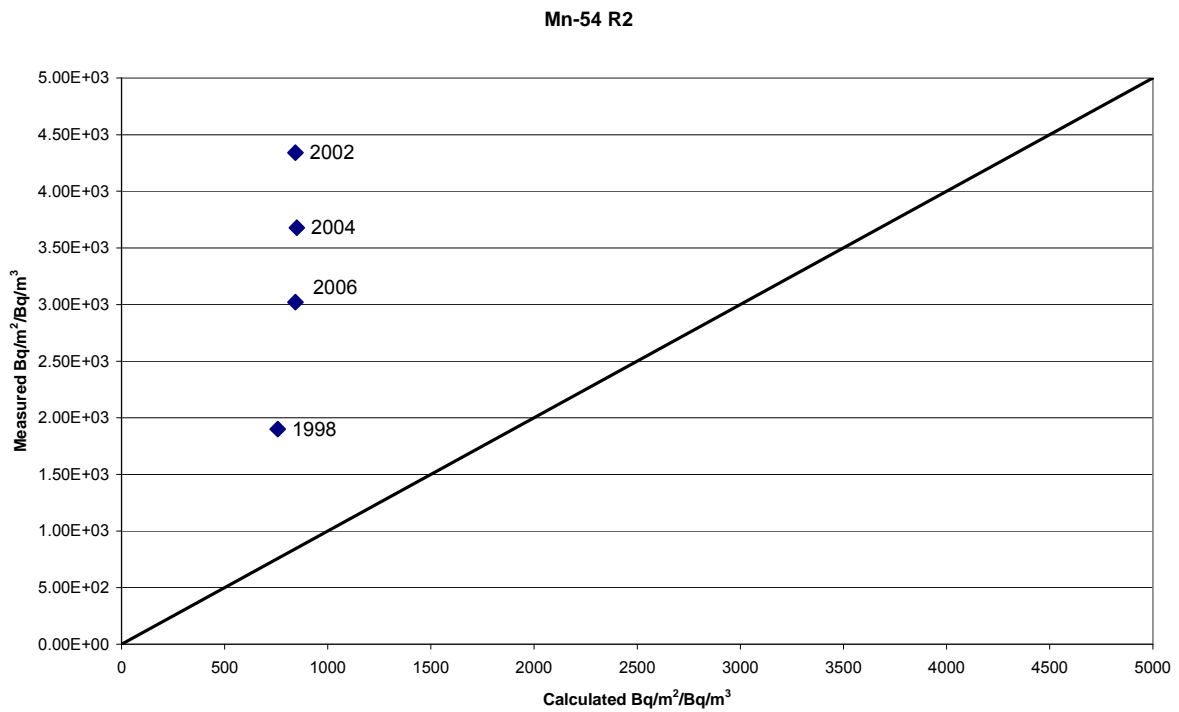


Figure 60: Measured versus calculated ratio between activity in the oxide and the activity in the coolant for Mn54.

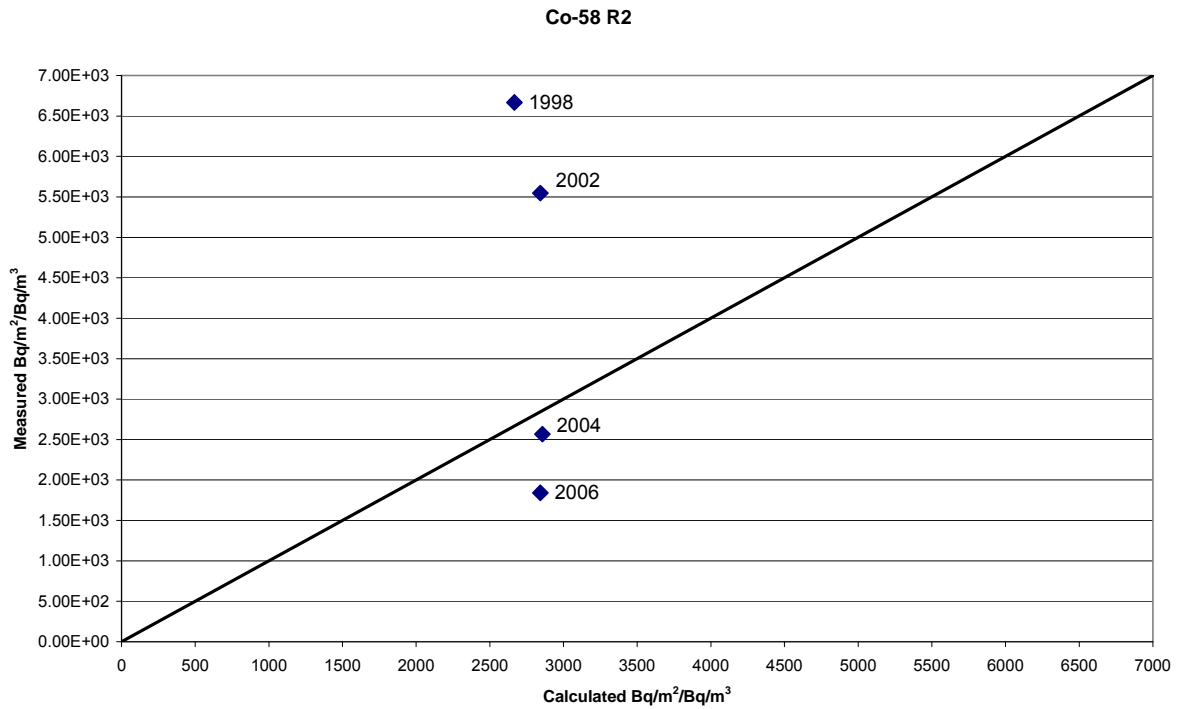


Figure 61: Measured versus calculated ratio between activity in the oxide and the activity in the coolant for Co58.

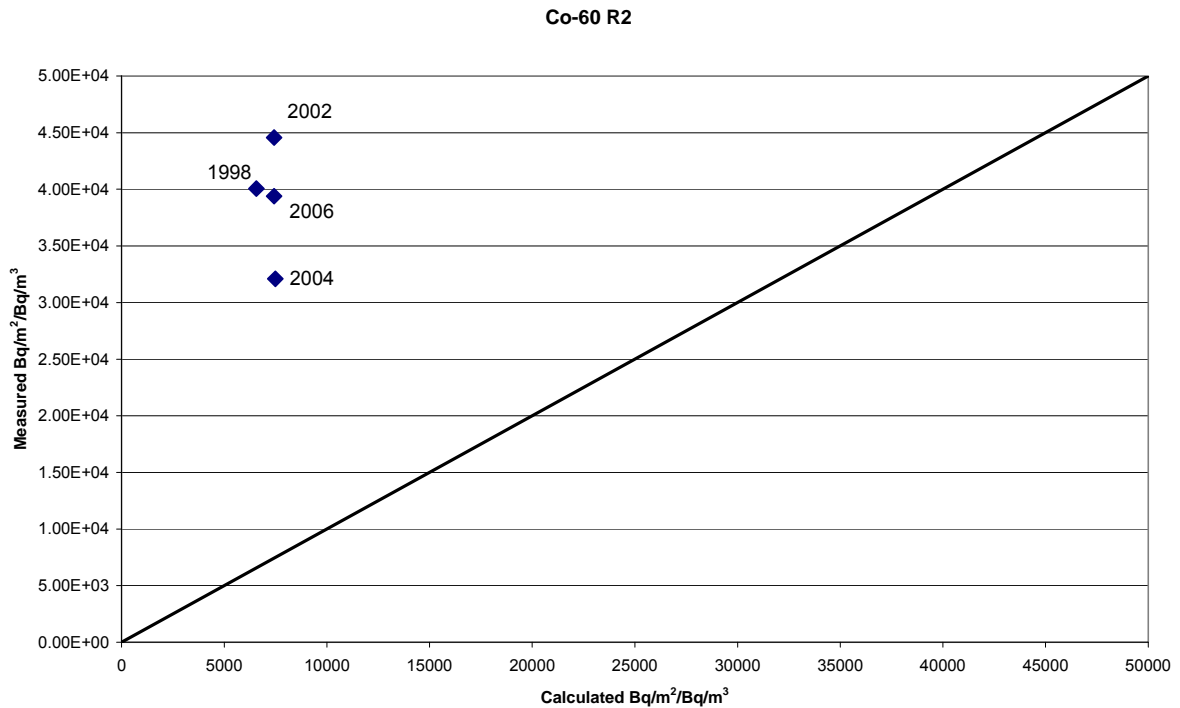


Figure 62: Measured versus calculated ratio between activity in the oxide and the activity in the coolant for Co60.

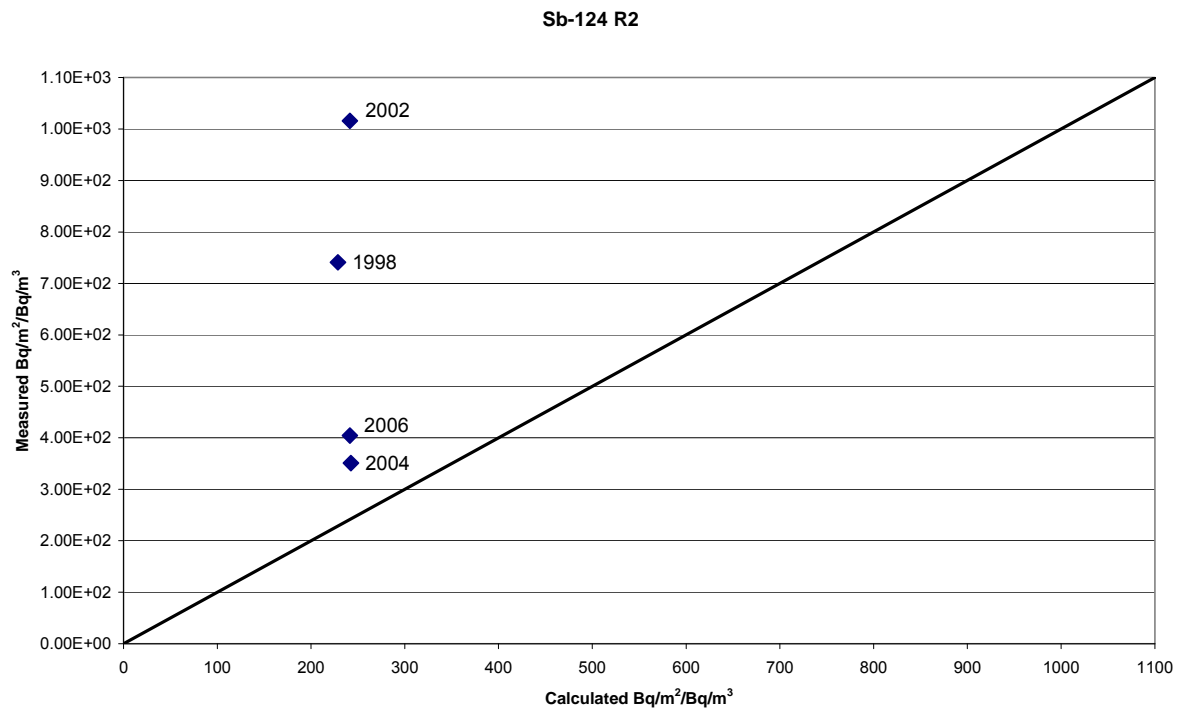


Figure 63: Measured versus calculated ratio between activity in the oxide and the activity in the coolant for Sb124.

As can be seen in the figures 58 – 63 the calculated ratios are somewhat underestimated for the nuclides Fe59, Mn54, Co60 and Sb124. In case of Cr51 the calculated ratio is somewhat overestimated and in the case of Co58 the calculated ratio is close to reference values. As in the case of BWR the measured ratios tend to fluctuate much more than the calculated ratios. The calculated ratios are closer to reference ratios for BWR than for PWR. The reason for this is that the activity in the oxide is no longer a linear function of the enrichment factor if the enrichment factor becomes large enough to effect the rate of which the oxide grows. Another reason for the somewhat lower correlation in case of the PWR activity ratios is that the enrichment factors are optimized in a different reactor, R3.

Since the water chemistry can differ largely between different years, which can be seen due to the large variety in the measured activity ratios, and especially between different reactors the calculated activity ratios can be considered to agree well with measured activity ratios. It should be noticed that the activity on steam generator tubing is measured through the steam generator vessel wall, i.e. the enrichment factors should be somewhat smaller due to shielding of the activity.

It should also be mentioned that the measured data is not corrected for the activity on steam generators is measured through the steam generator vessel wall, i.e. the enrichment factors should be somewhat smaller.

Table 15: Ringhals 2 – Corrosion product reactor water chemistry data – Annual average data during reactor operation

Year	C _w (t)				
	Fe [ppb]	Zn [ppb]	Ni [ppb]	Cr [ppb]	Mn [ppb]
1998	1.0	0.010	0.080	0.010	0.030
2002	2.0	0.010	0.060	0.010	0.025
2004	2.0	0.010	0.15	0.010	0.025
2006	2.0	0.010	0.060	0.010	0.020

Table 16: Ringhals 2 – Corrosion product reactor water chemistry data – Annual average data during reactor operation

Year	C _w (t)						
	Mn54 Bq/kg	Co58 Bq/kg	Co60 Bq/kg	Zn65 Bq/kg	Cr51 Bq/kg	Fe59 Bq/kg	Sb124 Bq/kg
1998	7.0E+02	1.5E+03	2.5E+02	4.0E+00	1.0E+03	3.0E+01	1.3E+03
2002	3.0E+02	1.0E+03	2.0E+02	4.0E+00	2.0E+03	3.0E+01	1.0E+03
2004	3.0E+02	2.5E+03	2.5E+02	4.0E+00	2.0E+03	4.0E+01	1.0E+03
2006	3.0E+02	1.5E+03	2.0E+02	4.0E+00	2.0E+03	6.0E+01	8.0E+02

5 Conclusion

As can be seen in the figures above the ratio between the activity in the oxide with the activity in the reactor water shows much greater variation in measured data for calculated ratios than for measured ratios in both BWR and PWR. This implies that build-up effects are generally not simple one-factor dependencies. This should not, however, be surprising. The main oxide forms are spinels and they can have a variable composition, encompassing all the important corrosion product ions (Fe, Ni, Cr, Mn, Co, Zn, ..). The fact that there are normal spinels and inversed spinels, and even “depleted” spinels (with vacancies instead of A in the general spinel structure AB₂O₄) as in γ -Fe₂O₃ (maghemite), and the fact that Ni²⁺, Zn²⁺, Mn²⁺, Co²⁺ and even Fe²⁺ all could be the A²⁺ ion, suggests a variation in the activity levels caused by memory effects from previous environmental conditions can be significant in the oxide films. The variation in the water chemistry conditions within the cycles, between the cycles, and between the plants will all affect the actual levels of activity (and of course the level of the corresponding non-active ions, although it is not as straight-forward to study them in the real BWR system) in the oxide films mainly due to the in-diffusion of the activity into the oxide film. Hence, a change in the water chemistry conditions can not immediately establish a new steady-state level. Instead, the actual activity level, especially for more long-lived nuclides, will be an integral result of possibly many effects of water chemistry or other environmental changes. However, as can be seen in the figures above the predicted ratio between the activity in the oxide and the activity in the reactor water are in general close to the measured ratios.

The main difference between the enrichment factors in NWC compared to HWC is the enrichment factor of Cr. It is increased with a factor of approximately 130 compared to its corresponding NWC value. Hydrogen injection decreases the activated corrosion products in the reactor water for Cr51 but since the enrichment factor is increased the ratio between the activity in the oxide and the activity in the reactor water is a factor of hundred larger in HWC compared to NWC, which can be seen in the figures above. In case of nuclides with short half-lives the nuclides only penetrates the inner oxide layer at the surface. However, the outer oxide layer is penetrated much deeper due to the larger diffusion coefficients in the outer oxide layer compared to the inner oxide layer.

As can be seen in the figures above the ratios between the activity in the oxide and the activity in the reactor water are decreased, especially for Sb124, when using DZO and HWC injection compared to only HWC injection. DZO injection also makes the oxide layers thinner, as can be seen in the figures above.

The enrichment factors used in PWR are greater than the corresponding values used in BWR. Therefore becomes also the ratio between the activity in the oxide and the activity in the reactor water greater than in a BWR, which can be seen in the figures above. As also can be seen in the figures above the oxide becomes thicker in PWR than in BWR. This is due to the larger enrichment factors in PWRs.

The measured data tend to fluctuate much more than calculated data. Since the input data for most calculations within a certain plant and certain water chemistry is almost the same the calculated data becomes also almost the same. However, the measured data can nevertheless show low correlation. It should be noticed that the activities of the nuclides Sb122 and Sb124 are governed by the shutdown transient. To make the model even more realistic more input data is needed. Perhaps make the enrichment factors depend on several variables.

6 References

/1/ Klas Lundgren, "ANTIOXI – Development of oxide model for activity build-up in LWRs – BWR plant data analysis", VTT Report VTT-R-04127-07 (June 2007).

/2/ Klas Lundgren, "ANTIOXI – Development of oxide model for activity build-up in LWRs – PWR and WWER plant data analysis", VTT Report VTT-R-03907-08 (June 2008).

/3/ Iva Betova, Martin Bojinov, Petri Kinnunen, Timo Saario, "ANTIOXI – Development and testing of an integrated corrosion and activity build-up model", VTT Report VTT-R-10525-08 (December 2008).

/4/ Zhang L.; Macdonald D.D. *Electrochim. Acta* 1998, 43, 2673-2685.